Communication of IUGS Geological Standards

335

by Miguel Company[1], Roque Aguado[2†], François Baudin[3], Rodolfo Coccioni[4], Mathieu Martinez[5], Peter F. Rawson[6], Helmut Weissert[7], Jean-François Deconinck[8], Fabrizio Frontalini[9], Luca Giusberti[10], Bruno Granier[11], Nico M. M. Janssen[12], Mathieu Moiroud[8], Fabrice Monna[13], Luis O'Dogherty[14], Pierre Pellenard[8], Laurent Riquier[3], Gregorio Romero[15], José Sandoval[1], and José M. Tavera[1]*

The Global Boundary Stratotype Section and Point (GSSP) of the Barremian Stage at Río Argos (Caravaca, SE Spain)

[1] Departamento de Estratigrafía y Paleontología, Universidad de Granada, 18002 Granada, Spain; *Corresponding author, *E-mail: mcompany@ugr.es*
[2] Departamento de Geología, CEACTEMA, Universidad de Jaén, 23700 Linares, Spain. †Deceased February 23, 2023
[3] Institut des Sciences de la Terre de Paris, UMR 7193, Sorbonne Université, CNRS, 75005 Paris, France
[4] Università degli Studi di Urbino "Carlo Bo", 61029 Urbino, Italy
[5] Géosciences Rennes, UMR 6118, Université de Rennes, CNRS, 35000 Rennes, France
[6] Scarborough YO11 2SS and Department of Earth Sciences, University College London, London WC1E 6BT, UK
[7] Geologisches Institut, ETH Zentrum, 8092 Zurich, Switzerland
[8] Biogéosciences, UMR 6282, Université de Bourgogne Franche-Comté, CNRS, 21000 Dijon, France
[9] Dipartimento di Scienze Pure e Applicate, Università degli Studi di Urbino "Carlo Bo", 61029 Urbino, Italy
[10] Dipartimento di Geoscienze, Università degli Studi di Padova, 35131 Padova, Italy
[11] Département des Sciences de la Terre et de l'Univers, Université de Bretagne Occidentale, 29238, Brest, France
[12] 3522SV Utrecht, The Netherlands
[13] CPTC, EA 4178, Université de Bourgogne Franche-Comté, 21000 Dijon, France
[14] Departamento Ciencias de la Tierra, CASEM, Universidad de Cádiz, 11510 Puerto Real, Spain
[15] Servicio de Patrimonio Histórico, Consejería de Educación y Cultura de la Región de Murcia, 30005 Murcia, Spain

(Received: September 5, 2023; Revised accepted: October 24, 2023)

https://doi.org/10.18814/epiiugs/2023/02330

Following votes by the Barremian Working Group, the International Subcommission on Cretaceous Stratigraphy and the International Commission on Stratigraphy, the Executive Committee of the International Union of Geological Sciences unanimously approved in March 2023 the Global Stratotype Section and Point (GSSP) for the Barremian Stage (Lower Cretaceous). The base of the Barremian Stage is defined at the base of bed 171 of the Río Argos section, near Caravaca (SE Spain) and correlated by the first appearance of the ammonite species Taveraidiscus hugii. This event falls within the NC5C calcareous nannofossil Subzone, the Lilliputianella semielongata planktonic foraminiferal Zone, and the Dorothia ouachensis benthic foraminiferal Zone. It roughly coincides with the beginning of a slightly negative trend interval in the $\delta^{13}C$ curve. Indirect calibration to the magnetostratigraphic scale suggests that the boundary falls in the lowermost part of polarity chron M3r. According to the astrochronological analysis, a time interval of 0.74 myr separates the beginning of the late Hauterivian Faraoni Episode from the base of the Barremian, which is dated at 125.77 MA.

Introduction

The Barremian Working Group was established in 1994 with the aim of defining the base of the Barremian Stage and proposing a candidate stratotype section. Following the discussions held before, during and after the 2nd Symposium on Cretaceous Stage Boundaries (Brussels, 1995) the members of the Working Group decided, by a large majority, to recommend drawing the lower boundary of the Barremian Stage at the base of the *Taveraidiscus hugii* ammonite Zone (AZ), defined by the first occurrence (FO) of the index species. Concurrently, the Río Argos section (Caravaca, SE Spain) was selected as the most appropriate to become the GSSP for this boundary (Rawson et al., 1996).

Between 1994 and 2015, several studies were conducted on the biostratigraphy and palaeobiology of various fossil groups in the Río Argos section: ammonites (Hoedemaeker, 1995, 2013; Hoedemaeker and Leereveld, 1995; Company et al., 2002, 2003, 2005, 2010), belemnites (Janssen, 1997), calcareous nannofossils (Hoedemaeker and Leereveld, 1995; Gea, 2004; Company et al., 2005; Aguado et al., 2014), and planktonic foraminifera (Coccioni and Premoli Silva, 1994; Hoedemaeker and Leereveld, 1995; Coccioni et al., 2004, 2006). The specific research work to prepare the proposal began in 2010. The Río

Argos section was re-measured and re-sampled for further bio–, chemo– and cyclostratigraphic studies (Martinez et al., 2012, 2015, 2020; Moiroud et al., 2012, Sauvage et al., 2013; Baudin and Riquier, 2014). Preliminary accounts of the proposal were presented at the International Cretaceous Symposia of Ankara (Company et al., 2013) and Vienna (Company et al., 2017), and at the Business meeting of the International Subcommission on Cretaceous Stratigraphy in Milan (2019). This report brings together the most relevant published, and some still unpublished, results on the Hauterivian–Barremian boundary in the Río Argos section.

Definition of the Base of the Barremian. Historical Background

Coquand proposed the Barremian Stage in 1862 for the upper part of the Neocomian, characterised by "*Belemnites minaret*, *Ammonites ligatus*, *Scaphites Yvani*, etc" (Coquand 1862, p. 535). As noted by Busnardo (1965a), Coquand's "Barremian" embraces both the upper Hauterivian and the Barremian of more recent usage. The modern interpretation of Barremian effectively dates from Kilian (1888), who, in his study of the Montagne de Lure succession in SE France, included *Crioceras angulicostatum* (= *Pseudothurmannia* spp.) among the Hauterivian species, and the "Horizon de Combe-Petite", with *Holcodiscus* and *Pulchellia*, in the Barremian.

Kilian's (1888, 1896, 1910) placing of the faunas of the *Pseudothurmannia* beds in the highest Hauterivian was followed by most subsequent workers, including the Pre-Albian Stages Working Group (predecessor of the Barremian Working Group), which regarded the *Spitidiscus hugii* (now *Taveraidiscus hugii*) AZ as the basal zone of the Barremian (Rawson 1983, table 1). However, Busnardo (in Rawson 1983) favoured to take the appearance of *Raspailiceras* and *Barremites* to mark the base of the stage, which would therefore lie within the *Pseudothurmannia angulicostata* AZ, while other specialists (Avram, 1983; Vašíček et al., 1983) preferred to place the boundary at the base of this zone. At a symposium on Cretaceous Stage Boundaries organised by the International Subcommission on Cretaceous Stratigraphy in Copenhagen in 1983 it was agreed that the boundary should be placed either at the base or at the top of the *P. angulicostata* AZ, and that one within the zone "should be avoided" (Birkelund et al., 1984, p. 8).

Following the establishment of the Barremian Working Group, it became evident during the first exchanges of views among its members that there was no obvious microfossil or non-biostratigraphic event that could convincingly replace the ammonites as a primary tool for defining the base of the Barremian Stage (Rawson et al., 1996). Thus, in the Working Group meeting held during the 2nd Cretaceous Stage Boundaries meeting in Brussels in 1995, the debate was focussed on which ammonite level would provide the best boundary. Three possible, and classical, horizons were discussed in Brussels: base of the *Pseudothurmannia* beds, middle of the *Pseudothurmannia* beds and base of the *S. hugii* AZ (i.e. above the *Pseudothurmannia* beds). By a large majority view (11 out of 13 votes in a subsequent postal ballot), the members of the Barremian Working Group recommended drawing the base of the Barremian Stage at the base of the *S. hugii* AZ. The other two alternatives were rejected mainly due to the difficulty in differentiating *Pseudothurmannia* species from each other and from other late Hauterivian crioceratitids and, consequently, in accurately recognizing the base of the *Pseudothurmannia* beds and their eventual subdivisions.

Conversely, the base of the *T. hugii* AZ is clearly defined and fits closer to the traditional concept of the Hauterivian–Barremian boundary. The index species is easy to recognise and does not present taxonomic identification problems (Busnardo et al., 2003; Vermeulen et al., 2018). It is common in both shallow and deep-water facies. However, in keeping with the strong endemism of marine fauna and flora during the late Hauterivian and early Barremian (Rawson et al., 1996), its geographic distribution is quite restricted and limited to the northern margin of the Mediterranean area (see below).

When introducing the Barremian Stage, Coquand (1862) cited several localities where this stage could be recognised, among them Barrême, Angles and Vergons, in the Basses-Alpes. In 1963 the *Colloque sur le Crétacé Inférieur* proposed the Angles roadside section as the Barremian "stratotype" (Busnardo 1965b) because of its apparent completeness, accessibility and lack of tectonic disturbance, as well as a sufficient richness in ammonites.

However, Busnardo (1965a) showed that in the Angles "stratotype" the crucial passage beds from Hauterivian to Barremian were hidden beneath fallen rocks and there were problems of exposure in the sequence. Hence, in 1983 during the meeting in Copenhagen it was recommended that sections in southeast France, southeast Spain, the Carpathians, the Crimea and the Caucasus should be considered for the boundary stratotype (Birkelund et al., 1984). Although Busnardo and Vermeulen (1986) subsequently obtained some specimens from the boundary interval at Angles, ammonites "are scarce around this interval and there are problems of exposure" (Rawson et al. 1996). After reporting several other possible sites in Europe, the Barremian Working Group recommended that the Río Argos section in SE Spain would represent an appropriate boundary stratotype section (supported in the subsequent postal vote by 12 out of 13 members) (Rawson et al., 1996).

The Río Argos Section: the GSSP for the Base of the Barremian Stage

Geographical and Geological Setting

The beds around the Hauterivian–Barremian boundary outcrop at several points along the river Argos and its tributaries (Hoedemaeker, 1995, 2013; Hoedemaeker and Leereveld, 1995). The GSSP (section Ag1 in Fig. 1, equivalent to section A in Hoedemaeker, 1995, 2013) is the most complete and continuous of these outcrops. It is located some 8 km WSW of Caravaca and 1.5 km NW of the small village of Benablón (Region of Murcia, SE Spain), on the southern bank of the river. The geographical coordinates of the base of the section are: 38°4′13.5″N 1°56′54.3″W, altitude: 771 m (sheet n° 910-IV of the 1:25000 IGN topographic map, and sheet n° 910 of the 1:50000 IGME geologic map) (Fig. 1).

Four other nearby sections were sampled to complement some observations and check the consistency of the records. Two of them (sections Ag5 and Ag4, equivalent to sections C and W in Hoede-

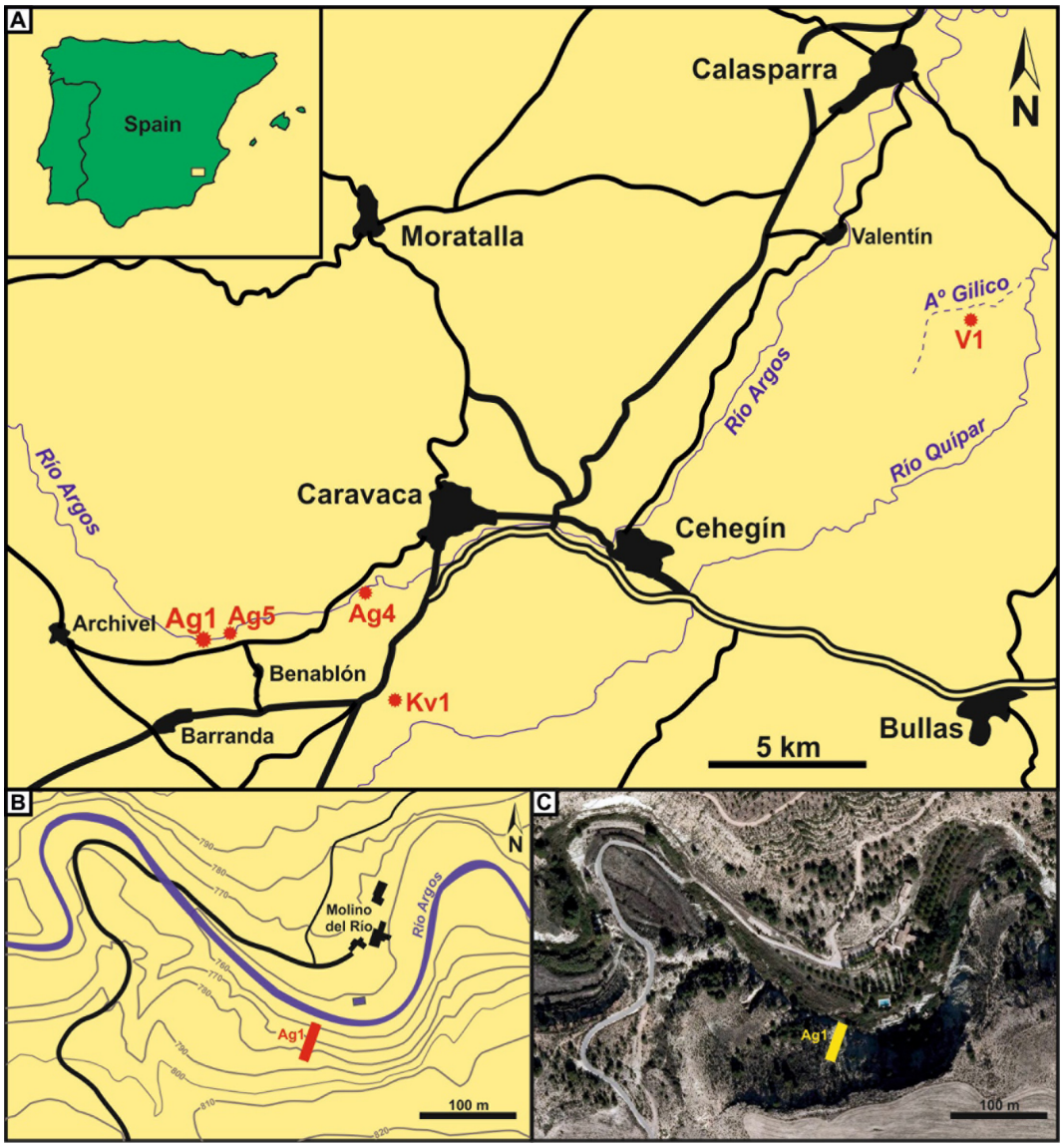

Figure 1. Geographic location of the Río Argos section. A, Map showing the location of section Ag1 (GSSP) and other sections studied in the Caravaca region (Ag5, Ag4, Kv1 and V1). B, Detailed location map of section Ag1. C, aerial view of section Ag1 (source: Cartomur).

maeker, 2013) are located also in the Río Argos area, 0.6 and 4.5 km downstream, respectively, from the GSSP. The other two are section Kv1, in the Barranco de Cavila, 6.5 km SSW of Caravaca (Company et al., 1995), and section V1 near the Arroyo Gilico, 17 km ENE of Caravaca and 8 km SES of Calasparra (Aguado et al., 2014; Premoli Silva et al., 2018; Martinez et al, 2020).

From a geological point of view, the Río Argos area is located in the Subbetic Domain, which together with the Prebetic Domain constitutes the External Zones of the Betic Cordillera (Fig. 2A, B). These are made of a complex of thrust sheets comprising thick successions of sedimentary rocks deposited during the Alpine tectonic cycle (Triassic to Early Miocene) on the southern margin of the Iberian Plate, which was located at the western end of Tethys, on the northern edge of the seaway connecting with the Central Atlantic Ocean (Fig. 2C). The proximal part of southern Iberian palaeomargin (Prebetic Domain) was, during the Cretaceous, a vast epeiric domain that extended from a shallow marine platform in the north to more distal environments to the south, giving way to a complex pelagic basin (Subbetic Domain). The morphology of this Subbetic Basin was quite irregular due to severe intracontinental rifting, which gave rise to well defined swells and troughs bordered by extensional faults that were tectonically active during the Jurassic and the Early Cretaceous (Vera, 2001; Vera et al., 2004). The Río Argos succession would be deposited in a subsident and relatively deep area within this basin (Rey, 1995; Gea, 2004) (Fig. 2D).

Description of the Section

A thick, well-exposed and tectonically almost undisturbed Lower Cretaceous succession crops out along the Río Argos west of Caravaca (Fig. 2B). It encompasses the entire Berriasian–Upper Albian interval, except for a hiatus comprising the Upper Aptian–Middle

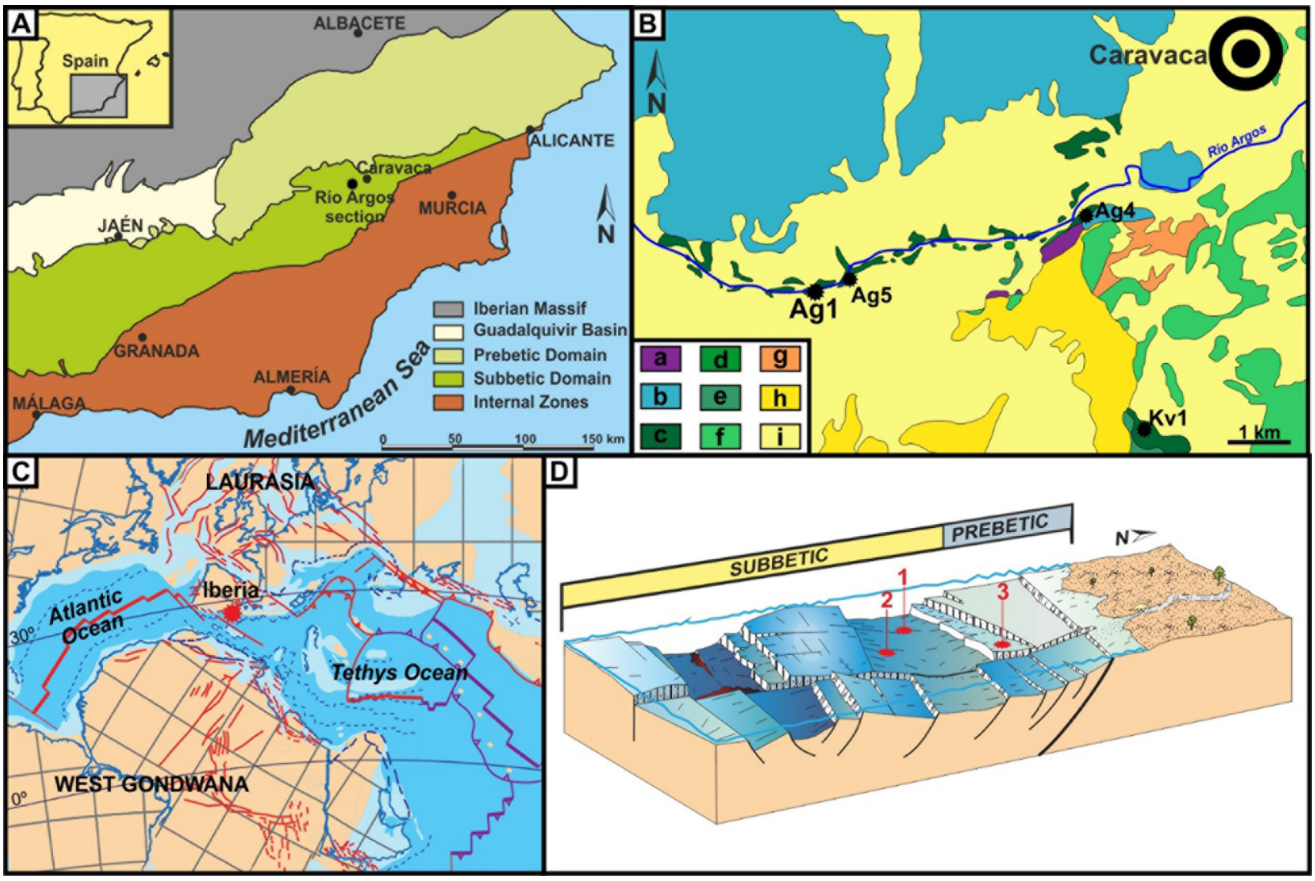

Figure 2. Geologic and palaeogeographic location of the Río Argos section. A, Simplified geologic map of the Betic Cordillera. B, Geological sketch map of the Río Argos area: a, Triassic; b, Jurassic; c, Miravetes Formation (Berriasian-upper Barremian); d, Argos Formation (upper Barremian-middle Aptian); e, Represa Formation (upper Albian); f, Upper Cretaceous; g, Palaeogene; h, Neogene; i, Quaternary. C, Palaeogeographic location of the Río Argos section (red star) in the Western Tethys (modified from Barrier et al., 2018). D, Hypothetical reconstruction of the southern Iberian palaeomargin with the relative position of the sections studied: 1, sections Ag1, Ag4 and Ag5; 2, section Kv1; 3, section V1.

Albian (van Veen, 1969; Gea, 2004). The lower part of this succession (Berriasian–Upper Barremian) consists of a marl–limestone rhythmite that corresponds to the Miravetes Formation (van Veen, 1966).

The entire section Ag1 extends from the lower Hauterivian (*Lyticoceras nodosoplicatum* AZ) up to the lower Barremian (*Kotetishvilia compressissima* AZ). However, for the present study, we have analysed only a ~40 m thick interval embracing the uppermost Hauterivian (*Pseudothurmannia ohmi* AZ) and lowermost Barremian (*T. hugii* AZ); i.e., between beds 144 and 193 (Figs. 3 and 4). For a better understanding, we have retained the original bed numbering of Hoedemaeker and Leereveld (1995), also used in most of the subsequent studies on this section.

The lower 8 m of the section (beds 144 to 154), belonging to the *Pseudothurmannia ohmi* ammonite Subzone (ASz) and most of the *Pseudothurmannia mortilleti* ASz, consist of a rhythmic alternance of light gray limestone beds (10–75 cm thick) and dark gray marlstone interbeds (10–65 cm thick). A thin laminated black shale interval occurs at the base of the *Pseudothurmannia mortilleti* ASz (bed 148), which represents the local equivalent of the Faraoni Level (Baudin, 2005; Company et al., 2005; Sauvage et al., 2013; Baudin and Riquier, 2014), a well-known organic-rich horizon that has been recognised within the uppermost Hauterivian sediments in several basins of the western Mediterranean Tethys. It was first described by Cecca et al. (1994a) in the Maiolica Formation of Umbria–Marche Apennines in central Italy, and subsequently documented in southern Alps, and in the Vocontian, Subbetic and Utrahelvetic basins (see Baudin and Riquier, 2014, for references). Its occurrence has been also suggested in other Mediterranean areas as well as outside the Mediterranean domain (Baudin and Riquier, 2014).

The uppermost part of the *P. mortilleti* ASz and the *Pseudothurmannia picteti* ASz (beds 155 to 170b, with a thickness of 15 m) are represented by a predominantly marly interval with yellowish limestone and marly limestone beds (10–45 cm thick) and light grey marlstone layers up to 120 cm thick.

The following 9 m of the section (beds 171 to 182, *T. hugii* ASz) correspond to a more regular succession of yellowish limestone beds (10–45 cm thick) and greyish marlstone interbeds (10–60 cm thick).

Finally, the uppermost 8 m of the section (beds 183 to 192, *Psilotissotia colombiana* ASz) are made of thick marlstone layers (up to 100 cm) alternating with thinner marly limestone beds (10–40 cm thick).

The lithological composition and succession of the complementary sections (Ag4, Ag5, Kv1 and V1) is very similar to that of section Ag1, although with some differences in the relative thicknesses of the intervals. All the five sections can be lithologically and biostrati-

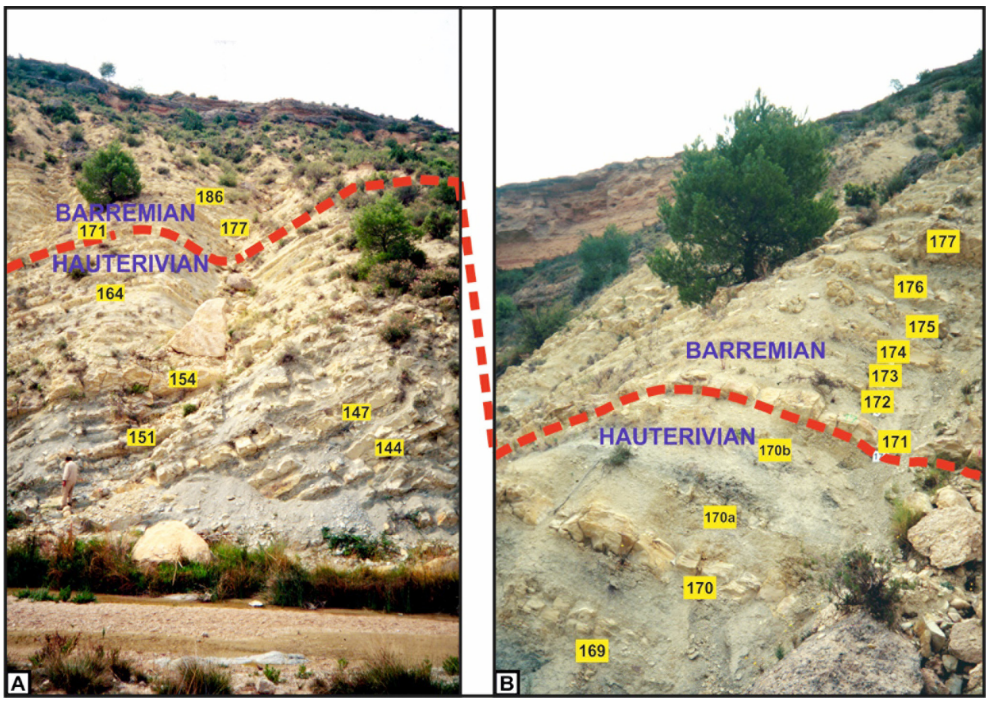

Figure 3. A, General view of section Ag1. B, Detailed view of the beds around the Hauterivian/Barremian boundary in section Ag1.

graphically correlated bed-to-bed (Fig. 4).

Texturally, the sediments composing the lithological successions are mudstones with calcitised radiolarians and scarce foraminifera. The lime fraction is mostly made up of calcareous nannofossil remains (Hoedemaeker and Leereveld, 1995; Gressier, 2010), while clay minerals (illite, smectite, chlorite and kaolinite) are, by far, the main components of the detrital fraction (Moiroud et al., 2012).

Macrofossil remains are common throughout the section, being overwhelmingly dominated by ammonites (>97%), which are accompanied by scarce irregular echinoids, brachiopods, belemnites, bivalves and gastropods. Ammonites are invariably preserved as casts and moulds; any trace of the original shell being absent. Most of the specimens are fairly complete, with phragmocone and body chamber, and even the peristome is fully or partially preserved in many of them. No signs of abrasion, encrustation, bioerosion or any other evidence of a prolonged residence of shells on the sea floor or taphonomic reworking have been detected. Body chambers are, in general, well preserved, although moderately compressed due to diagenetic compaction. Phragmocones are strongly flattened, even collapsed, indicating incomplete or no sediment filling. Irregular lumps or fine linings of limonitised pyrite can be frequently observed in the inner whorls. Most ammonites lie parallel to the bedding surfaces, suggesting a softground, rather than soupground, substrate consistency. All these taphonomic features point to a rapid burial of the shells in a low-energy environment with a relatively high sedimentation rate (Maeda and Seilacher, 1996; Fernández-López, 1997; Fernández-López et al., 2000).

In general, the bioturbation is intense and pervasive. Among the identified ichnotaxa, *Trichichnus*, *Chondrites*, *Thalassinoides* and *Planolites* are largely dominant, although some other traces like *Zoophycos* or *Rhizocorallium* have also been identified (Rodríguez-Tovar and Uchmann, 2017). This assemblage is characteristic of the *Zoophycos* ichnofacies, which has usually been related to lower offshore to bathyal, fine-grained substrates, below the storm wave base and free of turbidity currents (Seilacher, 2007).

Sedimentological, palaeontological, taphonomic and palaeoichnological data indicate that the Río Argos succession was deposited in a stable, distal, low-energy, deep-water marine environment. A several hundred metres depth has been estimated for these deposits (Rey, 1993; Hoedemaeker and Leereveld, 1995; Gea, 2004). Except for the Faraoni Level equivalent interval (FLE), the sediment deposition took place in oxic bottom waters, although dysoxic to anoxic conditions could develop within the sediment. Sedimentation seems to have been continuous throughout the studied interval, since no evidence of interruptions or condensations has been detected.

Protection, Access and Facilities

The Lower Cretaceous succession outcrops along the river Argos are listed in the geosite inventories of the Spanish Geological Survey (IGME) and the Region of Murcia. In the latter it is pointed out that the preservation conditions of the outcrops are optimal and that the risk of deterioration due to anthropic action is low (Arana et al., 2009). Even so, these outcrops have been catalogued as Site of Special Geological Interest in the General Urban Development Plan of the municipality of Caravaca, favouring their conservation and promotion and prohibiting the construction of any building or facility.

The succession of the river Argos is also included in the Archaeological and Palaeontological Chart of the Region of Murcia as a step prior to its declaration as a Site of Cultural Interest with the category of Palaeontological Zone, according to Law 4/2007 on Cultural Heritage of the Region of Murcia. This declaration will imply the prohibition of all types of intervention (works, landfills, quarries, constructions, etc.) except those that are aimed at the scientific study and safeguarding of the outcrops.

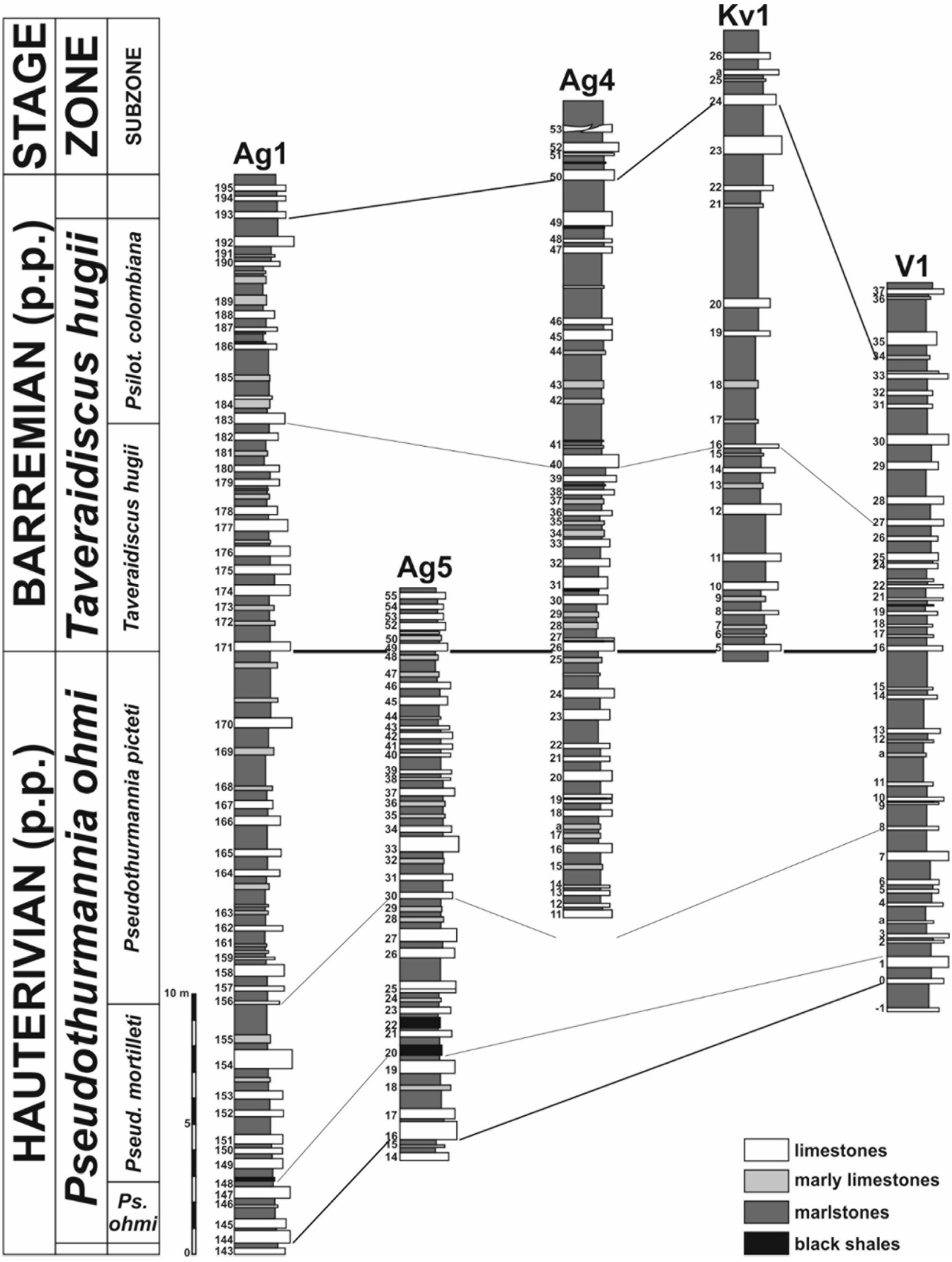

Figure 4. Lithological logs and correlation of the sections studied.

Furthermore, the Spanish Law 42/2007 of Natural Heritage and Biodiversity contemplates that stratotypes can be declared Natural Monuments, so the Río Argos section could enjoy the highest degree of protection.

The section can be reached following the local road between Caravaca and Archivel and then taking the turning to *Molino del Río*, a small countryside hotel that is placed just opposite the section (Fig. 1). The hotel offers accommodation, meals and other tourist services throughout the year, and there is a small parking area next to the entrance of the hotel.

We are currently in contact with officials from the Departments of Culture and Environment of the Region of Murcia and the Caravaca Town Council, and with the specialists in Geological Heritage and Geodiversity from the University of Murcia in order to outline the conditioning, signposting and maintenance of the Río Argos section and its use as a scientific and educational resource.

Biostratigraphy

Ammonites are by far the most abundant group of macrofossils in the Río Argos section and also the most useful for biostratigraphically characterising the Hauterivian–Barremian boundary. Among the other macroinvertebrates, only the belemnites have been shown to have a certain biochronological value. Other macroinvertebrates are very infrequent and have not been studied in detail. Among microfossils, calcareous nannofossils, foraminifera, and organic walled dynocists provide valuable information, while radiolarians, although frequent, are calcitised and impossible to determine.

Ammonites

Ammonite faunas are particularly rich, diversified and well preserved throughout the uppermost Hauterivian–lowermost Barremian interval in the Río Argos succession. First identified by van Veen (1966, 1969), these faunas and their stratigraphic distribution have been analysed in detail in several subsequent papers (Hoedemaeker, 1992, 1995, 2013; Hoedemaeker and Leereveld, 1995; Company et al., 2002, 2003, 2005, 2010; Vašíček and Hoedemaeker, 2003; Martinez et al., 2012). These studies have contributed decisively to the development and refinement of the Mediterranean standard ammonite zonal scheme proposed by the former Lower Cretaceous Cephalopod Team (Hoedemaeker and Bulot, 1990; Hoedemaeker et al., 1993) and the current Lower Cretaceous Ammonite Working Group (Hoedemaeker et al., 2003; Reboulet et al., 2009, 2018; Szives et al., 2023) for the latest Hauterivian and the earliest Barremian.

For the present study, the GSSP (section Ag1) and the four complementary sections (Ag4, Ag5, Kv1 and V1) were systematically sampled bed-by-bed. Almost 4000 ammonites were collected (more than 1000 from section Ag1), most of them being well enough preserved to be identified at the species level. They are housed in the palaeontological collections of the University of Granada. All these ammonites correspond to typical Mediterranean taxa. The analysis of their stratigraphic distribution has enabled us to accurately characterise the uppermost Hauterivian *P. ohmi* AZ and the lowermost Barremian *T. hugii* AZ of the standard zonation (Szives et al., 2023) in the sections studied (Figs. 4 and 5).

As stated above, the members of the Barremian Working Group decided to recommend drawing the lower boundary of the Barremian Stage at the base of the *T. hugii* AZ (Rawson et al., 1996). This zone had been introduced by Busnardo (1984) without formally defining its boundaries. It was in the first zonal scheme adopted by the Lower Cretaceous Cephalopod Team (Hoedemaeker and Bulot, 1990) where the lower boundary of the *T. hugii* Zone was defined by the FO of the index species (see also Company et al., 1995).

The first specimens of *T. hugii* (Fig. 6) have been recorded in bed 171 of section Ag1, and in a strictly equivalent stratigraphic position in the four complementary sections. It is a fairly common species, which extends throughout its nominal zone and reaches the lower part of the *Kotetishvilia nicklesi* AZ, although its acme is restricted to the beginning of its stratigraphic range. According to our interpretation (Company et al., 2006, 2008), the nominal species *Taveraidiscus oosteri* and *Taveraidiscus alcoyensis* can be considered synonyms of *T. hugii*. As thus conceived, the index species is quite uniform and easily identifiable, showing a certain variability in the strength of ornamentation, from very densely and finely ribbed specimens (morphotype *oosteri*) to others, such as the lectotype of the species, with moderately thicker and less dense ribs. The geographic distribution of *T. hugii* extends along the northern margin of the Mediterran–Caucasian subrealm (*sensu* Westermann, 2000), having been reported from Spain, France, Italy, Switzerland, Austria, Hungary, Slovakia, Romania, Bulgaria, Crimea and Georgia (see references in Klein, 2005). In the Betic Cordillera it is present both in pelagic and neritic settings.

In addition to the primary marker, several other ammonite events relevant to the characterisation of the Hauterivian–Barremian boundary have been recorded in the sections studied. One of them is the FO of *Taveraidiscus intermedius* (Fig. 7A). This highly variable species (herein considered a senior synonym of *Taveraidiscus heeri*, *T. kiliani*, *T. querolensis* and *T. vandeckii*) is a close relative of *T. hugii*, from which it differs in its more evolute and inflated shell, and the presence of constrictions from an earlier ontogenetic stage. In general, the FO of *T. intermedius* coincides with that of *T. hugii*, but in some sections its appearance slightly predates that of the index species. Such is the case with section Ag1, where the FO of *T. intermedius* has been recorded in bed 170.

As mentioned above, the genus *Pseudothurmannia* played an important role in the historical debate on the Hauterivian–Barremian boundary. This genus dominates the assemblages of the uppermost Hauterivian *P. ohmi* AZ. The successive FOs of the species *P. ohmi* (Fig. 7B) (bed 144 in section Ag1), *P. mortilleti* (Fig. 7C) (herein regarded as a senior synonym of *P. catulloi*) and *P. pseudomalbosi* (Fig. 7D) (bed 148), and *P. picteti* (Fig. 7E) (bed 156) mark the base of the three subzones of the zone. The last occurrence (LO) of the genus takes place in bed 160, i.e. well below the base of the Barremian. This event is traceable in the same stratigraphic position in the complementary sections Ag4, Ag5 and V1, as well as in systematically sampled sections in SE France (Busnardo and Vermeulen, 1986; Vermeulen, 2005; Busnardo et al., 2013; Vermeulen et al., 2018) and Switzerland (Busnardo et al., 2003). This strongly contrasts with the observations by Hoedemaeker (1995, 2013), who placed the LO of the genus *Pseudothurmannia* within the *T. hugii* AZ in the Río Argos succession. This and other discrepancies between Hoedemaeker's data and ours may

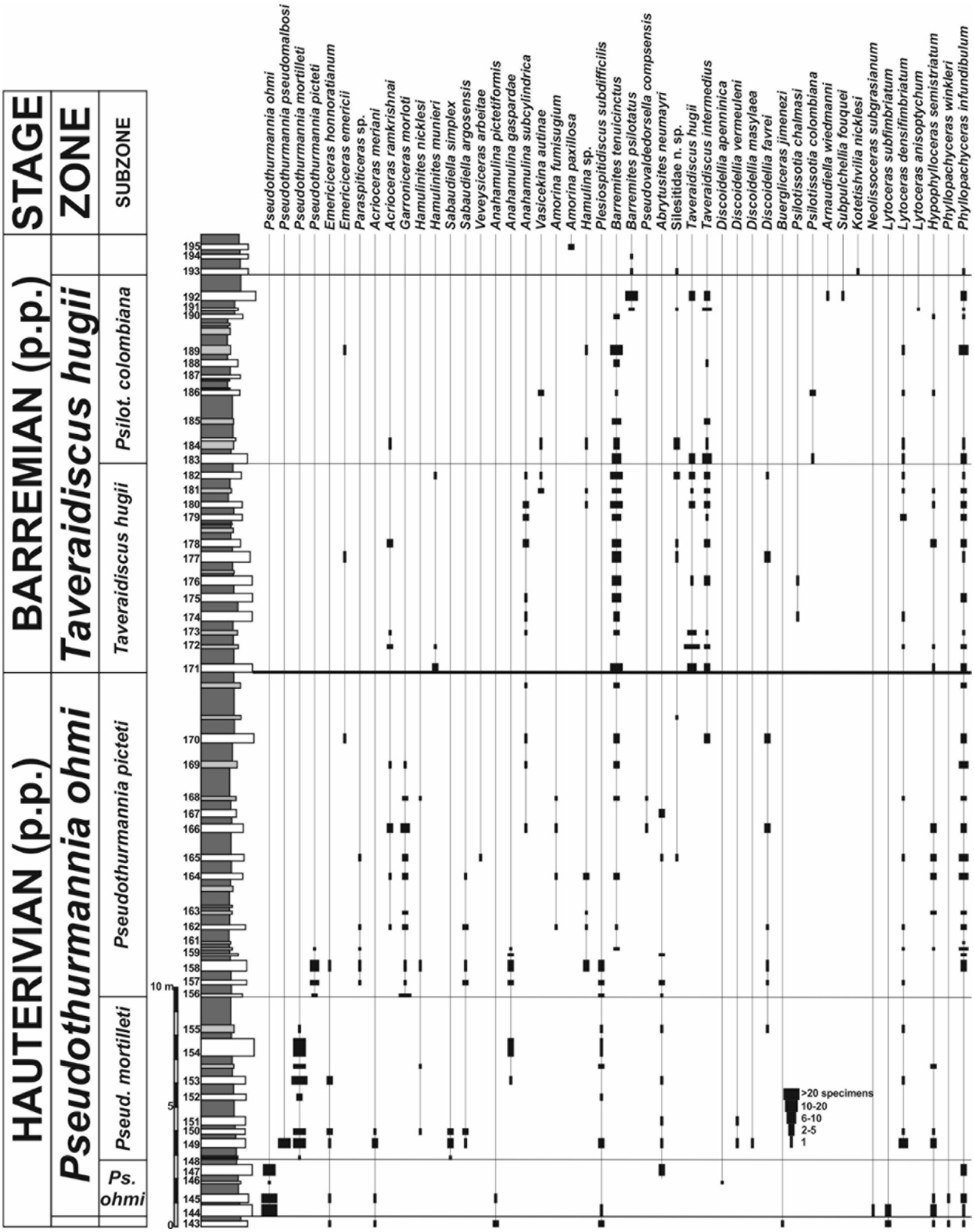

Figure 5. Ammonite stratigraphic distribution and zonation in the Río Argos section.

be due to problems in the bed numbering system used by our colleague. Hoedemaeker (2013, p. 3) indicated that the bed numbers of his sections C–K corresponded to those of section A. However, we have detected some errors in the bed-to-bed equivalences assumed by

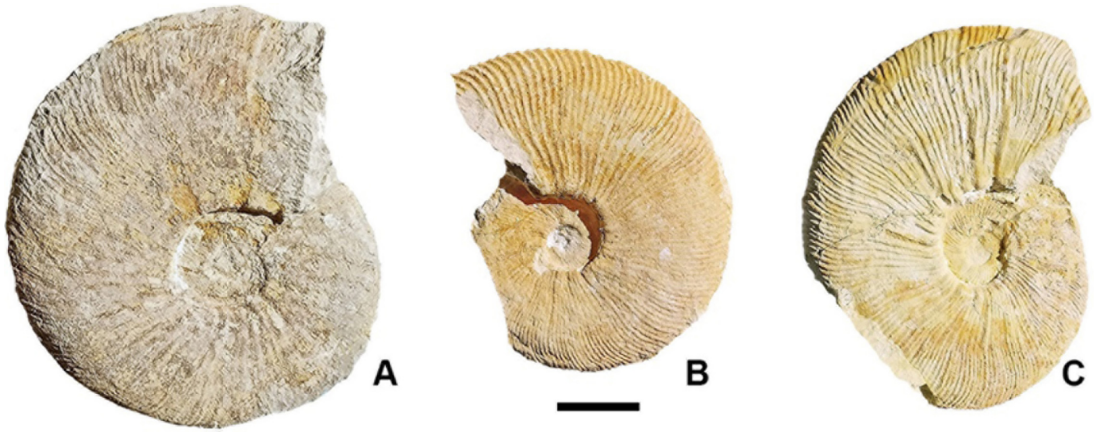

Figure 6. Three specimens of Taveraidiscus hugii showing the morphological variability of the species: A, specimen X.Ag1.172.55; B, specimen X.Ag1.172.29; C, specimen X.Ag4.28.104. Scale bar = 1 cm.

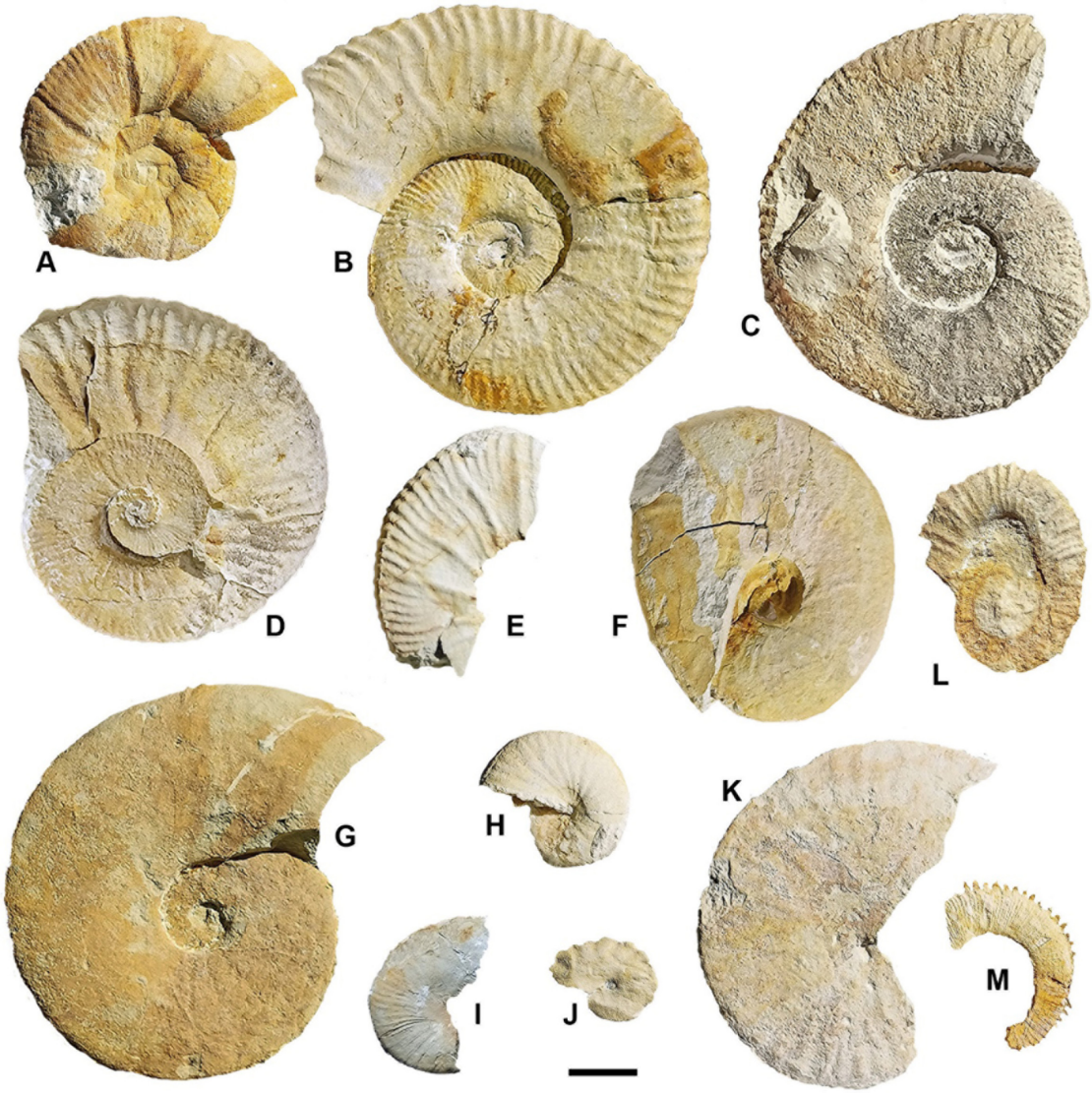

Figure 7. Other relevant ammonite species: A, Taveraidiscus intermedius. specimen X.Ag1.176.1; B, Pseudothurmannia ohmi, specimen X.Ag5.19r.1; C, Pseudothurmannia mortilleti, specimen X.Ag1.150.36; D, Pseudothurmannia pseudomalbosi, specimen X.V1.3.66; E, Pseudothurmannia picteti, specimen X.Ag1.158.1; F, Plesiospitidiscus subdifficilis, specimen X.V1.-2.22; G, Barremites tenuicinctus, specimen X.Ag1.181.3; H, Psilotissotia chalmasi, specimen X.V1.19.160; I, Psilotissotia colombiana, specimen X.Ag4.47.12; J, Kotetishvilia nicklesi, specimen X.Ag4.50.30; K, Discoidellia favrei, specimen X.Ag1.162.1; L, Sabaudiella argosensis, specimen X.Ag1.158.27; M, Garroniceras morloti, specimen X.Ag1.164.29. Scale bar = 1 cm.

Hoedemaeker for these sections, which could explain the differences in the stratigraphic position of some events.

Another event also used by some authors (Busnardo, 1965a; Busnardo and Vermeulen, 1986) to mark the base of the Barremian is the phylogenetic replacement of the genus *Plesiospitidiscus* (Fig. 7F) by *Barremites*. The first representatives of this latter genus, that can be ascribed to the species *B. tenuicinctus* (Fig. 7G), occur in bed 160 of the section, coinciding with the last specimens of *Pseudothurmannia*. They are not very frequent in the uppermost Hauterivian beds, but become common, even abundant, in the basal Barremian. The FO of *Barremites* has been recorded in an analogous stratigraphic level in the Angles (Busnardo and Vermeulen, 1986) and Veveyse de Châtel-Saint-Denis (Busnardo et al., 2003) sections.

Pulchelliids also provide secondary markers that may help to constrain the boundary position. One of them is the FO of *Psilotissotia chalmasi* (Fig. 7H), recorded in bed 174, slightly above the base of the Barremian, and in a position equivalent to that in the Angles section (referred as *P. mazuca* in Vermeulen, 2003, 2005). The FO of *Psilotissotia colombiana* (Fig. 7I), which defines the base of the upper subzone of the *T. hugii* Zone in the Mediterranean standard zonation, takes place in bed 183. *Kotetishvilia nicklesi* (Fig. 7J), the index species of the second zone of the Barremian, first appears in bed 193. Another interesting pulchelliid is *Discoidellia favrei* (Fig. 7K), a species that straddles the Hauterivian–Barremian boundary, having its FO in the upper part of the *P. mortilleti* ASz (bed 155), and its LO around the boundary between the *T. hugii* and *P. colombiana* ASzs (bed 182), in accordance with its stratigraphic range recorded in SE France (Vermeulen, 2005; Vermeulen et al., 2018). It should be noted, however, that the low frequency and the restricted geographical distribution of these species, known only from the western Mediterranean area, considerably limit their correlation potential.

Finally, it is worth mentioning two heteromorph species, which are common in the uppermost Hauterivian, and whose LOs are recorded near the boundary. They are *Sabaudiella argosensis* (Fig. 7L), which ranges from the base of the *P. mortilleti* ASz (bed 149) up to the middle part of the *P. picteti* ASz (bed 164), and *Garronicer as morloti* (Fig. 7M) (probably, a senior synonym of "*Holcodiscus*" *evolutus*), a species strictly confined to the *P. picteti* Subzone (beds 156–169).

Belemnites

Janssen (1997) described and figured part of the belemnite fauna collected from beds around the Hauterivian–Barremian boundary in the Río Argos section, and calibrated its stratigraphic distribution with the ammonite zonation. From this paper and additionally collected specimens, combined with the herein revised bed-to-bed correlation of the Río Argos sections (see above), the following main belemnite bio-events around the Hauterivian–Barremian boundary could be recognized: the LO of *Duvalia dilatata* at the boundary between the *P. mortilleti* and *P. picteti* ASzs (beds 154–158), the FO of *D. silesiaca* in the upper part of the *T. hugii* AZ (bed 188), and the FO of *Duvalia pontica* in the succeeding *K. nicklesi* AZ (bed 195). Other components of the uppermost Hauterivian include so far undescribed duvalids in the *P. mortilleti* and *Ps. picteti* ASzs (beds 151–167) and the abundant occurrence of *Hibolites* gr. *subfusiformis*. The latter can be found regularly up to lowermost part of the *T. hugii* AZ, eventually being replaced by *Hibolites jaculiformis*. Comparable associations have been reported from other areas of the Mediterran–Caucasian subrealm (see references in Janssen and Főzy, 2004, 2005; Janssen et al., 2012).

Calcareous Nannofossils

The calcareous nannofossil biostratigraphy and assemblage composition of sections Ag1 and V1 have been reported and analysed in Aguado et al. (2014) and Martinez et al. (2020). Calcareous nannofossils were investigated in 43 marlstone samples from section Ag1 and 38 from section V1 (Figs. 8 and 9), taken irregularly spaced. In addition, 15 samples were studied from section Ag5 (between beds 19 and 25) in order to detect the LO of *Lithraphidites bollii*. Finally, in Martinez et al. (2020), a set of 30 additional samples were studied in section V1 to gain precision in the location of FOs and LOs of biostratigraphic markers. For details about sample preparation and analysis we refer to Aguado et al. (2014) and Martinez et al. (2020).

A total of 62 taxa were identified (Figs. 8 and 9), and photomicrographs of the most representative of them are shown in Figs. 10 and 11. The nannofossil total abundance fluctuates from 2.4 nannofossils/field of view (n/fv) in average for section Ag1 to 6 n/fv in average for section V1, and preservation varies from moderate or moderate to poor (sections Ag1 and Ag5) to moderate to good (section V1).

Assemblages are composed of mainly cosmopolitan and Tethyan taxa (Figs. 8–11). They are dominated by the genera *Watznaueria* (14%–58%, average 39%), *Nannoconus* (9%–51%, average 26%) and *Micrantholithus* (2%–26%, average 12%). Other common taxa are *Assipetra terebrodentarius*, *Biscutum constans*, *Diazomatolithus lehmanii*, *Discorhabdus ignotus*, *Lithraphidites carniolensis*, *Rhagodiscus asper* and small *Zeugrhabdotus* (including *Z. noeliae*, and *Z. trivectis*).

Biostratigraphically, the complete interval studied in sections Ag1 and V1 (Figs. 8 and 9) and also in section Ag5 is assigned to the NC5 Zone of Bralower et al., (1995), based on the absence of the taxa *Cruciellipsis cuvillieri* and *Hayesites irregularis*. *Assipetra terebrodentarius* and *Lithraphidites bollii* are present from the lowermost samples in sections Ag1 and V1, and allow the assignment of these levels to the NC5B Subzone (Bralower et al., 1995; Company et al., 2005; Aguado et al., 2008, 2014; Fig. 12). Following Bralower et al. (1995), the LO of *L. bollii* marks the boundary between NC5B and NC5C subzones. In the studied sections (Tables 1 and 2), *L. bollii* is rare, but consistently recorded, along their lower part. The LO of *L. bollii* was recorded in sample 148b, at the base of FLE (Aguado et al., 2014; Fig. 12), in section Ag1, and in a similar position in sections Ag5 and V1 (Martinez et al, 2020; Fig. 12). These results are consistent with those obtained by Baudin et al., (1999) who observed the LO of *L. bollii* within the lower part of the FLE at Vergons (SE France). In most of the other previous literature, the LO of this species with respect to the position of the FLE is not clearly indicated (Cecca et al., 1994b; Bersezio et al., 2002; Godet et al., 2006), or located below (Channell et al., 1995; Coccioni et al., 1998; Bellanca et al., 2002; Tremolada et al., 2009) or above it (Channell et al., 1995; Erba et al., 1999).

The LO of *Calcicalathina oblongata* was used to separate the NC5C and NC5D subzones by Bralower et al. (1995), and the CC5

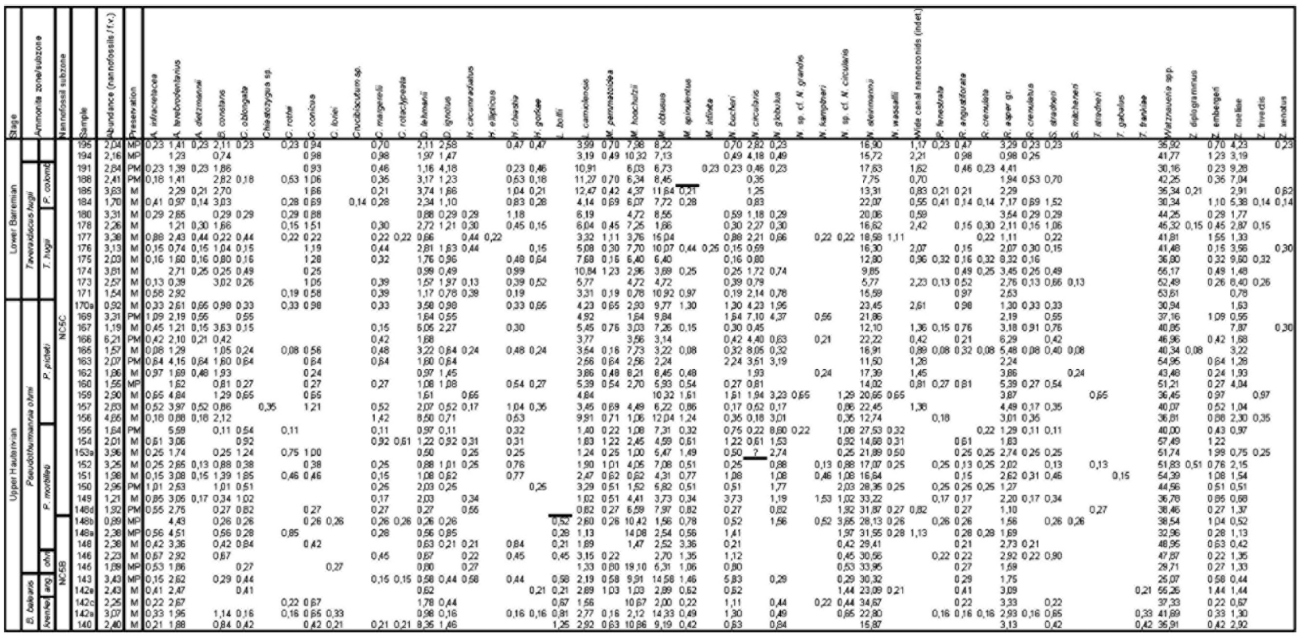

Figure 8. Range table showing percentage abundances for all calcareous nannofossil taxa recorded from section Ag1 and their correlation to ammonite zones. A minimum of 300 specimens per sample were counted for percentage determination (see Aguado et al., 2014 for details). Nannofossil zonation according to Bralower et al. (1995). Preservation (Roth and Thierstein, 1972): P=Poor; PM=Poor to moderate; MP=Moderate to poor; M=Moderate; MG=Moderate to good; G=Good. Watznaueria spp. includes: W. barnesiae, W. biporta, W. cynthae, W. fossacincta, and W. ovata. Solid black horizontal lines indicate stratigraphically relevant bioevents (FOs and LOs of key species).

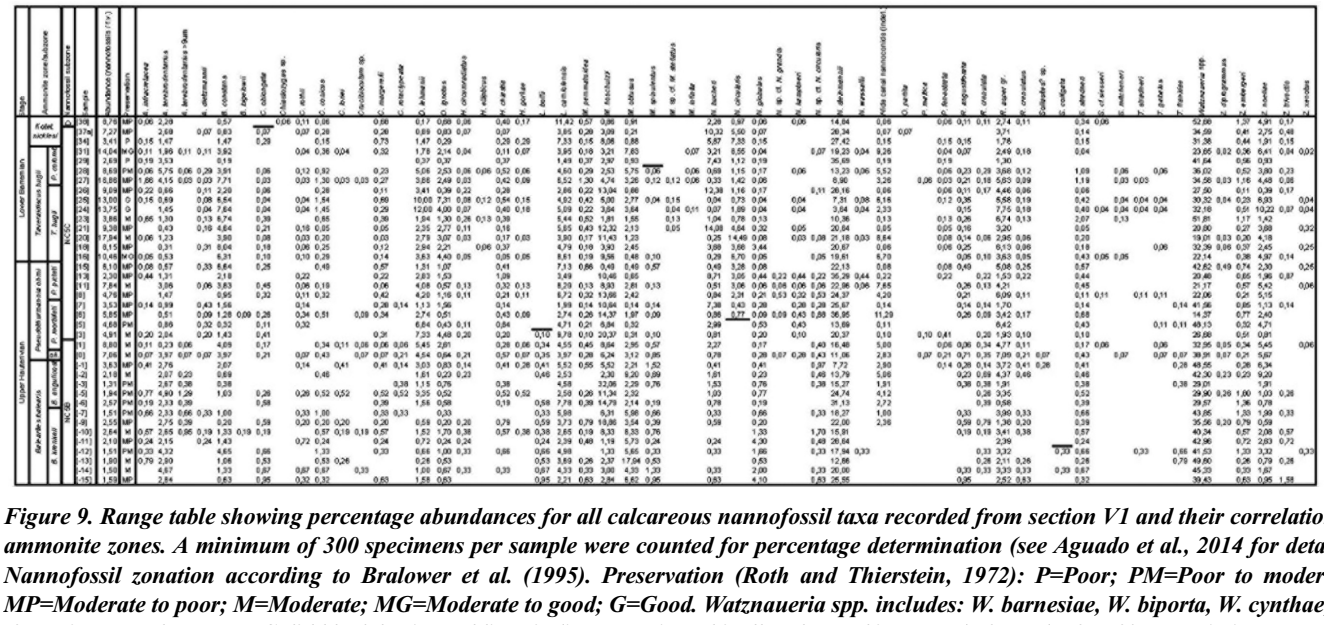

Figure 9. Range table showing percentage abundances for all calcareous nannofossil taxa recorded from section V1 and their correlation to ammonite zones. A minimum of 300 specimens per sample were counted for percentage determination (see Aguado et al., 2014 for details). Nannofossil zonation according to Bralower et al. (1995). Preservation (Roth and Thierstein, 1972): P=Poor; PM=Poor to moderate; MP=Moderate to poor; M=Moderate; MG=Moderate to good; G=Good. Watznaueria spp. includes: W. barnesiae, W. biporta, W. cynthae, W. fossacincta, and W. ovata. Solid black horizontal lines indicate stratigraphically relevant bioevents (FOs and LOs of key species).

and CC6 zones by Sissingh (1977) and Perch-Nielsen (1985). This bioevent lies above the last studied samples in the section Ag1 (corresponding to the lowermost part of the *K. nicklesi* AZ), and has been recorded in the uppermost part of the *K. nicklesi* AZ in section V1 (Martinez et al., 2020; Fig. 12).

According to all this, the NC5B and NC5C nannofossil subzones were identified in the studied interval of the Ag1 section, and NC5B, NC5C, and basal part of the NC5D subzones in the studied interval of section V1 (Fig. 12). The Hauterivian–Barremian boundary falls in the middle part of the NC5C subzone.

In addition, following the zonations proposed by Sissingh (1977) and Perch-Nielsen (1985) the interval studied in Ag1 section can be assigned to the CC5 Zone based on the absence of *Speetonia colligata* and the presence of *Calcicalathina oblongata*. As the LOs of *S. colligata* (sample -12) and *C. oblongata* (sample 37a) are recorded in V1 section, the uppermost part of CC4, CC5, and basal part of CC6 zones can be identified.

Coccioni et al. (1998) reported the presence of ‘large *Zeugrhabdotus*

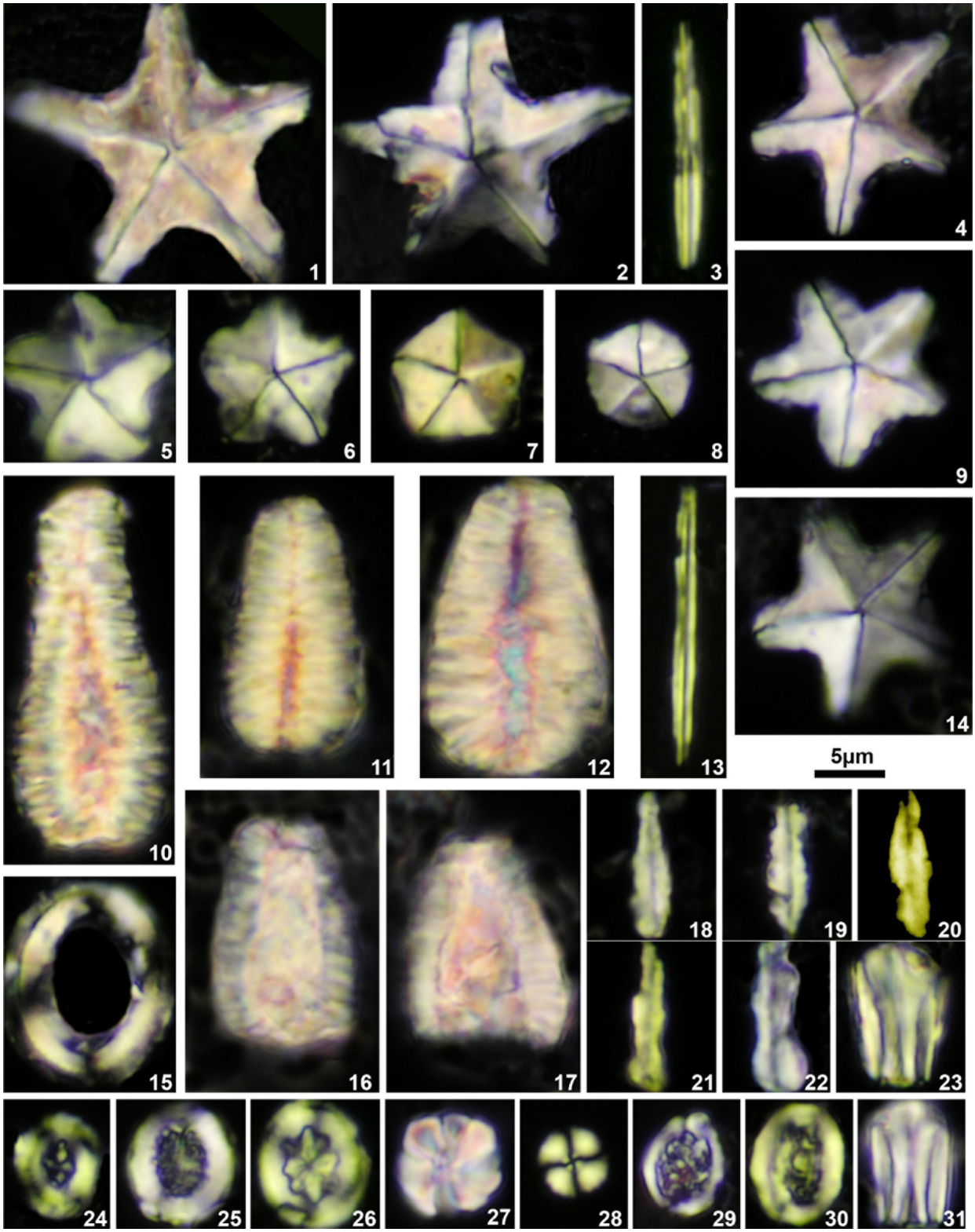

Figure 10. Light micrographs of the most relevant nannofossil taxa found throughout the study interval. All micrographs under cross-polarized light. (1, 2, 4, 9, 14) Micrantholithus spinulentus: 1, paratype, sample Ag5.20.2; 2, sample Ag1.157; 4, holotype, sample V1.-7; 9, sample V1.0; 14, paratype, sample V1.1. (3, 13) Lithraphidites carniolensis: 3, sample V1.25; 13, sample Ag1.184. (5, 6) Micrantholithus obtusus: 5, sample V1.25; 6, sample V1.0. (7, 8) Micrantholithus hoschulzii: 7, sample V1.0; 8, sample Ag5.20.2. (10) Nannoconus bermudezii, sample V1.-10. (11, 12) Nannoconus steinmannii: 11, sample V1.6; 12, sample V1.-9. (15) Manivitella pemmatoidea, sample V1.1. (16, 17) Nannoconus kamptneri: 16, sample V1.6; 17, sample V1.11. (18-22) Lithraphidites bollii: 18, 19, sample V1.1; 20, sample Ag1.137; 21, sample V1.-2; 22, sample Ag1.148.1. (23, 31) Conusphaera rothii: 23, sample Ag1.180; 31, sample V1.-1. (24) Helenea chiastia, sample V1.25. (25) Cretarhabdus conicus, sample V1.6. (26) Retecapsa angustiforata, sample V1.25. (27) Assipetra terebrodentaria, sample V1.24. (28) Cyclagelosphaera margerelii, sample Ag1.188. (29, 30) Rhagodiscus asper: 29, sample V1.1; 30, sample Ag1.184.

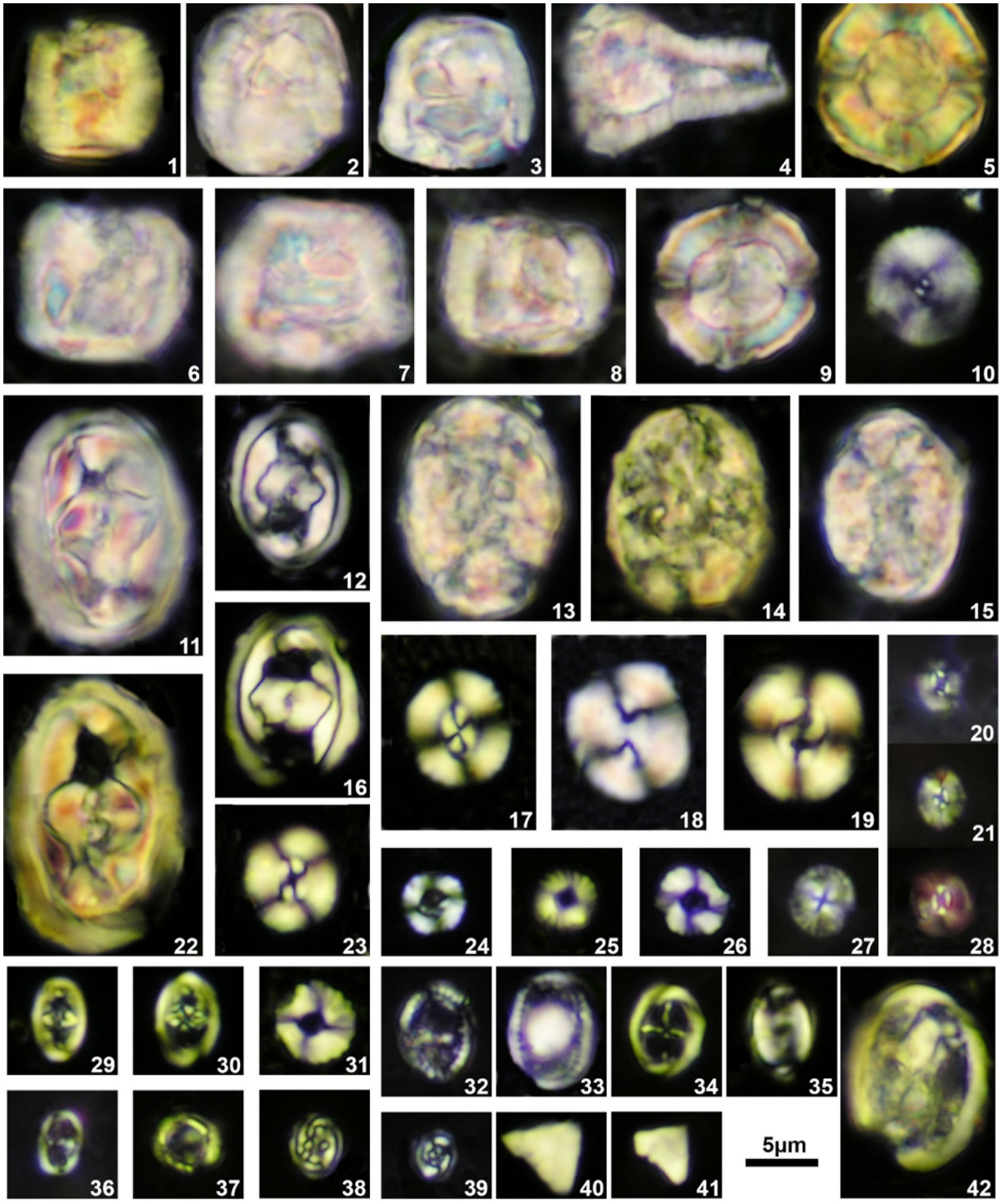

Figure 11. Light micrographs of the most relevant nannofossil taxa found throughout the study interval. All micrographs under cross-polarized light. (1–3) Nannoconus sp. cf. N. circularis: 1, sample V1.1; 2, sample V1.6; 3, sample V1.16. (4) Nannoconus wassallii, sample V1.28. (5) wide canal nannoconid (apical view), sample Ag5.20.4. (6-9), Nannoconus circularis: 6, sample V1.20; 7, sample V1.16; 8, sample V1.11; 9, sample V1.11, apical view. (10) Haqius circumradiatus, sample V1.40. (11, 12, 16, 22) Zeugrhabdotus embergeri: 11, 22, very large specimens, samples V1.-2 and Ag1.178; 12, 16, normal size specimens, samples V1.-9 and Ag5.20.3. (13-15) Calcicalathina oblongata: 13, sample V1.0; 14, sample V1.-9; 14, sample V1.16. (17, 23) Watznaueria barnesiae: 17, sample V1.24; 23, sample Ag1.184. (18, 19) Watznaueria biporta: 18, sample V1.24; 19, sample Ag1.184. (20, 21, 28) Biscutum ellipticum: 20, sample V1.1; 21, sample V1.16; 28, sample Ag1.184. (24-26, 31) Diazomatolithus lehmanii: 24, sample Ag5.20.1; 25, sample V1.0; 26, sample V1.11; 31, sample V1.16. (27) Discorhabdus ignotus, sample V1.24. (29, 30) Zeugrhabdotus noeliae: 29, sample V1.-1; 30, sample V1.0. (32) Podorhabdus gorkae, sample V1.28. (33) Axopodorhabdus dietzmannii, V1.11. (34) Staurolithites siesseri, sample Ag1.188. (35) Percivalia fenestrata, sample Ag1.148.2. (36) Zeugrhabdotus erectus, sample Ag1.184. (37) Rotelapillus laffittei, sample Ag1.184. (38, 39) Staurolithites mitcheneri: 38, sample Ag1.148.2; 39, sample V1.40. (40, 41) Micrantholithus hoschulzii, isolated elements, sample V1.1. (42) Mitosia infinita, sample V1.24.

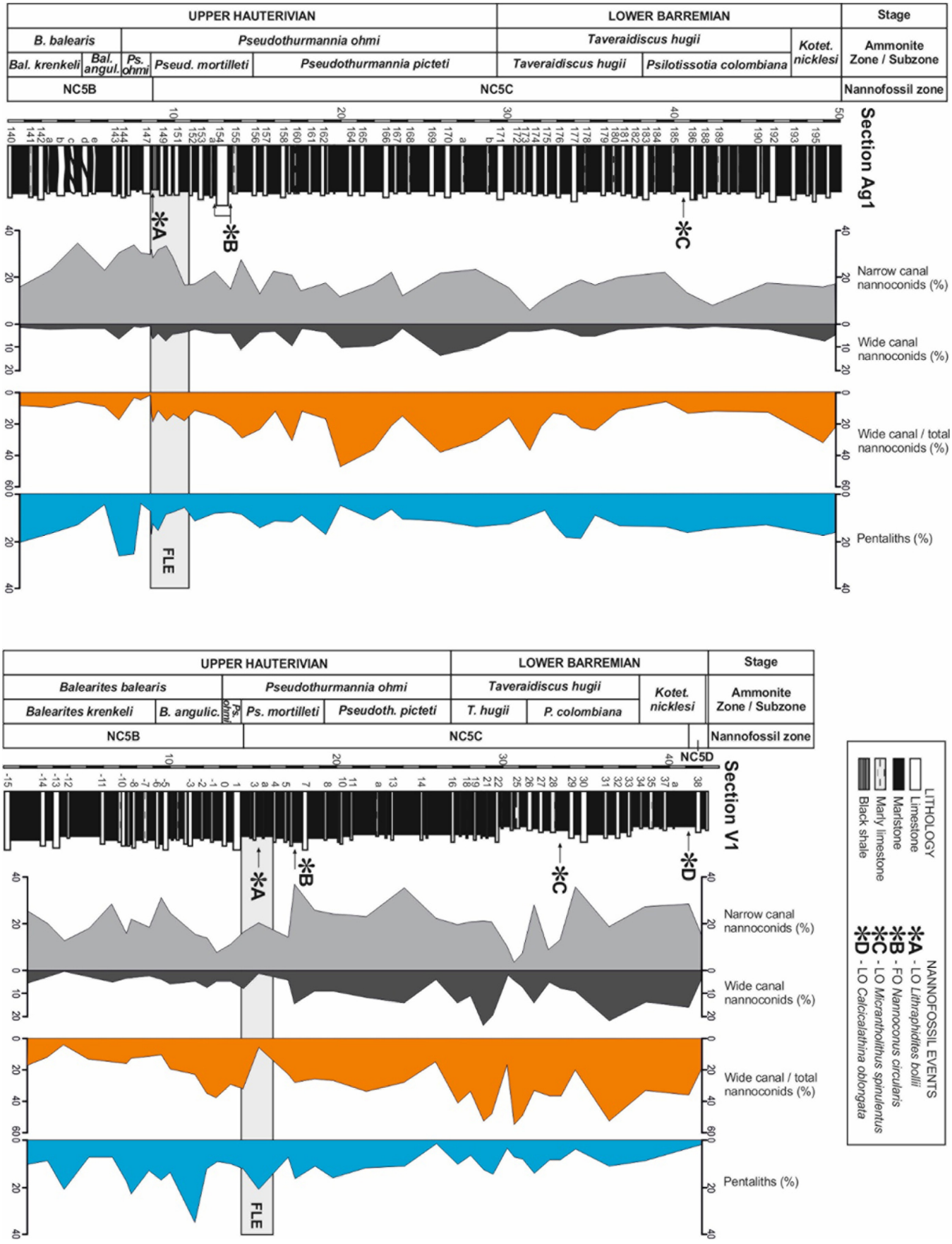

Figure 12. Fluctuations in the percentage abundances of nannoconids and pentaliths derived from the quantitative study in sections Ag1 and V1 (see text for details). The most relevant nannofossil events are also marked.

embergeri' within the levels of the Faraoni Level in the Fiume Bosso section. We have also found large to very large (14–20 μm) specimens of *Z. embergeri* (Fig. 11.11, 11.22) in all sections, but they were found scattered along the study interval and not restricted to the FLE.

As mentioned above, *Micrantholithus* is a major constituent of the late Hauterivian–early Barremian nannofossil assemblages in the studied sections. Our results show a discrete peak in the abundance of *Micrantholithus*, reaching percentages greater than 25–35%, within the upper part of the *Balearites angulicostatus* ASz and the *P. ohmi* ASz (Company et al., 2005; Aguado et al., 2008, 2014; Fig. 12). This event probably corresponds with the 'pentalith acme' reported by some previous authors below the FLE (Erba et al., 1999; Channell et al., 2000; Bellanca et al., 2002; Bersezio et al., 2002; Tremolada et al., 2009). *Micrantholithus spinulentus*, a species characterised by its very large size (14–25 μm) and deeply indented sides resulting in medium to long free rays (Aguado, 1994; Company et al., 2005; Aguado, 2012; Aguado et al., 2014; Figs. 10.1, 10.2, 10.4, 10.9, 10.14), was found from the base of the studied interval, and its LO was recorded in both Ag1 and V1 sections in the middle part of the *P. colombiana* ASz (Figs. 8, 9 and 12).

Our results also show that there are some fluctuations in the composition of the nannoconid assemblages throughout the studied interval (Company et al., 2005; Aguado et al., 2008, 2014). The most conspicuous change consists in an increase in the abundance of the wide canal nannoconid group (*Nannoconus bucheri*, *N. circularis*, *N. globulus*, *N. grandis*, *N. kamptneri*, *N.* sp. cf. *N. circularis*) compared to the narrow canal nannoconid group (*N. bermudezii*, *N. steinmannii*). This increase initiates below the FLE, in the uppermost part of the *B. angulicostatus* ASz and extends throughout the *P. ohmi* and *P. picteti* ASzs, having been identified in both Ag1 and V1 sections (Fig. 12). A group of *Nannoconus* characterised in side view by a very wide canal and thin and parallel walls, but being higher than wide (Figs. 11.1–11.3), were found throughout the *B. krenkeli–T. hugii* ASzs interval. These forms differ from the holotype of *N. circularis* (Déres and Achériteguy, 1980) and are reported here as *Nannoconus* sp. cf. *N. circularis*. The FO of typical *N. circularis* (forms as wider as high in side view, and similar to the holotype, Figs. 11.6–11.9) was recorded, in both sections, slightly above the FLE within the upper part of the *P. mortilleti* ASz (Company et al., 2005; Aguado et al., 2008, 2014; Fig. 12).

Our biostratigraphic results, and those derived from the quantitative analysis, are consistent between the three sections studied (Ag1, Ag5 and V1). Most of these results are also consistent with previous data from the upper Hauterivian–lower Barremian interval in Italy (Cecca et al., 1994b; Channell et al., 1995; Coccioni et al., 1998; Erba et al., 1999; Bersezio et al., 2002; Bellanca et al., 2002; Tremolada et al., 2009), SE France (Baudin et al., 1999) and some German sections (Mutterlose, 1989). The presence of *Micrantholithus spinulentus* as a taxon characterising the late Hauterivian to earliest Barremian interval, is documented for the first time in the sections studied (Company et al., 2005; Aguado et al., 2008, 2014; Aguado, 2012).

Foraminifera

Foraminifera from both marlstone and limestone layers of section Ag1 were investigated in a total of 139 samples collected bed-by-bed from bed 124 to interbed 195–196. This interval spans from the base of the upper Hauterivian *Balearites balearis* AZ, to the lower part of the lower Barremian *K. nicklesi* AZ (Hoedemaeker and Leereveld, 1995, Company et al., 2003).

All studied samples contain foraminifera. Their abundance fluctuates from rare to abundant. Their preservation varies from very poor to quite good, and specimens are mainly recrystallized and the original walls are not preserved. Planktonic foraminiferal diversity is moderately low (up to eighteen species) throughout. Benthic foraminifera usually occur in higher abundances and diversity when compared to the planktonic counterpart. Zonal marker species and some significant species have been imaged using SEM and are illustrated in Figures 13 to 15.

Planktonic foraminifera

Detailed studies on the stratigraphic distribution of planktonic foraminifera in the Río Argos succession were published by Coccioni and Premoli Silva (1994) and Coccioni et al. (2004, 2006, 2007). Here the planktonic foraminiferal zonation of Coccioni (2020) is followed.

According to the previous investigations mentioned above, *Hedbergella infracretacea* (reported as *Hedbergella delrioensis* in Coccioni and Premoli Silva, 1994) is already present in the lowermost sample. Consequently, the lower boundary of the *H. infracretacea* Zone lies below the base of the interval here considered. Higher in the succession, the FOs of *Lilliputianella semielongata* and *Lilliputianella roblesae* are recognized in bed 138, in the upper part of the *Balearites binelli* ASz (Company et al., 2003).

The FO of *L. semielongata* marks the base of the *L. semielongata* Zone and has been reported from the same stratigraphic position in the Angles (Coccioni et al., 2007) and the Arroyo Gilico sections (Premoli Silva et al., 2018). The upper boundary of this zone is marked by the FO of *Lilliputianella similis*, which has been recorded in interbed 198–199 in the Río Argos section, within the *K. nicklesi* AZ, slightly above the top of the studied interval (Coccioni and Premoli Silva, 1994). Therefore, the Hauterivian–Barremian boundary falls in the middle part of this zone.

The diversity of the assemblages is moderately low, being dominated by species of the genus *Hedbergella* (*H. aptiana*, *H. excelsa*, *H. infracretacea*, *H. laculata*, *H. praetrocoidea* and *H. sigali*) accompanied by *Lilliputianella* (*L. eocretacea, L. pauliani, L. roblesae* and *L. semielongata*), *Favusella hoterivica* and *Globigerinelloides paragottisi.* In addition, high numbers of gorbachikellids occur in the interval between beds 135 and 183, including the FLE. An overall increase in planktonic foraminiferal size (up to 250 μm) occurs at some levels and particularly within the FLE.

The occurrence of *L. eocretacea, L. roblesae* and *L. semielongata* in the lower part of the *L. semielongata* Zone, predating the onset of the Faraoni Episode, represents the first radiation of planktonic foraminifera with radially elongated chambers (Coccioni et al., 2004, 2006, 2007). However, from their first appearance up to the top of the studied interval, subclavate to clavate chambered forms are unevenly distributed and represent only a minor component of the assemblages. Remarkably, records of these morphotypes are scattered and very rare within the FLE.

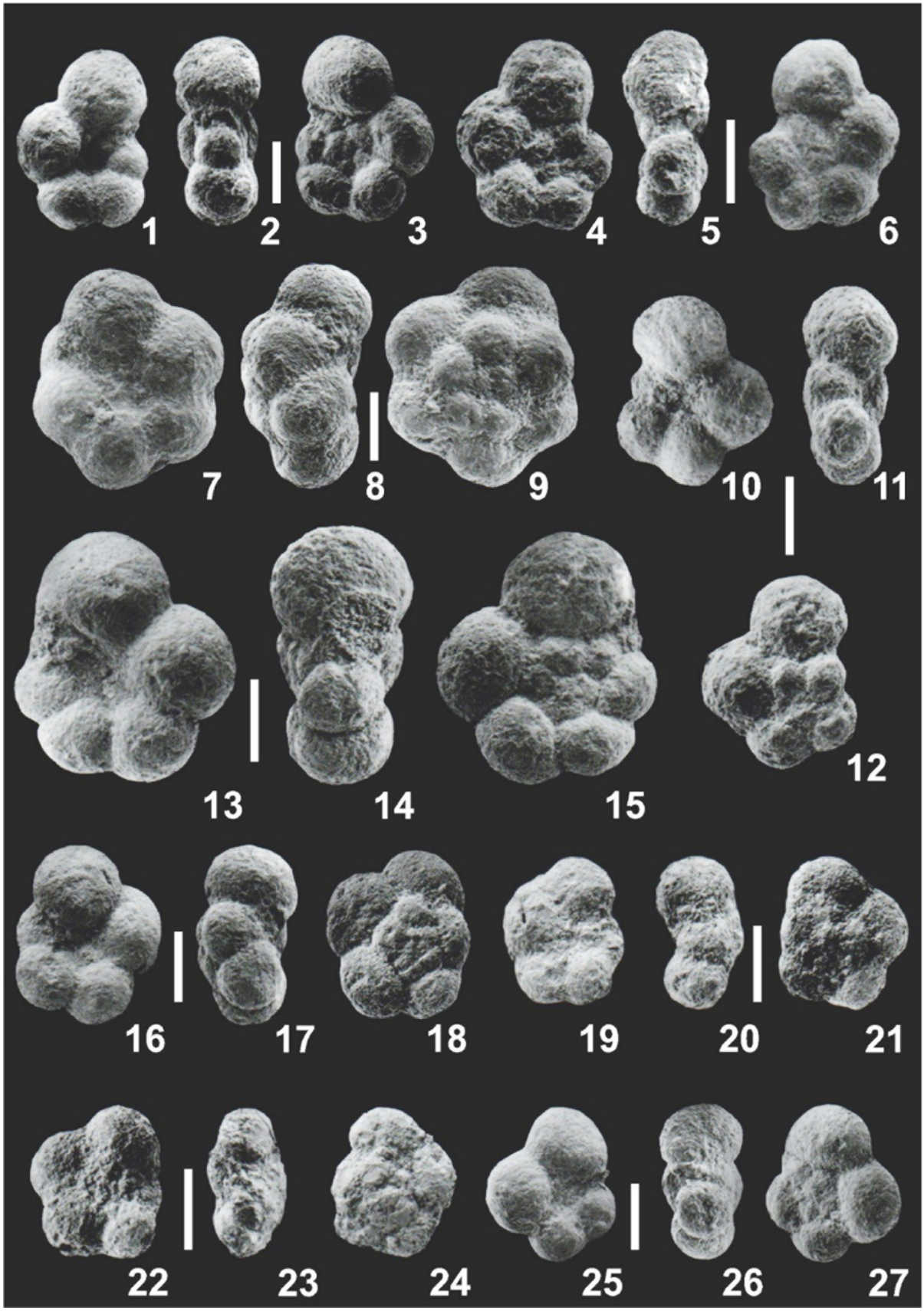

Figure 13. Scanning electron microscope micrographs of selected planktonic foraminiferal taxa. 1-3, Hedbergella aptiana, sample U34-35. 4-6, Hedbergella aptiana, sample V86-87. 7-9, Hedbergella excelsa, sample U28. 10-12, Hedbergella laculata, sample A196-199. 13-15, Hedbergella infracretacea, sample U34-35. 16-18, Hedbergella praetrocoidea, sample V118-119. 19-21, Hedbergella praetrocoidea, sample N47-48. 22-24, Hedbergella praetrocoidea, sample V118-119. 25-27: Hedbergella sigali, sample V118-119, x165. Scale bar = 50 µm.

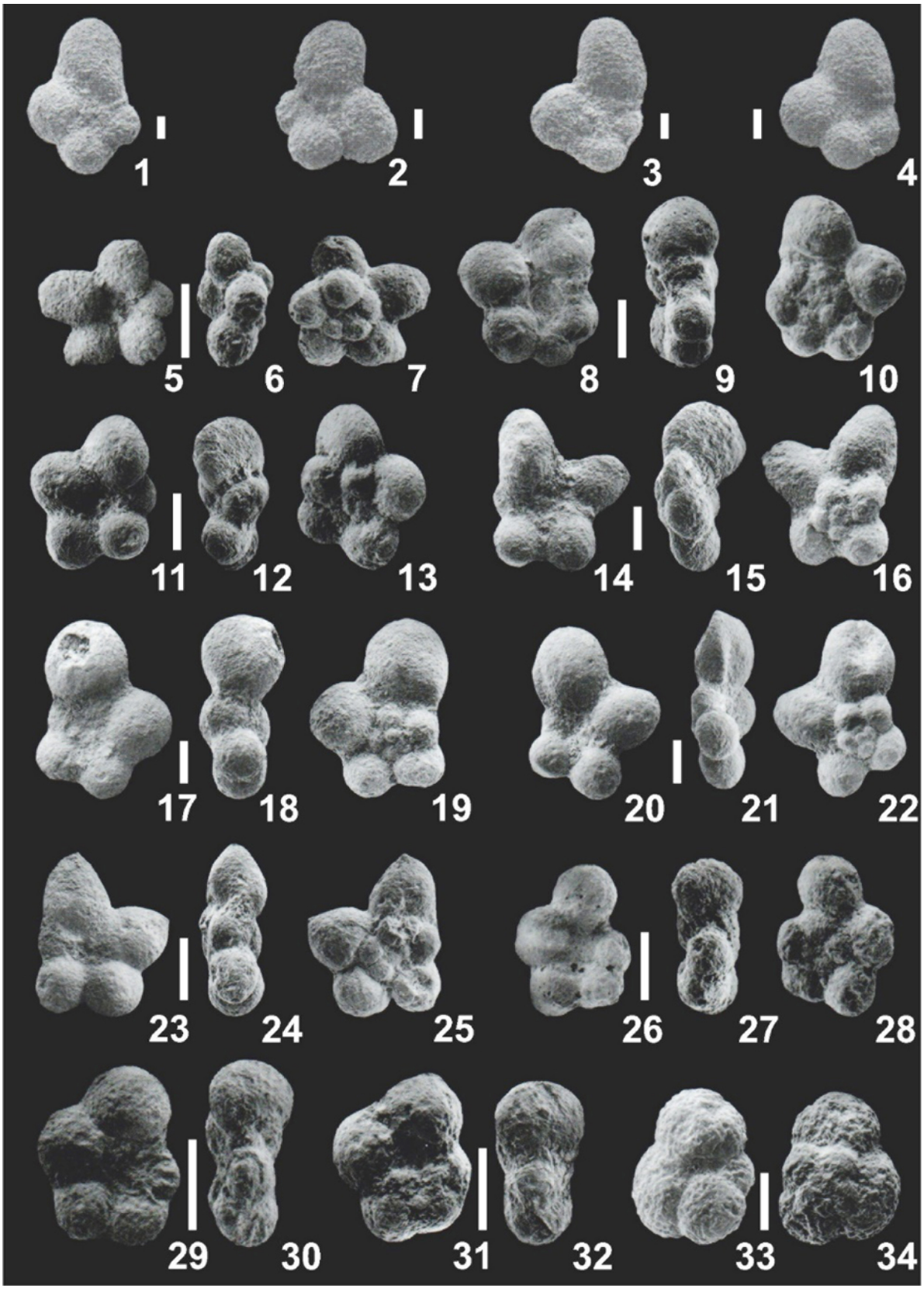

Figure 14. Scanning electron microscope micrographs of selected planktonic foraminiferal taxa. 1, Lilliputianella eocretacea, sample 138. 2, Lilliputianella eocretacea, sample 139. 3, Lilliputianella eocretacea, sample 138. 4, Lilliputianella eocretacea, sample 139. 5-7, Lilliputianella pauliani, sample U34-35. 8-10, Lilliputianella pauliani, sample U34-35. 11-13, Lilliputianella pauliani, sample A207-208. 14-16, Lilliputianella roblesae, sample A207-208. 17-19, Lilliputianella semielongata, sample A207-208. 20-22, Lilliputianella semielongata, sample A207-208. 23-25, Lilliputianella semielongata, sample U34-35. 26-28, Lilliputianella similis, sample A218-219. 29-30, Globigerinelloides paragottisi, sample N1. 31-32, Globigerinelloides paragottisi, sample P65-66. 33-34, Favusella hoterivica, sample A57-58. Scale bar = 50 µm.

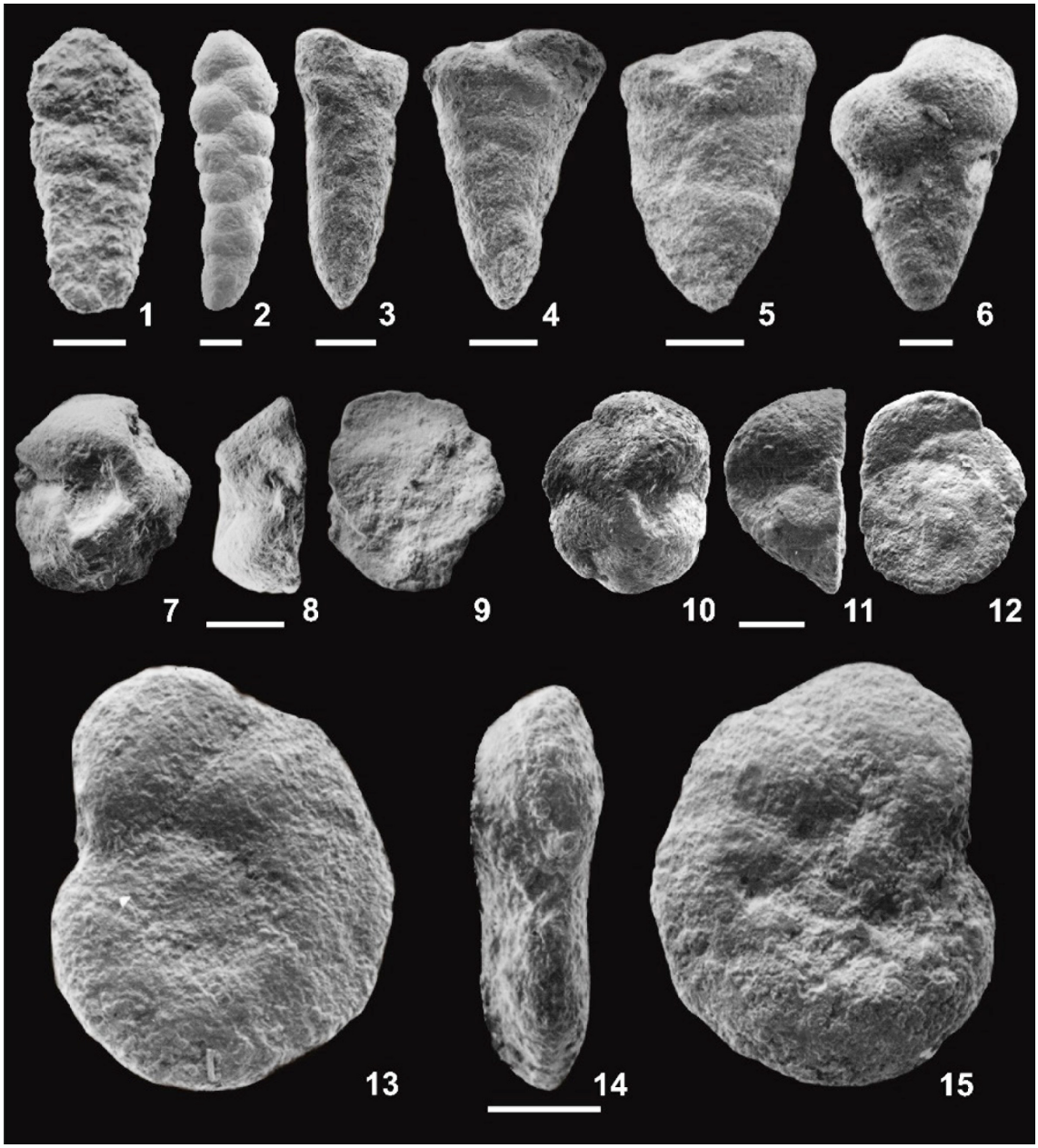

Figure 15. Scanning electron microscope micrographs of selected benthic foraminiferal taxa. 1, Textularia bettenstaedti. 2, Dorothia ouachensis. 3, Dorothia hauteriviana. 4, Dorothia kummi. 5, Dorothia praeoxycona. 6, Dorothia zedlerae. 7-9, Conorotalites cf. bartensteini. 10-12, Conorotalites intercedens. 13-15, Gavelinella barremiana. Scale bar = 100 μm.

Benthic foraminifera

Several benthic foraminiferal events have been identified in the Río Argos section: the FOs of *Dorothia praeoxycona* (interbed 128–129), *Conorotalites bartensteini* (interbed 175–176), *Gavelinella barremiana* (interbed 175–176), and *Conorotalites intercedens* (interbed 185–186), the LO of *Dorothia kummi* (interbed 195–196), and the temporary disappearance of Dorothiinae (between interbed 143–144 and interbed 191–192). A new zonation based on some of these bioevents is here proposed for the studied interval, revising the Early Cretaceous zonal scheme introduced by Moullade (1984).

The *Dorothia ouachensis* Zone is subdivided into two subzones using the FO of *D. praeoxycona*. The assemblages of the lower *Textularia bettenstaedti* Subzone (up to bed 128) are quite well diversified and mainly represented by the genera *Ammodiscus*, *Dorothia*, *Spirillina*, *Laevidentalina*, *Lenticulina*, and *Astacolus*. The upper *Dorothia praeoxycona* Subzone corresponds to the interval between the FO of the index species (interbed 128–129) and the FO of *G. barremiana*. Its assemblages are well diversified and dominated by different species of *Ammodiscus*, *Glomospirella*, *Spirillina*, *Laevidentalina*, *Lenticulina*, *Astacolus*, and *Reussoolina* and of polimorphinids. The Hauterivian–Barremian boundary falls in the uppermost part of this subzone.

The base of the overlying *Gavelinella barremiana* Zone is defined by the FO of the index species (interbed 175–176), and its top by the FO of *Conorotalites aptiensis* (above the interval studied). The assemblages in this zone are quite well diversified and dominated by *Ammodiscus*,

Glomospirella, *Spirillina*, *Laevidentalina*, *Lenticulina*, *Astacolus*, and *Gavelinella*.

Benthic foraminifera are abundant and quite well preserved throughout the FLE, showing higher abundances than planktonic foraminifera, with assemblages dominated by epifaunal taxa and representatives of the genera *Ammodiscus*, *Spirillina*, *Laevidentalina* and *Lenticulina*. A marked decline in the relative abundance of agglutinants has been recognised, with the agglutinated tubular taxa partially replaced by laevidentalinids and lenticulinids that are interpreted to be highly tolerant to oxygen deficiency (e.g., Nyong and Ramanathan, 1985; Tronchetti and Grosheny, 1991; Coccioni and Galeotti, 1993; Moullade et al., 2000; Holbourn and Kuhnt, 2002; Friedrich et al., 2003; Grosheny et al., 2006). These findings suggest an overall increase in fertility of surface waters associated with dysoxic bottom waters during the Faraoni Episode. It is also worth mentioning the temporary disappearance of Dorothiinae throughout the interval between interbed 143–144 and interbed 191–192, encompassing the FLE and the Hauterivian–Barremian boundary.

Dinoflagellate Cysts

The stratigraphic distribution of organic-walled dinoflagellate cysts from the Lower Cretaceous Río Argos succession was thoroughly examined by Leereveld (1995, 1997). He also integrated data from ammonite controlled sections in SE France and Switzerland, and proposed a zonal scheme valid for the whole western Mediterranean region. The Hauterivian–Barremian boundary falls within the upper part of the *Subtilisphaera perlucida* dinocyst Zone. The base of this zone is defined by the LO of *Aprobolocysta eilema* (in the marlstone interbed 138–139 of section Ag1, corresponding to the *B. binelli* ASz, see Company et al., 2003), and its top by the FO of *Subtilisphaera scabrata* (interbed 195–196, in the lowermost part of the *K. nicklesi* AZ). According to Leereveld (1995, 1997), other significant events recorded in this interval are the LO of *Palaecysta complicata* and the FO of *Subtilisphaera senegalensis* in interbed 154–155, and the LO of *Exiguisphaera phragma* in interbed 170–171. In any case, it should be taken into account that, as pointed out by Leereveld (1997, p. 433), no sample between beds 171 and 195 (i. e., the whole *T. hugii* AZ) yielded identifiable dinocysts, so the position of this last event cannot be accurately calibrated against the ammonite zonation.

Chemostratigraphy

Organic Matter

Previous data on the organic geochemistry of the Río Argos succession, largely on the FLE, were provided by Baudin (2005), Sauvage et al. (2013) and Baudin and Riquier (2014). For the present study, 61 samples taken in the middle part of the marlstone interbeds between interbed 135–136 (top of the *B. balearis* ASz) and interbed 185–186 (lower part of the *P. colombiana* ASz) from section Ag1, and 14 samples around the FLE (beds 18–25) from section Ag5 have been analysed (Figs. 16 and 17; Tables 1 and 2).

Information on the thermal evolution of the organic matter can be achieved by pyrolytic measurements, especially using the Tmax parameter (Espitalié et al., 1985). Tmax values are relatively low (~ 427°C on average), which indicates that the organic matter did not experience high temperature during burial and is still immature with respect to petroleum generation. This is in agreement with the moderate burial diagenesis deduced from clay mineralogy (Moiroud et al., 2012). Such a moderate diagenesis suggests that the Rock-Eval parameters (TOC, HI) represent a primary signal and reflect the environmental changes during the deposition of uppermost Hauterivian and lowermost Barremian strata.

If we except the FLE, the background sediment from section Ag1 shows a low organic carbon content with TOC ranging from 0 to 0.4% (0.13% on average), while calcium carbonate content varies from 39 to 68.5% with an average of 52% (Fig. 16, Table 1). The calcium carbonate and organic matter contents of marlstone interbeds appear very homogeneous throughout the studied interval and no trend may be drawn along this interval of section Ag1. No relationship between the percentages of carbonate and organic carbon content can be observed (Fig. 18A), which suggests that organic matter is not diluted by the carbonate flux and argues for a more or less constant ratio of the carbonate flux vs organic matter flux through time, at least during the background marlstone interbed deposition.

According to the low range of HI values (25 to 147 mg HC/g TOC), the organic matter of the studied samples is distributed between oxidised Type II and Type IV (Fig. 18C). The small amount of sedimentary organic matter in marlstone interbeds is probably the result of slightly enhanced preservation of organic matter, that mainly corresponds to land-derived organic matter (Type III) and the non-metabolisable fraction of marine organic matter (oxidised Type II and Type IV). The low amount of organic matter, associated with low HI values, argues for deposition in fully oxic pelagic waters. However, anoxic conditions were developed within the sediment as pyrite is a ubiquitous mineral in all the studied interval.

The lithological succession of the FLE in sections Ag1 and Ag5 is comparable to the Italian and French occurrences, but its thickness reaches 2 meters that is the most expanded record of the Faraoni Episode (Baudin and Riquier, 2014). The TOC varies from 0.03 to 3.8% within the FLE (Tabs. 1 and 2). HI values of the FLE fluctuate between 52 and 338 mg HC/g TOC that indicates a good preservation of marine phytoplanktonic (Type II) organic matter (Fig. 18C). Calcium carbonate content is in the same range than the background sedimentation (Fig 18A), which suggests that the organic enrichment of the FLE is not related to dissolution of carbonate but rather to an increase of primary productivity. The better preservation of sedimentary organic matter suggests the development of dysoxic conditions during the Faraoni Episode time interval.

Carbon Isotope Stratigraphy

Data on carbon and oxygen isotope stratigraphy in the Río Argos section were reported by Aguado et al. (2014), who performed a high-resolution analysis of 137 bulk carbonate samples from limestone, marlstone and marly limestone beds. The $\delta^{13}C$ values fluctuate between -0.09‰ and 1.75‰. The $\delta^{18}O$ values, which vary between -1.9‰ and -3.42‰, display a high frequency oscillation very likely due to diagenetic alteration; therefore, they have not been taken into account as a stratigraphic tool (Fig. 19).

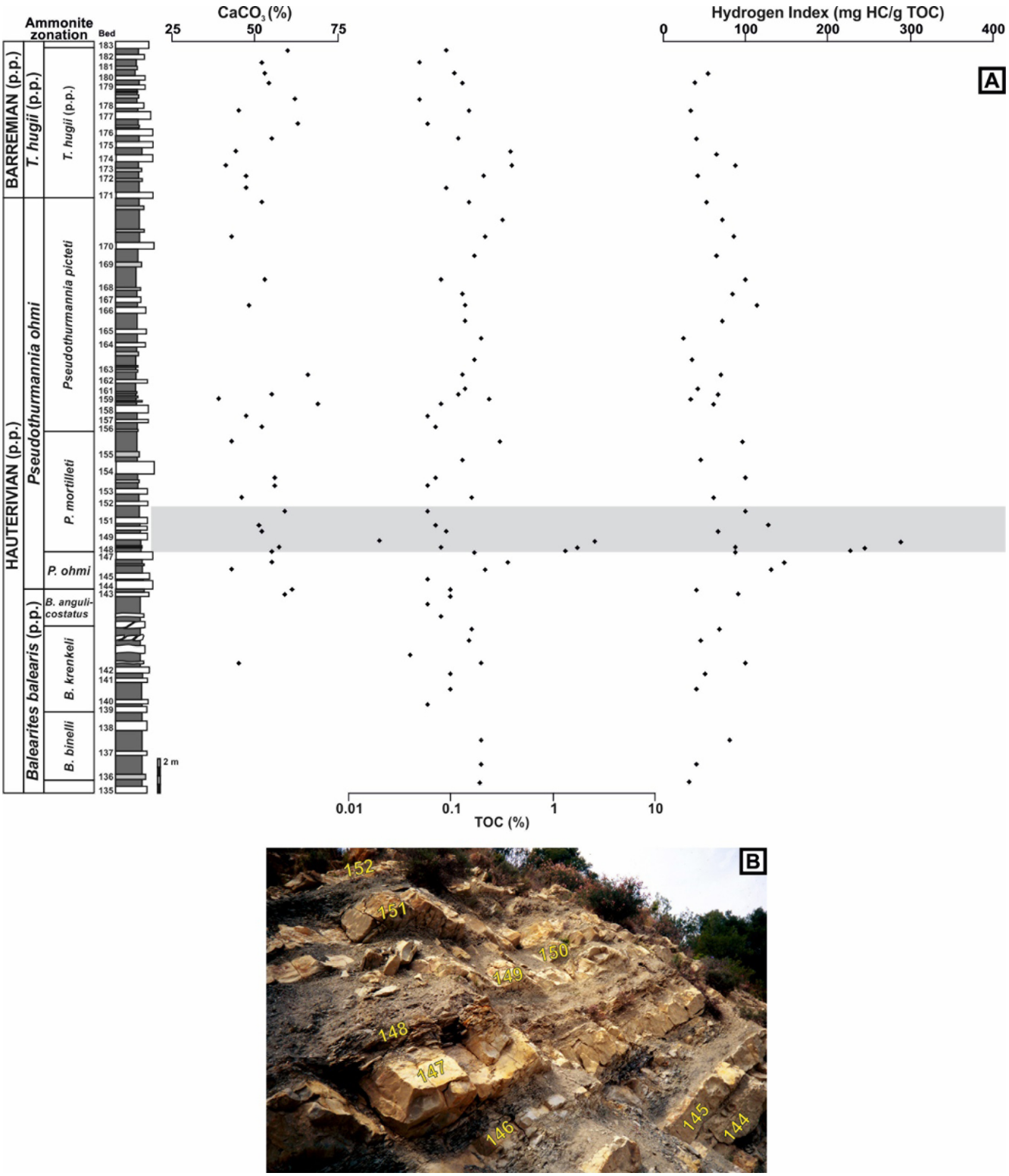

Figure 16. Section Ag1. A, Vertical distribution of $CaCO_3$ percentages (in wt%), the total organic carbon content (TOC, in weight %) and the Hydrogen Index (HI, mg HC/g TOC). B, Detailed view of the Faraoni Level equivalent interval.

The carbon isotope curve shows a small negative spike (around 0.7‰) measured in the laminated black shale interval (bed 148) that marks the beginning of the FLE at the base of the *P. mortilleti* ASz (bed 148). This anomaly is rapidly followed by a positive excursion leading to the maximum value (1.75‰) towards the top of the FLE (bed 152). After a decrease in the upper part of the *P. mortilleti* ASz, the values remain more or less stable, around 1‰, throughout most of the *P. picteti* ASz. The Hauterivian–Barremian boundary falls into a time of slightly decreasing carbon isotope values, which reach their minimum (-0.09‰) in the uppermost part of the *T. hugii* AZ. A

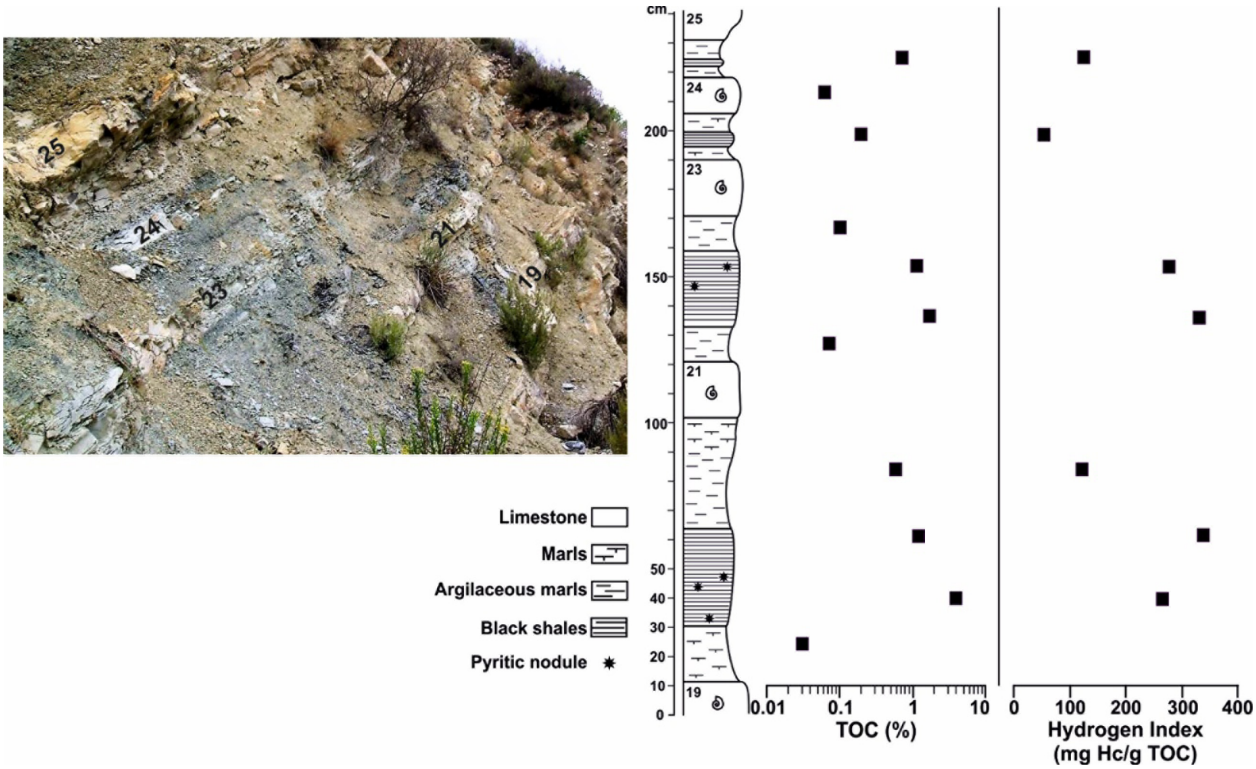

Figure 17. Section Ag5. Detailed view of the Faraoni Level equivalent interval and vertical distribution of the total organic carbon content (TOC, in weight %) and the Hydrogen Index (HI, mg HC/g TOC).

trend to increasing values is observed at the transition to the *K. nicklesi* AZ.

A similar general pattern can be observed in the carbon isotope curve of the section V1 (Aguado et al., 2014; Martinez et al., 2020), and in the curves established for other pelagic and hemipelagic successions from the Apennines (Gorgo a Cerbara and Fiume Bosso), the Ultrahelvetic domain (Veveyse de Châtel-Saint-Denis) and the Vocontian Basin (Angles) (Godet et al., 2006). In all these sections, with differences in detail, the positive excursion associated with the Faraoni Level is recognised, followed by a stable phase and, finally, a smooth trend towards more negative values from terminal Hauterivian and including the Hauterivian/Barremian boundary. Carbon isotope record is thus revealed as a useful tool for the recognition and characterisation of the base of the Barremian Stage.

Strontium Isotope Stratigraphy

No systematic analysis of $^{87}Sr/^{86}Sr$ has been performed in the Río Argos section. However, high-resolution Sr-isotope curves are available for the Hauterivian–Barremian interval based mainly on data from the Vocontian Basin (McArthur et al., 2007; Bodin et al., 2009; Mutterlose et al., 2014). According to these curves, the Hauterivian–Barremian boundary falls within an interval of steadily increasing values from 0.707442 in the *Subsaynella sayni* AZ (early late Hauterivian) to a relative maximum of 0.707504 in the *Kotetishvilia compressissima* AZ (late early Barremian), from which the curve shifts to lower values. The measure on a belemnite coming from the very base of the Barremian in the Angles section yielded a value of 0.707470 ± 0.000011 (Bodin et al., 2009).

Magnetostratigraphy

The Early Cretaceous limestones of the Río Argos succession are affected by an intense Neogene remagnetisation that, unfortunately, prevents any magnetostratigraphic analysis (Hoedemaeker et al., 1998).

Bartolocci et al. (1992) and Channell et al. (1995) placed the Hauterivian/Barremian boundary in the uppermost part of polarity chron M5n (= CM4), mainly on the basis of the calibration between the magnetostratigraphic record in Gorgo a Cerbara (Lowrie and Alvarez, 1984) and the ammonite findings in this and other central Italian sections (Cecca et al., 1994b, 1995). Although it is generally accepted nowadays (Ogg, 2020; Gale et al., 2020), the revision of some taxonomic assignments leads us to nuance or slightly modify this correlation.

In the Gorgo a Cerbara section the magnetic polarity reversal from chron M5n to M3r was recorded at 829.5 m (Lowrie and Alvarez, 1984). Cecca et al. (1994b, 1995) reported a rich and diversified ammonite fauna from the guide-bed of the Faraoni Level (base of the *P. mortilleti* ASz) at 822 m, and typical Barremian *Taveraidiscus intermedius* at 833 m. In the absence of other significant ammonites between metres 822 and 833, Cecca et al. (1994b, 1995) choose to draw the Hauterivian/Barremian boundary between metres 824 and 828 (i. e. in the upper part of chron M5n) “on the basis of data from other sections (Mount Petrano)” (Cecca et al., 1995, p. 192). These data refer to the presence, in several sections of the Monte Petrano area, of a bed with

Table 1. Calcium carbonate content and Rock-Eval pyrolysis results of the upper Hauterivian and lower Barremian strata along section Ag1. Tmax is not determined for S_2 peaks below 0.1 mg/g. HI is not determined for S_2 = 0 mg/g or TOC ≤ 0.05%. The grey part corresponds to the FLE

Sample	$CaCO_3$ %	Tmax °C	S_1 mg/g	S_2 mg/g	TOC %	HI mg HC/g TOC
185-186	41		0.03	0.00	0.00	
182-183	60		0.02	0.03	0.09	
181-182	52		0.02	0.02	0.05	
180-181	53		0.04	0.06	0.11	54
179-180	54		0.05	0.05	0.13	38
178-179	62		0.02	0.01	0.05	
177-178	45		0.02	0.05	0.15	33
176-177	63		0.04	0.02	0.06	
175-176	55		0.05	0.05	0.12	41
174-175	44	424	0.03	0.25	0.39	64
173-174	41	428	0.07	0.35	0.40	87
172-173	47		0.10	0.09	0.21	42
171-172	47		0.03	0.02	0.09	
170b-171	52		0.06	0.08	0.15	53
170a-170b	43	426	0.03	0.23	0.32	71
170-170a		420	0.04	0.19	0.22	86
169-170			0.04	0.11	0.17	64
168-169	53		0.01	0.08	0.08	100
167-168		438	0.02	0.11	0.13	84
166-167	48	439	0.03	0.16	0.14	114
165-166		428	0.02	0.10	0.14	71
164-165			0.02	0.05	0.20	25
163-164			0.02	0.06	0.17	35
162-163	66		0.04	0.09	0.13	69
161-162	55		0.04	0.06	0.14	42
160-161	39		0.01	0.08	0.12	67
159-160			0.06	0.08	0.24	33
158-159	69		0.02	0.05	0.08	62
157-158	47		0.01	0.01	0.06	
156-157	52		0.01	0.01	0.07	
155-156	43	431	0.03	0.29	0.30	96
154-155			0.02	0.06	0.13	46
153a-154	56		0.02	0.07	0.07	100
153-153a	56		0.01	0.03	0.06	
152-153	46	424	0.01	0.10	0.16	62
151-152	59		0.01	0.06	0.06	100
150-151	51		0.02	0.09	0.07	128
149-150	52		0.02	0.06	0.09	67
148-149 top			0.01	0.00	0.02	
148-149 base	57	425	0.14	7.38	2.56	288
148			0.02	0.07	0.08	87
147-148 top	55	426	0.11	4.25	1.73	245
147-148 middle		426	0.08	2.98	1.31	227
147-148 base			0.03	0.15	0.17	88
146-147	55	429	0.02	0.53	0.36	147
145-146	43	425	0.03	0.29	0.22	131
144-145			0.03	0.03	0.06	

Table 1. (continued)

Sample	$CaCO_3$ %	Tmax °C	S_1 mg/g	S_2 mg/g	TOC %	HI mg HC/g TOC
143-144	61		0.02	0.04	0.10	40
142e-143	59		0.13	0.09	0.10	90
142d-142e			0.05	0.04	0.08	
142c-142d			0.06	0.11	0.16	68
142b-142c			0.04	0.07	0.15	46
142a-142b			0.02	0.01	0.04	
142-142a	45	425	0.03	0.20	0.20	100
141-142			0.04	0.05	0.10	50
140-141			0.02	0.04	0.10	40
139-140			0.02	0.01	0.06	
138-139			0.00	0.00	0.00	
137-138			0.05	0.16	0.20	80
136-137			0.03	0.08	0.20	40

Table 2. Calcium carbonate content and Rock-Eval pyrolysis results of the upper Hauterivian FLE along section Ag5. Tmax is not determined for S_2 peaks below 0.1 mg/g. HI is not determined for S_2 = 0 mg/g or TOC ≤ 0.05%. The grey part corresponds to the FLE

Sample	$CaCO_3$	Tmax	S_1	S_2	TOC	HI
25m	58.5		0.16	0.00	0.05	
24m	52.5	431	0.40	0.92	0.74	124
24	72.3		0.18	0,01	0.06	
23m	40.0	424	0.12	0.10	0.19	52
22D	51.5		0.12	0.03	0.10	
22C	54.5	429	0.15	3.28	1.18	277
22B	64.4	424	0.25	5.49	1.65	332
22A	46.5		0.20	0.00	0.07	
20D	63.4	430	0.29	0.72	0.59	122
20C	70.3	426	0.18	4.20	1.24	338
20B	59.5	423	0.16	10.15	3.81	266
20A	68.5		0.10	0.00	0.03	
18m2 middle	44.5	437	0.09	0,01	0.14	
18m1 base	55.5	430	0.11	0.65	0.52	125

heteromorph ammonites attributed by Cecca et al. (1995) to "*Paraspinoceras*" *evolutum*. The bed, situated 4–5 m above the Faraoni Level, was dated as lowermost Barremian according to the data available at that time. However, these ammonites were later correctly reinterpreted (Vašíček and Hoedemaeker, 2003) as *Sabaudiella argosensis*, a species that, as seen above, has its LO in the middle part of the *P. picteti* ASz. This implies that the Hauterivian/Barremian boundary in the Gorgo a Cerbara section should rather be drawn between metres 829 and 833, practically coinciding with the boundary between chrons M5n and M3r or, more likely, in the lowermost part of chron M3r. This conclusion would be in full agreement with the results by Lukeneder et al. (2016, fig. 3) in the Puez section (Southern Alps, Italy), where they recorded the M5n/M3r magnetic reversal in the uppermost Hauterivian, a little above the LOs of *Pseudothurmannia picteti* and *Sabaudiella* sp. (see Lukeneder, 2012, fig. 3). According to the calibration proposed, the base of chron M3r would lie approximately between beds 166 to 171 in the Río Argos section.

Sequence Stratigraphy

The sequence chronostratigraphic framework developed by Hardenbol et al. (1998) for the European basins, as modified by Arnaud (2005a, b) for the Vocontian Basin, fits very well with the observations in the Betic Cordillera for the latest Hauterivian–earliest Barremian interval (Company et al., 2005). See, however, Hoedemaeker (1998) for a somewhat different interpretation.

The maximum flooding surface of sequence Ha6 coincides with the base of the *P. mortilleti* ASz (bed 148 in section Ag1). It corresponds to a second-order peak transgression, coeval and very likely linked to the onset of the Faraoni Episode, as reported from many pelagic and hemipelagic settings of the western Mediterranean Tethys (Baudin, 2005; Company et al., 2005, 2008; Bodin et al., 2006a; Baudin & Riquier, 2014). It also represents an important drowning episode in the evolution of the Prebetic platform in the south Iberian margin during the

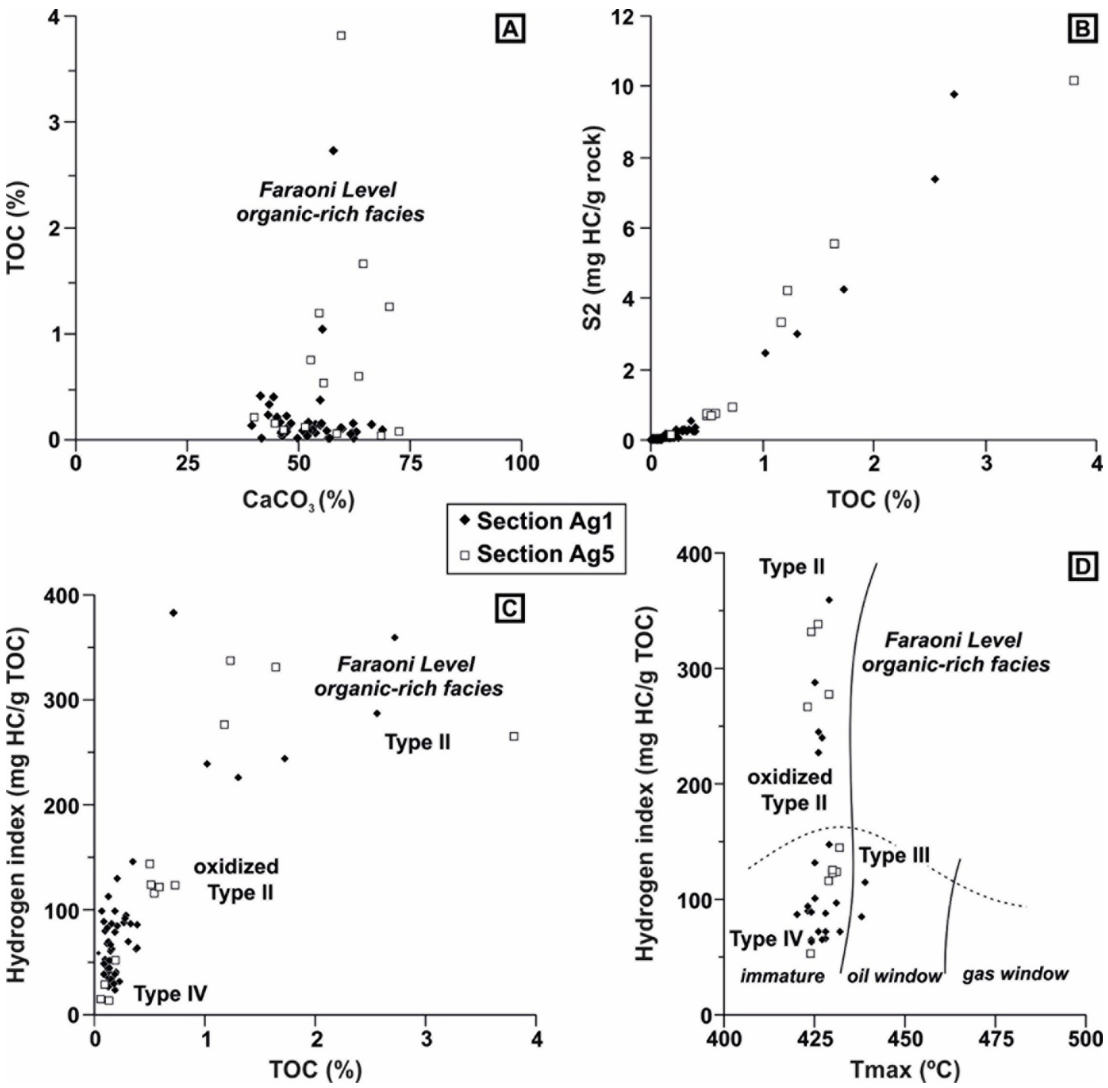

Figure 18. A, Carbonate vs. organic carbon content (TOC) of studied samples. B, S_2 vs TOC diagram of studied samples. C, Kerogen type according to TOC and HI parameters. D, Origin and thermal maturation of the studied samples.

Early Cretaceous (Castro et al., 2008).

Arnaud (2005b) placed the sequence boundary Ha7 in the middle part of the *P. picteti* ASz, namely at the base of bed 67 of the Angles section. Accurate bio– and cyclostratigraphic calibration between the Angles and Río Argos sections (see Martinez et al., 2012) allows correlation of this bed with bed 164 of section Ag1, coinciding with the last records of the genus *Sabaudiella*, and little after the disappearance of the genus *Pseudothurmannia*. This sequence boundary, which constitutes the base of a second order regressive cycle, reflects a drastic relative sea level fall responsible for a major unconformity in the perimediterranean platforms (Arnaud-Vanneau and Arnaud, 1990; Company et al., 1992, 2008; Jacquin et al., 1998; Arnaud, 2005a; Bodin et al., 2006b; Pictet, 2021). It also coincides with the start of deposition of the turbiditic Cerrajón Formation in the Subbetic Domain (Braga et al., 1982; Ruiz-Ortiz et al., 2006).

According to Arnaud (2005a, b) the maximum flooding surface of sequence Ha7 would correlate with the middle part of the *T. hugii* ASz (bed 78 of the Angles section, equivalent to bed 178a of section Ag1). It is around this stratigraphic level that sedimentation resumed after the Ha7 sequence boundary discontinuity in several areas of the Prebetic Domain (our personal observations) and also in the western High Atlas (Company et al., 2008).

It can be concluded, therefore, that the Hauterivian–Barremian boundary is located in the depositional sequence Ha7 and would correspond approximately to the top lowstand surface of the sequence (Hoedemaeker, 1998; Arnaud, 2005b) (see Clavel et al., 1995 for an alternative interpretation).

Cyclostratigraphy and Astrochronology

Magnetic Susceptibility (MS), Gamma-Ray Spectrometry (GRS), $CaCO_3$ content and clay mineral assemblages were acquired every 0.20 m during two sampling visits in order to detect the sedimentary cycles through spectral analyses, determine their climatic origin, and provide an orbital time scale in section Ag1. The methods applied to perform these measurements have been detailed in Martinez et al. (2012, 2015) and in Moiroud et al. (2012). We will outline here the

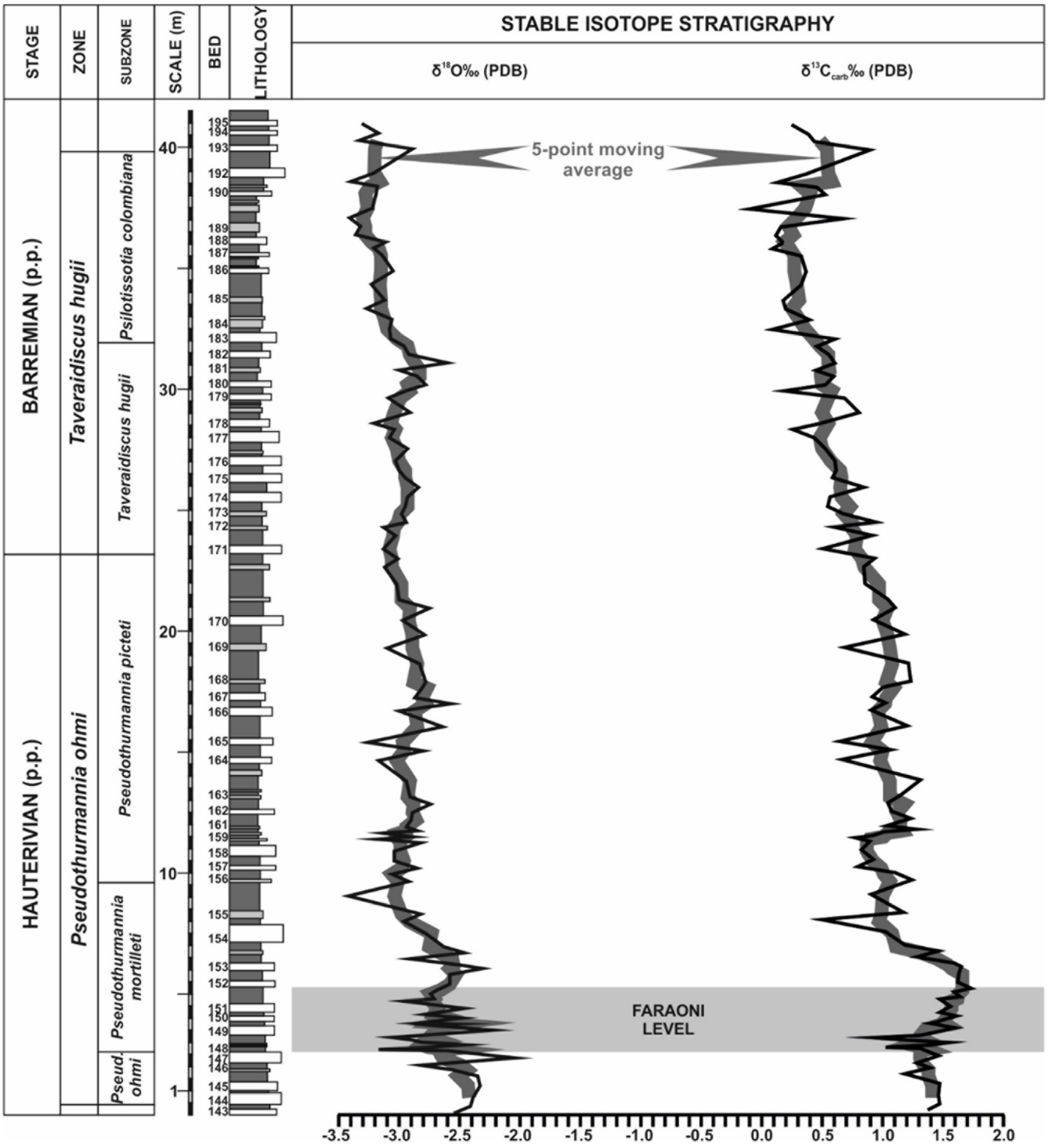

Figure 19. Carbon and oxygen isotope stratigraphy in the Río Argos section.

results from signals, the link between sedimentary cycles and astroclimatic cycles and the astrochronology of section Ag1.

Results

MS and GRS show a strong inverse correlation with $CaCO_3$ content (Fig. 20). MS and GRS values are higher in marlstone interbeds than in limestone beds. Higher MS values in marlstone interbeds reflect a higher content in paramagnetic clay minerals (such as smectite and illite) than in limestone beds, in which diamagnetic minerals (e.g. calcite and dolomite) are dominant (see Martinez et al., 2012; Martinez, 2018). Higher GRS values in marlstone interbeds reflect a higher content in potassium and thorium (associated with clay minerals) than in limestone beds. GRS values show a marked peak at the base of the Faraoni Level coinciding with high TOC values, which reflects enrichment in uranium under oxygen-deficient conditions

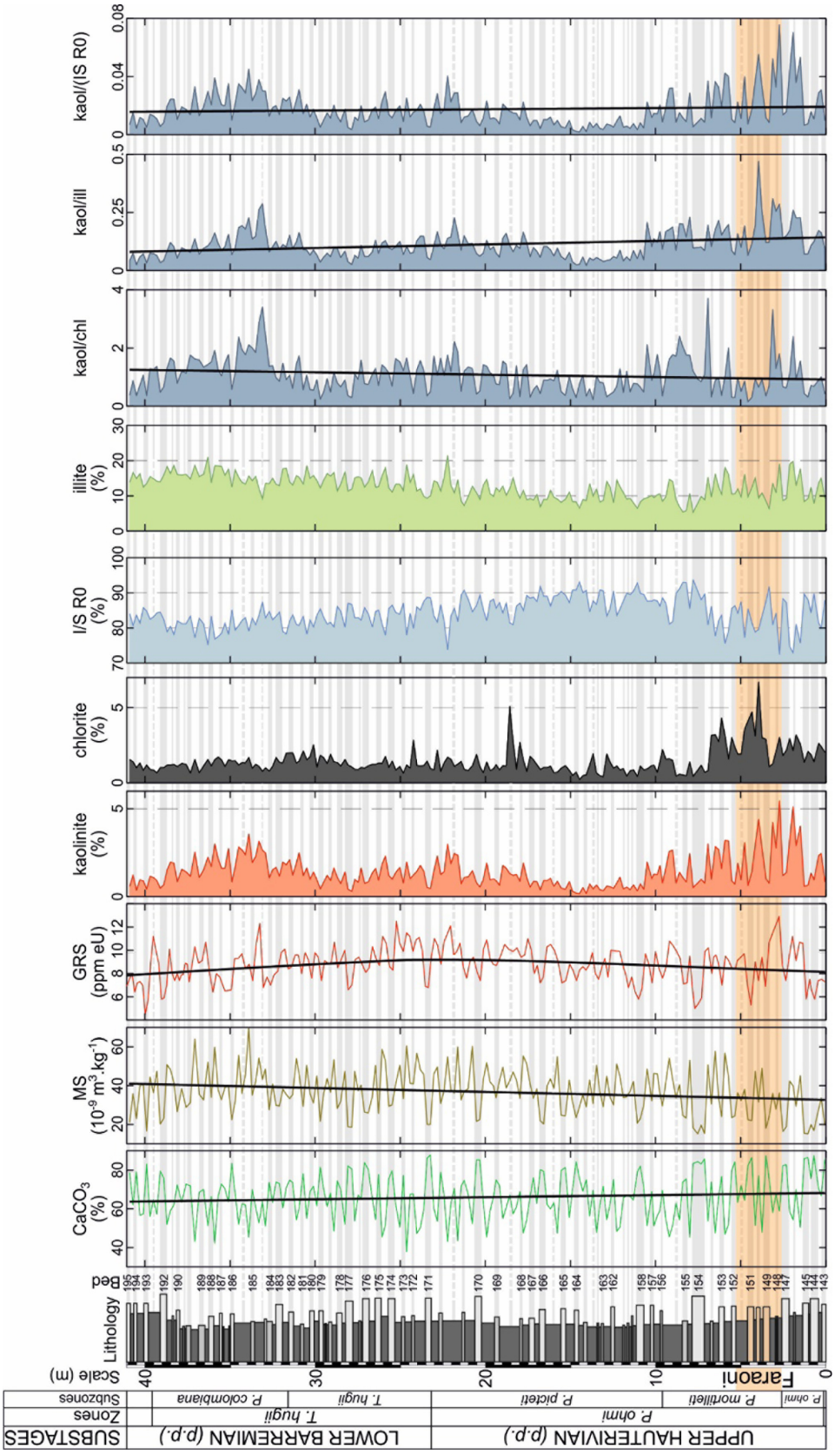

Figure 20. $CaCO_3$ (% wt), Magnetic Susceptibility (MS), Gamma-Ray Spectrometry (GRS), clay mineral content within the clay fraction and ratio between the clay content throughout section Ag1.

(Sauvage et al., 2013).

Marlstone interbeds also show higher contents in kaolinite and illite and lower content in IS R0 (thereafter referred as smectite) than limestone beds. This reflects that marlstone interbeds were deposited

under annually humid conditions while limestone beds were deposited under seasonally-arid conditions. The marl-limestone alternations of the Río Argos section correspond to climatic cycles with varying levels of humid conditions, continental weathering and detrital supply to the basin. The marl-limestone alternations have an average thickness of 0.65 m (standard deviation: 0.29 m, min: 0.10 m, max: 1.50 m). In addition to these elementary sequences, kaolinite, kaolinite/smectite, kaolinite/illite and kaolinite/chlorite show three sequences of ~14 m each, while MS, GRS and $CaCO_3$ show sequences of ~3 m.

Spectral analyses of MS, $CaCO_3$ and GRS show a high-power period at 3.5 m, a period at 13.7 m in the MS signal corresponding to the 405-kyr eccentricity, periods from 1.3 m to 1.0 m and periods from 0.75 m to 0.54 m (Fig. 21). Another period is observed at 1.8 m in the GRS series. In the MS signal, the period ratios between the cycles of 13.7 m, 3.5 m, 1.15 m and 0.65 m (21.1 : 5.4 : 1.7 : 1) is close to the ratios of 20 : 4.9 : 1.9 : 1 of the astronomical cycles of the 405-kyr eccentricity, ~100-kyr eccentricity, 38.5-kyr obliquity and ~20-kyr precession. The application of CO efficient CO rrelation analysis (COCO; Li et al., 2018) shows the maximum correlation between the spectrum of the MS series and the astronomical solution at sedimentation rate of 3.2 $cm.kyr^{-1}$ (Fig. 22A). Applying an average sedimentation rate of the periods of 13.7 m, 3.5 m, 1.15 m and 0.65 m leads to respective durations of 428 kyr, 109 kyr, 35.9 kyr and 20.3 kyr. The COCO analysis provides here a statistical justification of the interpretation deduced from the comparison of period ratios. In the $CaCO_3$, GRS, kaolinite/chlorite and kaolinite/illite series, the COCO analysis provides maximum correspondence between the sedimentary and the astronomical spectra for sedimentation rates ranging from 2.6 to 3.4 $cm.kyr^{-1}$ (Fig. 22B, C, E, F). In the kaolinite/smectite series (Fig. 22D, maximum correspondence is not observed. This is a consequence of maximum of kaolinite/smectite ratio during the Faraoni Episode, which corresponded to an event of reinforced weathering and hydrolysing conditions. Comparatively, the maximum of the first 405-kyr cycle in the MS series is recorded 6 m above the base of the Faraoni Episode (Fig. 23).

In the spectra of the clay mineral assemblages, the highest powers

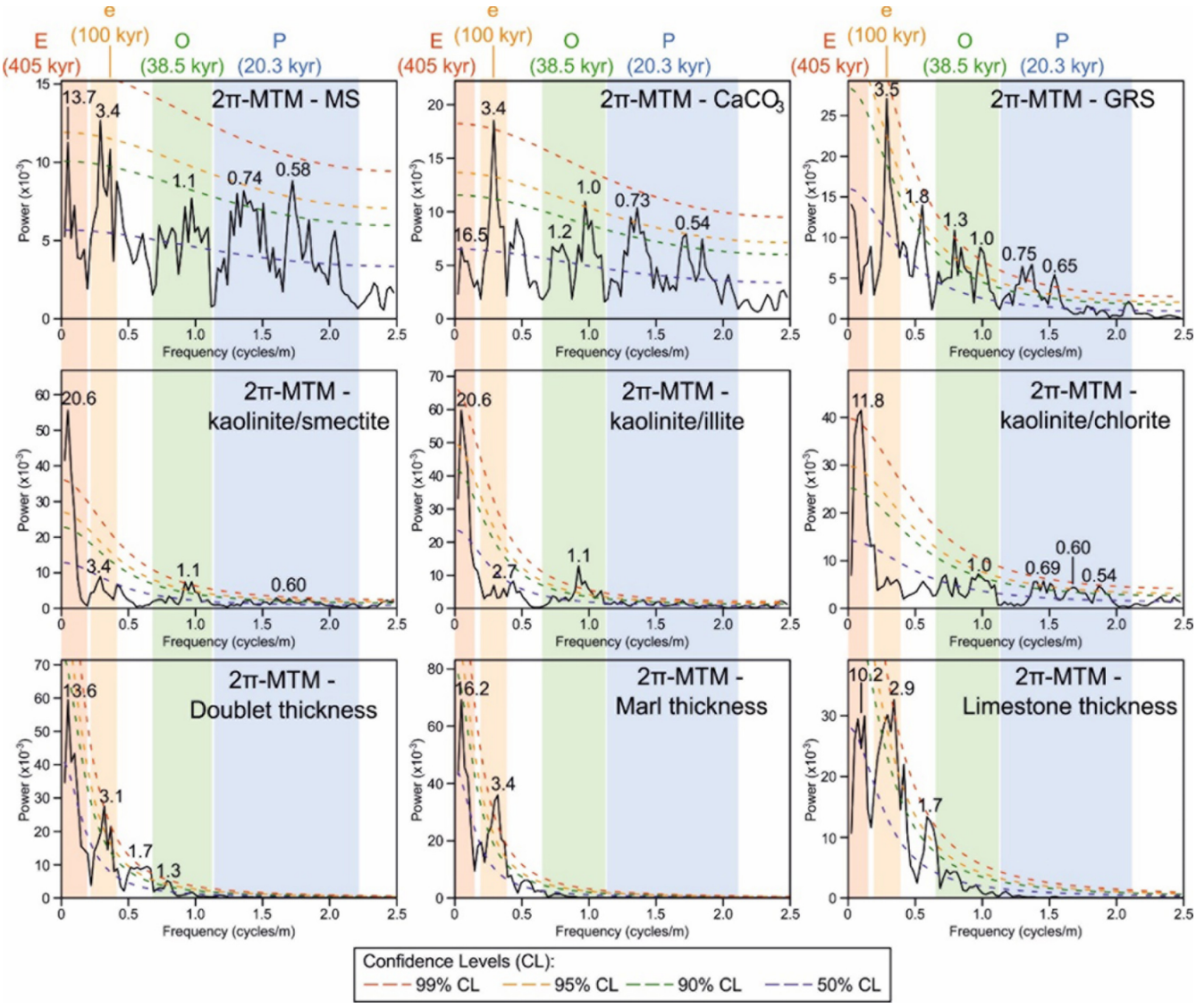

Figure 21. 2π-Multi-Taper spectra of the various proxies considered.

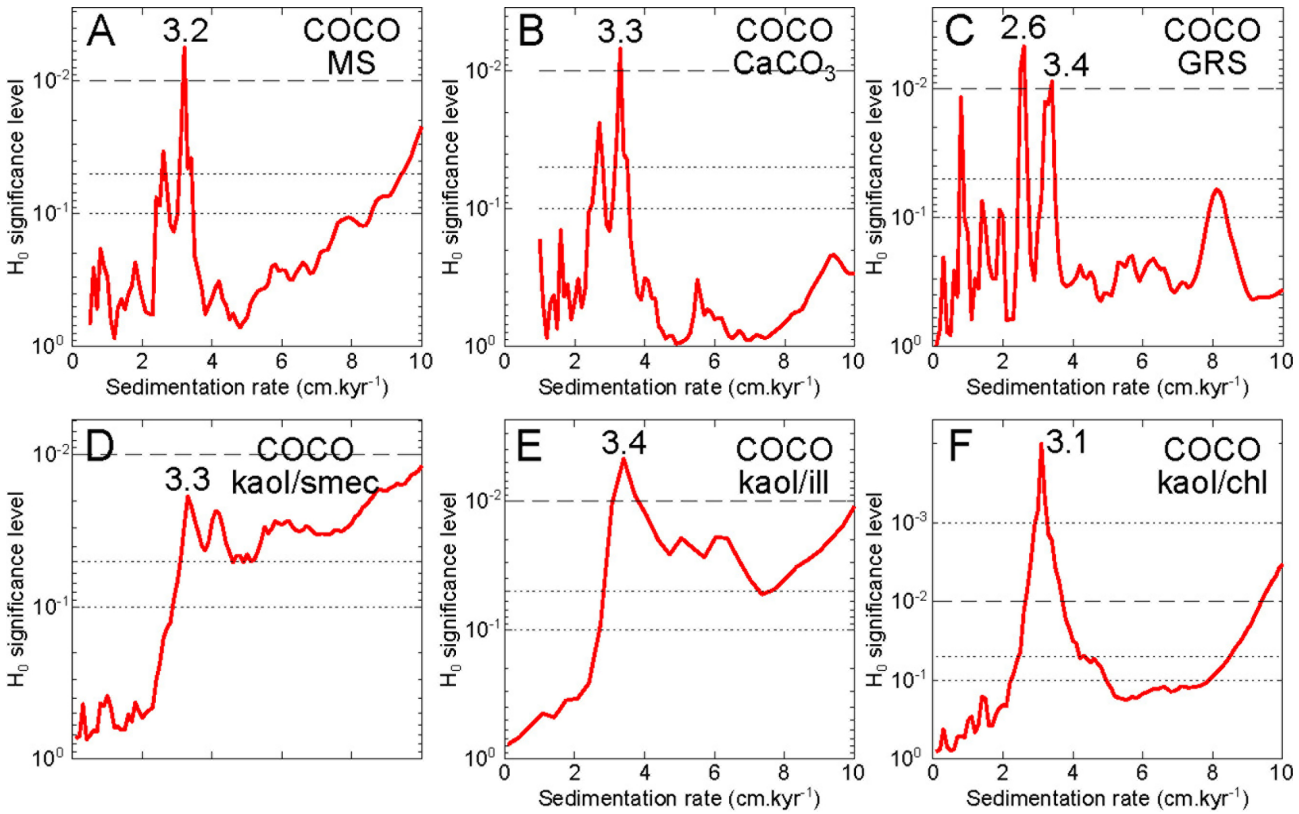

Figure 22. COefficient COrrelation (COCO) analyses of the proxies used for cyclostratigraphy.

are observed in the 405-kyr eccentricity band, although with longer periods than in the MS signal, related to the strong asymmetry of the lowest cycle, due to the maximum of humidity during the Faraoni Episode (Bodin et al., 2007). Spectral analyses of the marl-limestone couplets show periods at 13.6 m, 3.1 m and 1.3 m, respectively corresponding to the 405-kyr, 100-kyr and obliquity. Another period is observed at 1.7 m. Marl thicknesses show periods at 16.2 m and 3.4 m corresponding to the 405-kyr and 100-kyr eccentricity, while limestone bed thicknesses show periods at 10.2 m and 2.9 m, respectively corresponding to the 405-kyr band and the 100-kyr eccentricity. Another period at 1.7 m is observed. It is noteworthy that the spectra of the marl thicknesses and the couplet thicknesses have similar shapes with highest powers in the 405-kyr band while the spectrum of the limestone thicknesses shows highest powers in the 100-kyr band. This shows that (i) the eccentricity cycles control the variations in the sedimentation rates at short terms and (ii) these short-term variations in the sedimentation rates are mainly controlled by variations in the detrital supply although there is also a response of the carbonate supply at Milankovitch scale.

In general, the proxies of detrital supply (clay mineral assemblages, marl and couplet thicknesses) show highest powers in the 405-kyr eccentricity band, while the proxies which incorporate a carbonate component ($CaCO_3$, MS, GRS, limestone thicknesses) show highest periods in the 100-kyr band. This was explained by the fact the carbonate system has variegated responses to the orbital forcing disrupting the power of the 405-kyr eccentricity cycle (Martinez, 2018).

Astrochronology

The filter of the 100-kyr band in the MS signal shows that the Río Argos section contains thirteen repetitions of the 100-kyr cycle and three repetitions of the 405-kyr cycle (Fig. 23; Martinez et al., 2012, Martinez, 2018). Interestingly, the amplitude modulation of the 100-kyr filter in the MS follows the 405-kyr cycle (Fig. 23), as expected in the astronomical models (Laskar et al., 2011). A total of twelve repetitions of the 100-kyr cycle are observed from the filter of the GRS signal (Fig. 23). The difference is at the base of the FLE, where a maximum in GRS values corresponds to a minimum in the MS values. This maximum in the GRS values is due to enrichment in uranium and corresponds to a different phenomenon than the detrital supply. The filter of the GRS also shows maxima in amplitude every ~14 m, in phase with the maxima observed in the filter of the MS signal. In addition, the filter of the precession cycle shows amplitude modulation controlled by this 405-kyr cycle, as expected in the astronomical models (Laskar et al., 2011). These observations demonstrate the quality of the record of the orbital cycles in the section Ag1, making it an exceptional site to reconstruct the past changes of the Earth orbit. A difference of 150 kyr is observed in the maximum of amplitude related to the base of e405-B1 between the amplitude modulation of the 100-kyr cycle in the MS and GRS and the precession cycles of the GRS signal.

The astronomical tuning is based on the record of the 405-kyr eccentricity cycles, anchored to a radiometric age obtained in the Neuquén Basin at the base of the *Holcoptychites agrioensis* Andean AZ (Aguirre-Urreta et al., 2017), correlated to the base of the *Olco-*

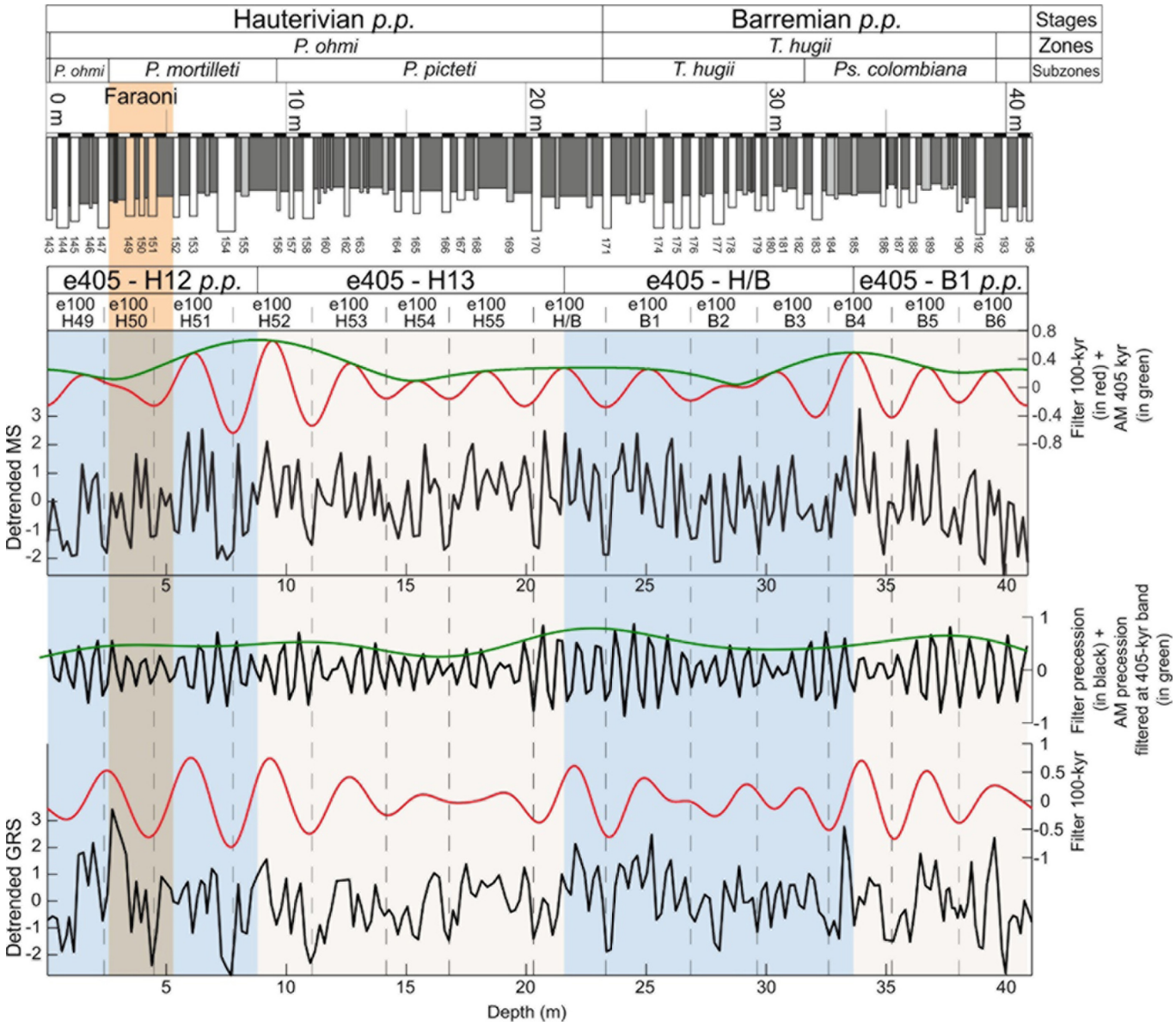

Figure 23. Astrochronology of the Río Argos section.

Table 3. Ages of the base of ammonite zones and subzones in the Río Argos section

Horizon	Selected age (Ma)
Base *K. niclesi* AZ	-125.21
Base *P. colombiana* ASz	-125.48
Base *T. hugii* AZ (base Barremian stage)	**-125.77**
Base *P. picteti* ASz	-126.20
End Faraoni Episode	-126.39
Base *P. mortilleti* ASz (start Faraoni Episode)	-126.51
Base *P. ohmi* AZ	-126.57

stephanus (Jeannoticeras) jeannoti Mediterranean AZ (Aguirre-Urreta et al., 2019). The ages of the base of the ammonite zones and subzones of the Ag1 section are shown in Table 3.

The Boundary Level: Primary and Auxiliary Markers

The base of the Barremian Stage is placed at the base of bed 171 (at 22.8 m from the base of the section), coinciding with the FO of the ammonite species *Taveraidiscus hugii*. There are, in addition, several other bioevents with regional to global correlation potential, which can be used as secondary markers to constrain the boundary in the absence of the index species. Their stratigraphic position, from bottom to top in the section, is as follows (Fig. 24):

- Bed 138: FO of the planktonic foraminifera species *Lilliputianella roblesae* and *Lilliputianella semielongata*. These events mark the base of the *L. semielongata* Zone. Both species have been recorded in the western Tethys (from Spain to Iran) and Mexico. *Lilliputianella semielongata* is also present in boreholes

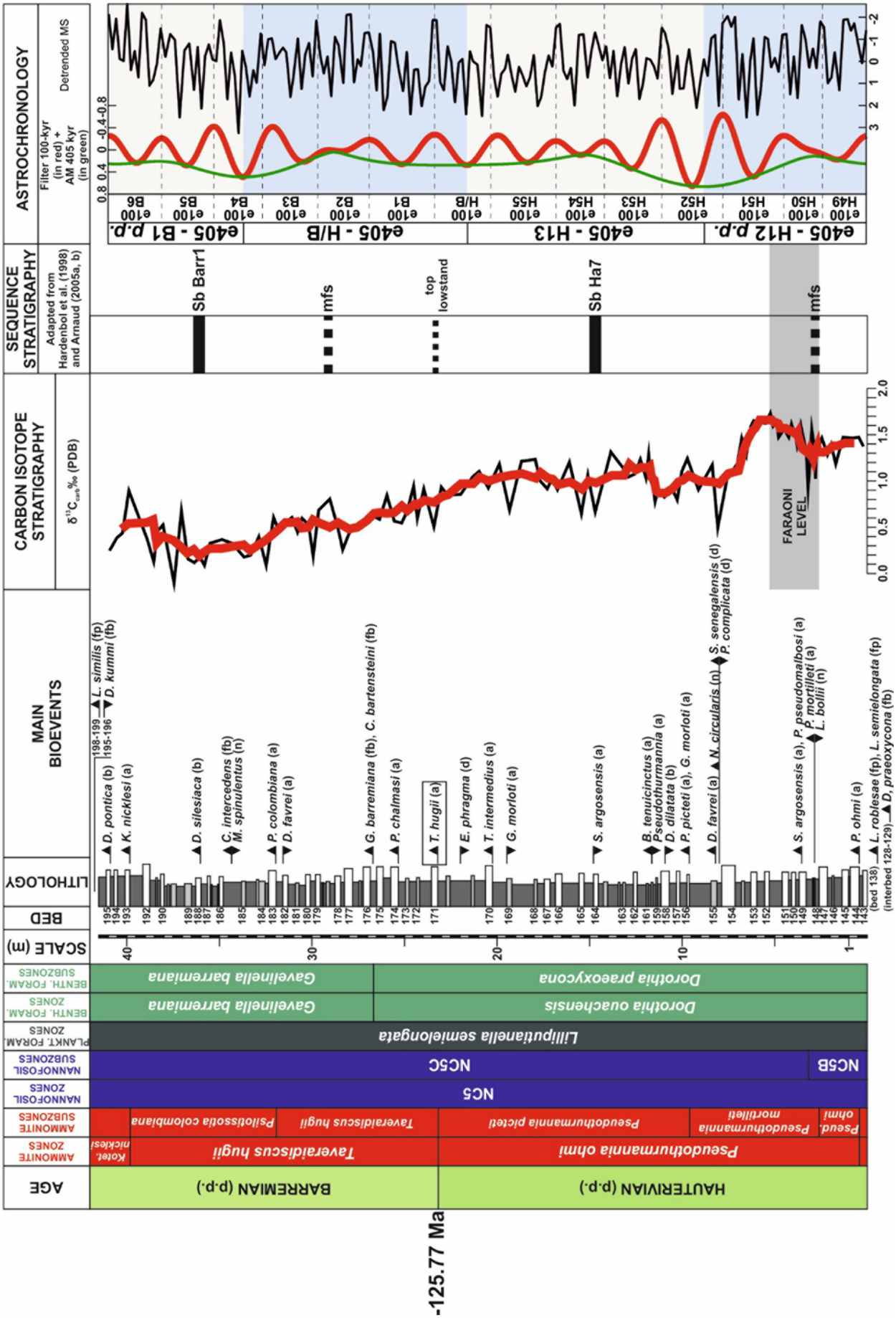

Figure 24. Río Argos section. Primary and secondary biostratigraphic markers (a: ammonite; b: belemnite; d: dinocyst; fb: benthic foraminifer; fp: planktonic foraminifer); n: calcareous nannofossil) for the Hauterivian/Barremian boundary, C isotope stratigraphy, sequence stratigraphy and astrochronology.

in the eastern North Atlantic and western North Pacific.

- Bed 144: FO of the ammonite genus *Pseudothurmannia* (species *Pseudothurmannia ohmi*). This genus is present throughout the western Tethys (from Morocco to Georgia) and also in the Caribbean area (Mexico and Cuba).
- Bed 148: LO of the calcareous nannofossil species *Lithraphidites bollii*. This event, which coincides with the base of the FLE, marks the boundary between NC5B and NC5C calcareous nannofossil Subzones. It is a rather reliable event in moderate to well preserved nannofossil assemblages. However, in poor to moderate assemblages, *L. bollii* can be difficult to differentiate from etched/overgrown broken specimens of *Lithraphidites carniolensis*. Poor preservation and/or reworking could artificially extend the LO of *L. bollii* and the upper range of the NC5B Subzone. This could explain some records of this species above the FLE (e.g., Channell et al., 1995; Erba et al., 1999). *L. bollii* is a typically Tethyan species, having been reported from Spain to Iran, but it is also present in the southern Andes (Neuquén and Magallanes basins) and North Atlantic boreholes.
- Bed 148: FO of the ammonite species *Pseudothurmannia mortilleti* and *Sabaudiella simplex*. The latter species is the first representative of the genus *Sabaudiella*, which is present in both the Mediterranean and Andean regions.
- Bed 149: FO of the ammonite species *Pseudothurmannia pseudomalbosi* and *Sabaudiella argosensis*. Both species are restricted to the Mediterranean region.
- Interbed 154–155: FO of the calcareous nannofossil species *Nannoconus circularis* (typical forms). *Nannoconus circularis* is mostly recorded from low-latitude assemblages, but also in some temperate latitudes (NW Germany) in periods of Tethyan warm-water influxes (Mutterlose and Ruffell, 1999).
- Interbed 154–155: FO of the dinoflagellate species *Subtilisphaera senegalensis*, and LO of the dinoflagellate species *Palaecysta complicata*. The former species is a typically low latitude taxon, whereas the latter one has also been found in higher latitudes (eastern Canada, England, Germany, Siberia).
- Bed 155: FO of the ammonite species *Discoidellia favrei*, reported from the Mediterranean region and Cuba.
- Bed 156: FO of the ammonite species *Pseudothurmannia picteti* and *Garroniceras morloti*. Both species are restricted to the Mediterranean region.
- Bed 158: LO of the belemnite species *Duvalia dilatata*, distributed throughout the Mediterran–Caucasian Subrealm.
- Bed 160: LO of the ammonite genus *Pseudothurmannia*, and FO of the ammonite species *Barremites tenuicinctus*. The latter is the first species strictly attributable to *Barremites*, a genus that has been reported from the western Tethys (from Morocco to Georgia), Caribbean area (Mexico and Cuba), California and Japan.
- Bed 164: LO of the ammonite species *Sabaudiella argosensis*.
- Bed 169: LO of the ammonite species *Garroniceras morloti*.
- Bed 170: FO of the ammonite species *Taveraidiscus intermedius*, widely distributed in the western Tethys (from Spain to Georgia).
- Interbed 170–171: LO of the dinoflagellate species *Exiguisphaera phragma*. This species has been recorded in both Tethyan and Boreal realms, and in boreholes in the North Atlantic and Indian Oceans. However, as indicated above, the exact position of this event cannot be accurately calibrated as none of the samples from the *T. hugii* AZ yielded identifiable dinocysts.
- Bed 171: FO of the ammonite species *Taveraidiscus hugii* (base of the Barremian). As mentioned above, the geographic distribution of the primary marker extends along the northern margin of the Mediterran–Caucasian Subrealm (from Spain to Georgia).
- Bed 174: FO of the ammonite species *Psilotissotia chalmasi*, known from the Mediterranean region. Specimens attributed of this species have also been reported from Colombia, but their identity is doubtful.
- Interbed 175–176: FO of the benthic foram species *Gavelinella barremiana* and *Conorotalites bartensteini*. The two species have a wide geographic distribution. *Gavelinella barremiana* is considered to be an important stratigraphic marker of the Barremian, occurring in both Tethyan and Boreal realms, and in boreholes in the Atlantic, Indian and Pacific Oceans (Giraldo-Gómez et al., 2022). *Conorotalites bartensteini* has been reported from the Mediterranean region and NW Europe, and in boreholes in North Atlantic and Arctic Oceans.
- Bed 182: LO of the ammonite species *Discoidellia favrei*.
- Bed 183: FO of the ammonite species *Psilotissotia colombiana*, known from France, Spain and Colombia.
- Interbed 185–186: LO of the calcareous nannofossil species *Micrantholithus spinulentus*. This species has been recorded in the Mediterrran–Caucasian subrealm (Spain, Iran), and boreholes in the North Atlantic Ocean (Blake Basin and Galicia Margin).
- Interbed 185–186: FO of the benthic foram species *Conorotalites intercedens*, widely distributed in the Mediterranean region and NW Europe, and boreholes in North Atlantic and Arctic Oceans.
- Bed 188: FO of the belemnite species *Duvalia silesiaca*, known from the Mediterranean region.
- Bed 193: FO of the ammonite species *Kotetishvilia nicklesi*, reported throughout the Mediterran–Caucasian subrealm, from Morocco to Armenia.
- Bed 195: FO of the belemnite species *Duvalia pontica*, recorded throughout the Mediterranean region.
- Interbed 195–196: LO of the benthic foram species *Dorothia kummi.* This species has been found in the Mediterranean region, NW Europe, and boreholes in the North Atlantic Ocean.

Further auxiliary marker criteria, with global correlation potential, are provided by non-biostratigraphic methods:

- The base of the Barremian correlates with the beginning of a gradual negative trend in the C-isotope curve near bed 170. The trend to lower C-isotope values is preceded by a 10-meter interval with stable C-isotope compositions. The positive C-isotope excursion related to the Faraoni Episode follows below the stable interval.
- Published data (Bodin et al., 2009) provide a Sr-isotope value of 0.707470 for the lowermost Barremian in the Angles section.
- Indirect calibration to the magnetostratigraphic scale suggests that the Hauterivian–Barremian boundary falls in the lowermost part of polarity chron M3r.
- The boundary is located in the depositional sequence Ha7, corresponding approximately to the transgressive surface of the sequence.
- The cyclostratigraphic analysis indicates a duration of 0.80 myr for the *P. ohmi* AZ and of 0.56 myr for the *T. hugii* AZ. The time

interval from the start of the Faraoni Episode to the Hauterivian–Barremian boundary is assessed at 0.74 myr. The base of the Barremian Stage is dated at 125.77 Ma.

Correlation

Outer Platform to Basin Settings

Due to a persistent regressive sea level trend during the latest Hauterivian and the early Barremian (Hardenbol et al., 1998; Haq, 2014), many marine basins became isolated, or even emerged, which triggered a high degree of endemicity among many organic groups, strongly hampering interregional correlation (Mutterlose, 1992; Rawson et al., 1996; Lehmann et al., 2015). This is the case, in particular, for ammonites, belemnites and calcareous nannofossils, whereas the record of planktonic foraminifera is, in general, rather poor, and mostly restricted to the western Tethys and North Atlantic Ocean. As previously mentioned, the ammonite species *T. hugii*, the primary marker for the Hauterivian/Barremian boundary, has not been reported outside the Mediterran–Caucasian subrealm, but no other event appears to constitute a better alternative for defining and correlating the base of the Barremian. In the following paragraphs we will discuss, using available biostratigraphic and non-biostratigraphic markers, the possibilities of correlation of the Hauterivian/Barremian boundary in open marine successions in other geographic areas outside the Tethyan realm.

Historically, particular attention has been paid to the correlation between Tethyan and Boreal realms. In the Boreal Atlantic subrealm, the Hauterivian/Barremian boundary has been placed either at the base of the *Fissicostaticeras rarocinctum* AZ (Rawson, 1971; Kemper, 1976; Mutterlose and Wiedenroth, 2009) or at the base of the *Craspedodiscus variabilis* AZ, equivalent to the upper part of the *Craspedodiscus discofalcatus* AZ (Kemper et al., 1981; Rawson, 1995). These correlations were based on the occurrence in this stratigraphic interval, in both NE England and N Germany, of trituberculate crioconic ammonites, such as *Paracrioceras spathi* and *Paracrioceras strombecki,* closely resembling *Emericiceras* gr. *thiollierei*/*emericii*, a group of Tethyan species that appears in the uppermost part of the *P. picteti* ASz and ranges into the *T. hugii* AZ. Nevertheless, Kakabadze and Hoedemaeker (2010) noted that similar trituberculate heteromorphs are already present in lower levels in N Germany, so resemblances with the Tethyan species may merely be due to morphological convergence. More relevant for correlation purposes are data from Crimea and North Caucasus. In these two regions, *Craspedodiscus discofalcatus* and other Boreal simbirskitids co-occur with specimens of the genus *Pseudothurmannia* (Kakabadze, 1983; Baraboshkin, 2002, 2004a), which confirms that the *C. discofalcatus* AZ of the Boreal standard scale proposed by Baraboshkin (2004b) is, at least in part, equivalent to the *P. ohmi* AZ of the Mediterranean standard scheme. To gain further insight on the Hauterivian/Barremian boundary correlation it is necessary to resort to non-biostratigraphic events. In the Russian Platform, Baraboshkin and Guzhikov (2018) reported the probable local equivalent of the Faraoni Level at the base of the *C. discofalcatus* AZ, in the middle part of chron M5n, i.e. in the same magnetostratigraphic position as in the central Italian sections. Also, according to these authors, the Boreal Hauterivian/Barremian boundary, drawn at the top of the *C. discofalcatus* AZ, is placed in the lowermost part of chron M3r, coinciding with the magnetostratigraphic calibration proposed here for the base of the Barremian in the Mediterranean region (see above). This chronostratigraphic coincidence of the Hauterivian/Barremian boundary in the two realms is furtherly supported by the available strontium-isotope stratigraphic record (Mutterlose et al., 2014), and by the recorded LO of the dinocyst *E. phragma* at the base of the *F. rarocinctum* AZ in the Boreal realm (Leereveld, 1995).

Not less problematic is the correlation with the Andean region. In the Neuquén Basin (west-central Argentina), Aguirre-Urreta and Rawson (2012) proposed the *Sabaudiella riverorum* AZ for beds, at the top of the Agrio Formation, that had previously not yielded ammonites and had been included in the upper part of the *Paraspiticeras groeberi* AZ. They correlated this latter zone with the *Pseudothurmannia catulloi* ASz (= *P. mortilleti* ASz) and the lower part of the *P. picteti* ASz of the Mediterranean standard zonation, and the *S. riverorum* AZ with the upper part of the *P. picteti* AZ and the lower part of the basal Barremian *T. hugii* AZ. More recently, however, Aguirre-Urreta et al. (2019) have correlated the *S. riverorum* AZ with the uppermost part of the *B. balearis* AZ and the whole *P. ohmi* AZ. In our opinion, the stratigraphic coincidence, both in the Neuquén Basin (Aguirre-Urreta et al., 2019) and in the Mediterranean region, of the LO of the calcareous nannofossil *Lithraphidites bollii*, the FO of the genus *Sabaudiella*, and a negative excursion in the carbon isotope ratios rather suggests that the base of the *S. riverorum* AZ should be equated to the base of the *P. mortilleti* ASz. The *S. riverorum* beds are overlain by continental sediments of the basal Huitrín Formation, which mark a regression and the beginning of the disconnection of the Neuquén Basin from the Pacific Ocean. This regression could be related to the sea level fall associated with the sequence boundary Ha7 (Hardenbol et al., 1998), dated from the upper part of the *P. picteti* ASz.

Analogously, in the Chañarcillo Basin (northern Chile), the beds with *Paraspiticeras* and *Sabaudiella* from the lower part of the Upper Nantoco Member were correlated by Mourgues (2007) with the *P. mortilleti* and *P. picteti* ASzs. These beds are followed by the subtidal to supratidal deposits of the uppermost Nantoco Formation evincing an important regression phase in the basin. The lower part of the overlying Totoralillo Formation is barren of ammonites. Its middle part has yielded an ammonite assemblage composed exclusively by endemic species (*Shasticrioceras* AZ) that was tentatively correlated with the upper part of the *T. hugii* AZ and the lower part of the *K. nicklesi* AZ (Aguirre-Urreta et al., 2007).

The late Hauterivian–early Barremian interval is represented in most of the Austral Basin (southern Patagonian Andes) by the organic-rich, outer shelf to basinal facies of the Río Mayer Formation (Arbe, 2002). Two ammonite associations, made up mostly of endemic taxa, have been recognized in this interval (Riccardi, 1984; Aguirre-Urreta, 1993): a lower *Favrella wilckensi* AZ, in which the index species coexists with *Protaconeceras patagoniense* and *Homeomorphites varicostatus*, and an upper *Hatchericeras patagonense* AZ, with several species of the genus *Hatchericeras*, *Cryptocrioceras yrigoyeni*, *Malgasaynella besairiei*, *Sanmartinoceras africanum insignicostatum* and *Homeomorphites varicostatus*. Other species of the genus *Protaconeceras* have been recorded from the *Craspedodiscus gottschei* Zone in eastern England and the *Subsaynella sayni* Zone in SE France

(Kemper et al., 1981), which has led to the assignment of an early late Hauterivian age to the *F. wilckensi* AZ (Riccardi et al., 1987). The age of the *H. patagonense* Zone is more debatable, but the presence of *C. yrigoyeni*, a species that shows affinities with some members of the subfamily Gassendiceratinae, would suggest an early late Barremian age for this biostratigraphic unit. In fact, both ammonite assemblages are separated by a barren interval about 200 meters thick (Riccardi et al., 1987), so the Hauterivian/Barremian boundary would most likely lie somewhere in that interval. Unfortunately, the results of foraminifera and calcareous nanofossils studies (Malumián & Náñez, 2002; Concheyro and Angelozzi, 2002) are also inconclusive and there are no data available on other non-biostratigraphic markers.

Hauterivian and Barremian marine sediments are also well represented in different lithostratigraphic units of central and northern Colombia, with the Paja Formation in the Villa de Leyva region being the best documented succession (Patarroyo, 2020). This thick unit (up to 940 m), Hauterivian to late Aptian in age, and composed mainly of slightly calcareous, finely laminated dark shales, contains a diverse and well-preserved fossil pelagic fauna (marine reptiles, fish and ammonites), plant remains and a depauperate benthic association (microbial mats, thin-shelled bivalves, and very rare foraminifera and other invertebrates) (Noè and Gómez-Pérez, 2020). The middle member of the Paja Formation bears a rich ammonite fauna, which has many elements in common with the Mediterranean assemblages and which enables the identification of most of the Barremian (Bürgl, 1956; Etayo-Serna, 1968; Patarroyo, 2000, 2004). The base of this member, where *Psilotissotia colombiana* has been recorded, correlates with the upper part of the *T. hugii* AZ. The underlying lower member of the Paja Formation, a ~350 m thick interval of black shales with some siltstone and limestone intercalations, has yielded identifiable ammonites only near its base, namely several species of early Hauterivian *Olcostephanus* (Etayo-Serna, 1968). It is therefore not possible to accurately fix the position of the Hauterivian/Barremian boundary in this succession. Also, the available C- and Sr-isotope stratigraphic data (Moreno-Sánchez and Hincapié-Jaramillo, 2010) are not detailed enough to allow a reliable correlation.

In the North American Pacific Coast ranges, rocks of Hauterivian and Barremian age occur only in a few localities in northern California, southwestern Oregon, and British Columbia (Popenoe et al., 1960; Jeletzky, 1970). The best known succession, corresponding to the lower part of the Buden Canyon Formation, outcrops in the Ono–Cottonwood area (Shasta County, northern California). Ammonite faunas of the latest Hauterivian–early Barremian interval show marked endemism also in this region, where two local range zones, the *Hertleinites aguila* AZ and the *Shasticrioceras patricki* AZ, have been recognized. Imlay (1960) dated the association of *H. aguila* AZ, present in the Ogo Member, as late Hauterivian, based mainly on its stratigraphic position and on the morphological similarity between the index species, *H. aguila*, and the genus *Craspedodiscus*, whose species characterize the sediments of that age throughout the Boreal realm. Murphy (1975) introduced the *S. patricki* AZ for the ammonite assemblage present at the base of the Lower Chickabally Member and attributed to it a late early Barremian age, arguing for the presence in this assemblage of a pulchelliid similar to *Kotetishvilia compressissima*. It should be noted that both ammonite assemblages are separated by an interval several hundred meters thick, mostly corresponding to the conglomeratic Roaring River Member, in which no identifiable ammonites have been found. Murphy (1975) also pointed out that the base of the Barremian would probably have to be located in the upper part of the *H. aguila* AZ, where the first representatives of the genus *Barremites* appeared. This idea was later confirmed by Fernando et al. (2011) in a study that combined calcareous nannofossil biostratigraphy, which did not provide conclusive data on the position of the Hauterivian–Barremian boundary, and magnetostratigraphy, which placed the base of the M3r chron in the upper part of the Ogo Member.

Late early to late Barremian open marine sediments, with rich ammonite assemblages, are widely distributed in Japan (Obata and Matsukawa, 2007, 2009; Matsukawa and Obata, 2015; Matsukawa, 2017, 2018, 2022). In contrast, ammonite reports from terminal Hauterivian or basal Barremian are very scarce. Matsukava et al (2007) and Matsukawa and Fukui (2009) described an ammonite assemblage from the Hida–Furukawa region composed of *'Pseudothurmannia* aff. *baleare*, *Phyllopachyceras infundibulum*, and *Acrioceras (Paraspinoceras)* sp.'. Simultaneously, Goto (2007) reported the finding in the Uchinamigawa area of a specimen of *Pseudothurmannia* sp., a determination later corroborated by Matsukawa and Asahara (2010). Both ammonite records come from the middle part of the Tetory Group, a thick Middle Jurassic–Early Cretaceous sequence mainly consisting of continental deposits with some marine intercalations. This unit outcrops in the Inner Zone of central Japan and is a key element to better understand the tectonic events and the evolution of the terrestrial ecosystems in East Asia (Matsukawa et al., 2006; Sano, 2015). In this context, the mentioned ammonite records were taken as evidence of a transgressive episode around the Hauterivian/Barremian boundary (Matsukawa et al, 2007; Matsukawa and Fukui, 2009; Sano, 2015). However, the revision of the Japanese specimens reveals that those attributed to the genus *Pseudothurmannia* show closer affinities with *Crioceratites* gr. *duvalii/villiersianus*, whereas *Acrioceras (Paraspinoceras)* can be reinterpreted as *Megacrioceras* cf. *doublieri*. Consequently, the actual age of this ammonite assemblage is more likely early late Hauterivian, more in line with the radiometric age (130.7 ± 0.8 Ma) obtained in supposedly age equivalent units (Sano, 2015). With the currently available data it is therefore not possible to accurately locate the Hauterivian/Barremian boundary in the Tetori Group succession. However, detailed ongoing studies on C-isotope stratigraphy (T. Hasegawa, 2022, pers. com.) might shed light on this issue in the near future.

As can be seen, the aforementioned endemicity problems and the presence of discontinuities and facies changes in the stratigraphic successions, together with the lack of continuous, detailed and reliable records of biostratigraphic and non-biostratigraphic events, make the correlation with other palaeogeographic domains particularly difficult. These same issues preclude, for now, the selection of Standard Auxiliary Boundary Stratotypes, as recently approved by ICS (Head et al. 2022), whose designation broadly follows the same requirements established for GSSPs. Hopefully, in the future, some of these sequences will be known in sufficient detail to meet these requirements and allow us to extend our knowledge and understanding of the Hauterivian/Barremian boundary to other palaeogeographical contexts.

Shallow-water Carbonate Platforms

These environments are represented by the Urgonian limestones in many of the Tethyan margins during the Early Cretaceous. Organisms such as rudist bivalves, corals, large benthic foraminifera, and dasycladalean algae dominate in these facies, while ammonites, benthic foraminifera, and calcareous nannofossils are virtually absent. This has hindered the accurate dating of the Urgonian formations and the study of their palaeogeographical evolution. In recent years, however, reliable calibration of the stratigraphic ranges of orbitolinids against ammonite scales for the late Hauterivian–early Aptian interval has been provided (Clavel et al., 2009, 2010; Granier et al., 2013, 2021; Frau et al., 2021, 2023). These authors studied several sections in SE France in which strata bearing orbitolinids are immediately overlying or underlying or even bounded by strata bearing ammonites.

According to the latest version of this calibration (Granier et al., 2021), most of the orbitolinids present in the Upper Hauterivian span the Hauterivian–Barremian boundary and have little biostratigraphic value. Two species (*Paleodictyoconus beckerae* and *Valserina primitiva*) have their LOs in the in the uppermost Hauterivian *P. ohmi* AZ. Six other species have their FOs in the lowermost Barremian *T. hugii* AZ: *Valserina turbinata* (which is restricted to the lower Barremian), *Cribellopsis schroederi*, *Orbitolinopsis cuvillieri*, *Orbitolinopsis kiliani*, *Orbitolinopsis buccifer*, and *Vanneauina vercorii*., although there is a recent striking record of the last two species in upper Berriasian limestones of eastern Serbia (Schlagintweit & Bucur, 2021). *Eopalorbitolina pertenuis* has its LO near the boundary between the *T. hugii* and *K. nicklesi* AZs, whereas the emblematic *Palorbitolina lenticularis* appears somewhat higher, in the *Nicklesia pulchella* AZ.

Dasycladalean algae are also diverse in the Urgonian facies from the Hauterivian to the Aptian. Most of them have long stratigraphic ranges, although some are of stratigraphic interest. A preliminary calibration against ammonite zonation was presented by Clavel et al (2007), later modified by Clavel et al. (2014). According to the data of these authors, among the species present in the Hauterivian, *Angioporella neocomiensis* and *Suppiluliumaella corbarica* seem to become extinct in the late Hauterivian, while *Deloffrella hauteriviana* reaches the Barremian and would have its LO around the limit between the *T. hugii* and *K. nicklesi* AZs.

Non-marine Settings

No analysis has been carried out on the distribution of sporomorphs in the Río Argos section. According to Leereveld (1997), these fossil remains are scarce and poorly preserved.

It seems that charophytes are the most promising group for long-distance correlations in continental environments. Pérez-Cano et al. (2021) have recently proposed a Barremian–early Aptian Eurasian charophyte biozonation, whose index species were widely distributed from Western Europe to China. The lowest unit of this zonation is the *Atopochara trivolvis* var. *triquetra* Zone, which correlates the interval between the uppermost Hauterivian and the lower Barremian *N. pulchella* AZ. This calibration is based on the finding of lacustrine layers containing charophytes interfingered between Urgonian limestones with orbitolinids and dasycladales in the French Jura and Subalpine Chains (Martín-Closas et al., 2009) and on dating by means of strontium isotope stratigraphy in sections of the Iberian Chain (NE Spain) (Pérez-Cano et al., 2021). Other charophytes occurring in the *A. trivolvis* var. *triquetra* Zone in the so-called Tethyan Archipelago (Western Europe and North Africa) are *Globator maillardii* var. *trochiliscoides*, *G. maillardii* var. *biutricularis*, *Clavator grovesii* var. *gautieri*, *Clavator harrisii* var. *dongjingensis*, *C. harrisii* var. *harrisii*, *C. harrisii* var. *reyi*, *Clavator calcitrapus* var. *jiangluoensis*, *Ascidiella stellata* var. *stellata*, *A. stellata* var. *lata*, *Ascidiella triquetra*, *Ascidiella iberica* var. *iberica*, *Hemiclavator adnatus*, *Hemiclavator neimongolensis* var. *posticecaptus*, and *Pseudoglobator fourcadei*.

According to Pérez-Cano et al. (2021), the *A. trivolvis* var. *triquetra* Zone would be equivalent to the *Ascidiella iberica* Zone proposed by Feist et al. (1995) in the Wealdean Basin in England, in which *A. trivolvis* var. *triquetra* and *A. iberica* var. *iberica* co-occur. This validates the placing of the Hauterivian/Barremian boundary "near the base of the upper division of the Weald Clay" suggested by Feist et al. (1995). A similar conclusion was reached by Hoedemaeker (1999) and Hoedemaeker and Herngreen (2003) by sequence stratigraphy correlation.

The association of *A. trivolvis* var. *triquetra* and *C. harrisii* var. *harrisii* has been reported from several localities in NE China (Wang and Lu, 1982; Martín-Closas and Wang, 2008; Martín-Closas, 2015; Pérez-Cano et al., 2021). It is present in the Jiufotang Formation of the Jehol Group (Wang et al., 2008), which would suggest a latest Hauterivian–early Barremian age for this formation containing the late Jehol Biota. However, radiometric dating indicates a younger age for the Jiufotang Formation, between ~123 and ~119 Ma (Yu et al., 2021), which corresponds to the late Barremian–early Aptian according to the most up-to-date numerical age models (Gale et al. al., 2020; Martinez et al., 2020; Zhang et al., 2021). In contrast, an earliest Barremian age fits better for the lower–middle part (Lujiatun, Lower Lava and Jianshangou members) of the underlying Yixian Formation, which hosts the middle Jehol Biota and is radiometrically dated between ~125.3 and ~125.9 Ma, according to the most recent data (Chang et al., 2017; Zhong et al., 2021; Li et al., 2022). Nevertheless, as highlighted by Li et al. (2022), at least part of this stratigraphic interval, namely the Lower Lava and Jiufotang members, show a normal magnetic polarity (Pan et al., 2001; Zhu et al., 2007), whereas the earliest Barremian coincides, according to what is currently accepted, with chron M3r (Gale, 2020; Ogg, 2020; see above). These inconsistencies deserve further scrutiny in order to pinpoint the temporal evolution of the exceptional Jehol Biota.

The assemblage of the *A. trivolvis* var. *triquetra* Zone, represented by the index species and *C. calcitrapus* var. *jiangluoensis* has also been recognized in Argentina (Musacchio, 1989; Pérez-Cano et al., 2020, 2021). It has been recorded in the lower part of the La Amarga Formation, a continental unit which unconformably overlies the uppermost Hauterivian marine sediments of the Agrio Formation in the southern sector of the Neuquén Basin, and is equivalent to the above mentioned Huitrín Formation (Leanza and Hugo, 2011).

Conclusions

The Río Argos section (Caravaca, SE Spain) has been confirmed as the Global Boundary Stratotype Section (GSSP) for the base of the

Barremian Stage. The section meets most of the requirements of the ICS guidelines for the establishment of global chronostratigraphic standards. The interval analysed is ~40 m thick and embraces the uppermost Hauterivian *P. ohmi* AZ and the lowermost Barremian *T. hugii* AZ. It is very well exposed, without synsedimentary or tectonic disturbances. The lithological succession, consisting of a rhythmic marlstone-limestone alternation, without gaps, condensations or facies changes, evidences a continuous sedimentation, accumulated at an average rate of 2.9 cm.kyr^{-1} in an open marine environment. Both macrofossils (mainly ammonites) and microfossils (mainly calcareous nannofossils and foraminifera) are abundant and well preserved.

The base of the Barremian Stage is defined at the base of bed 171 of the Río Argos section (at 22.8 m from the base of the section) by the first appearance of the ammonite species *Taveraidiscus hugii*. In addition to the primary marker, about thirty secondary biostratigraphic markers with regional to global correlation potential are identified in the studied interval. These bioevents correspond to ammonites, belemnites, calcareous nannofossils, benthic and planktonic foraminifera, and organic-walled dinocysts. The Hauterivian/Barremian boundary falls in the middle part of the NC5C calcareous nannofossil Subzone, in the middle of the *Lilliputianella semielongata* planktonic foraminifera Zone, and near the top of the *Dorothia ouachensis* benthic foraminifera Zone.

Further auxiliary marker criteria, with global correlation potential, are provided by non-biostratigraphic tools. The base of the Barremian correlates with the beginning of a gradual negative trend in the C-isotope curve, preceded by a stable interval, which follows the positive excursion related to the Faraoni Episode. Previously published data provide a Sr-isotope value of 0.707470 for the lowermost Barremian. Indirect calibration to the magnetostratigraphic scale suggests that the boundary falls in the lowermost part of polarity chron M3r. It is located in the depositional sequence Ha7, corresponding approximately to the transgressive surface of the sequence. Finally, according to the astrochronological analysis, a time interval of 0.74 myr separates the start of the Faraoni Episode from the base of the Barremian, which is dated at 125.77 MA.

Acknowledgements

We thank the Voting Members of the International Subcommission on Cretaceous Stratigraphy and of the International Commission on Stratigraphy for comments that helped to improve the final version of the proposal. Maria Rose Petrizzo, Chair of the International Subcommission on Cretaceous Stratigraphy, deserves special thanks for her many suggestions and her constant support and encouragement. We also thank the reviewer Camille Frau for his useful comments and corrections. We acknowledge financial support by the Spanish Ministry of Science and the International Subcommission on Cretaceous Stratigraphy.

References

Aguado, R., 1994, Nannofósiles del Cretácico de la Cordillera Bética (sur de España). Bioestratigrafía. Universidad de Granada, Granada, 413 p.

Aguado, R., 2012, Two new Cretaceous calcareous nannofossils from SE Spain and Tunisia. Journal of Nannoplankton Research, v. 32, pp. 53–57.

Aguado, R., Company, M., O'Dogherty, L., Palomo, I., Sandoval, J., and Tavera, J.M., 2008, Integrated stratigraphy of the uppermost Hauterivian–lower Barremian pelagic sequence of Arroyo Gilico (Betic Cordillera, SE Spain). Abstracts 1st International Meeting on Correlations of Cretaceous Micro– and Macrofossils, 2008, Berichte der Geologischen Bundesanstalt, v. 74, pp. 36–37.

Aguado, R., Company, M., O'Dogherty, L., Sandoval, J., and Tavera, J.M., 2014, Late Hauterivian–early Barremian calcareous nannofossil biostratigraphy, palaeoceanography, and stable isotope record in the Subbetic domain (southern Spain). Cretaceous Research, v. 49, pp. 105–124.

Aguirre-Urreta, M.B., 1993, Neocomian ammonite biostratigraphy of the Andean basins of Argentina and Chile. Revista Española de Paleontología, v. 8, pp. 53–74.

Aguirre-Urreta, M.B., and Rawson, P.F., 2012, Lower Cretaceous ammonites from the Neuquén Basin, Argentina: A new heteromorph fauna from the uppermost Agrio Formation. Cretaceous Research, v. 35, pp. 208–216.

Aguirre-Urreta, M.B., Mourgues, F.A., Rawson, P.F., Bulot, L.G., and Jaillard, E., 2007, The Lower Cretaceous Chañarcillo and Neuquén Andean basins: ammonoid biostratigraphy and correlations. Geological Journal, v. 42, pp. 143–173.

Aguirre-Urreta, M.B., Schmitz, M., Lescano, M., Tunik, M., Rawson, P.F., Concheyro, A., Buhler, M., and Ramos, V.A., 2017, A high precision U–Pb radioisotopic age for the Agrio Formation, Neuquén Basin, Argentina: Implications for the chronology of the Hauterivian Stage. Cretaceous Research, v. 75, pp. 193–204.

Aguirre-Urreta, M.B., Martinez, M., Schmitz, M., Lescano, M., Omarini, J., Tunik, M., Kuhnert, H., Concheyro, A., Rawson, P.F., Ramos, V.A., Reboulet, S., Noclin, N., Frederichs, T., Nickl, A.L., and Pälike, H., 2019, Interhemispheric radio-astrochronological calibration of the time scales from the Andean and the Tethyan areas in the Valanginian–Hauterivian (Early Cretaceous). Gondwana Research, v. 70, pp. 104–132.

Arana Castillo, R., Guillén Mondéjar, F., Mancheño Jiménez, M.A., Manteca Martínez, J.I., Ramo Jiménez, A. del, Rodríguez Estrella, T., Santisteban Bové, C. de, and Romero Sánchez, G., 2009, Actualización del inventario de lugares de interés geológico en la Región de Murcia. Consejería de Agricultura y Agua, Murcia, 254 p.

Arbe, H.A., 2002, Análisis estratigráfico del Cretácico de la Cuenca Austral. In: Haller, M.J. (Ed.), Geología y recursos naturales de la provincia de Santa Cruz. Relatorio del XV Congreso Geológico Argentino, 2002, pp. 103–128.

Arnaud, H., 2005a, The South-East France Basin and its Mesozoic evolution. Géologie Alpine, série "Colloques et excursions", v. 7, pp. 5–28.

Arnaud, H., 2005b, Sequence stratigraphy interpretation. Géologie Alpine, série "Colloques et excursions", v. 7, pp. 174–179.

Arnaud-Vanneau, A., and Arnaud, H., 1990, Hauterivian to Lower Aptian carbonate shelf sedimentation and sequence stratigraphy in the Jura and northern Subalpine chains (southeastern France and Swiss Jura). In: Tucker, M.E., Wilson, J.L., Crevello, P.D., Sarg, J.R., and Read, J.F. (Eds.), Carbonate platforms: Facies, sequences and evolution. International Association of Sedimentologists, Special Publication 9, pp. 203–233.

Avram, E., 1983, Barremian ammonite zonation in the Carpathian area. Zitteliana, v. 10, pp. 509–514.

Baraboshkin, E.J., 2002, Early Cretaceous seaways of the Russian Platform and the problem of the Boreal/Tethyan correlation. In: Michalík, J. (Eds.), Tethyan/Boreal correlation. Mediterranean and Boreal Cretaceous paleobiogeographic areas in central and eastern Europe. VEDA, Bratislava, pp. 39–78

Baraboshkin, E.J., 2004a, Boreal–Tethyan correlation of Lower Cretaceous ammonite scales. Moscow University Geology Bulletin, v. 59, pp. 9–20.

Baraboshkin, E.J., 2004b, The Lower Cretaceous ammonite zonal stan-

dard of the Boreal Realm. Bulletin of the Moscow Society of Naturalists, Geological series, v. 79, pp. 44–68 (in Russian).

Baraboshkin, E.J., and Guzhikov, A.Y., 2018, The Boreal Lower Cretaceous of Russia: revision of the stage boundaries on the base of non-paleontological data. Proceedings of 9th All-Russian Conference, 2018, Belgorod, pp. 47–53 (in Russian).

Bartolocci, P., Beraldini, M., Cecca, F., Faraoni, P., Marini, A., and Pallini, G., 1992, Preliminary results on correlation between Barremian ammonites and magnetic stratigraphy in Umbria–Marche Apennines (Central Italy). Palaeopelagos, v. 2, pp. 63–68.

Barrier, E., Vrielynck, B., Brouillet, J.F., and Brunet, M.F., 2018. Paleotectonic Reconstruction of the Central Tethyan Realm: Tectono-Sedimentary-Palinspastic maps from Late Permian to Pliocene. Commission for the Geological Map of the World (CGMW), Paris, Atlas of 20 maps.

Baudin, F., 2005, A Late Hauterivian short-lived anoxic event in the Mediterranean Tethys: the 'Faraoni Event'. Comptes Rendus Geoscience, v. 337, pp. 1532–1540.

Baudin, F., and Riquier, L., 2014, The late Hauterivian Faraoni 'Oceanic Anoxic Event': an update. Bulletin de la Société Géologique de France, v. 185, pp. 359–377.

Baudin, F., Bulot, L.G., Cecca, F., Coccioni, R., Gardin, S., and Renard, M., 1999, Un équivalent du "Niveau Faraoni" dans le Bassin du Sud-Est de la France, indice possible d'un événement anoxique fini-hauterivien étendu à la Téthys méditérranéenne. Bulletin de la Société Géologique de France, v. 170, pp. 487–498.

Bellanca, A., Erba, E., Neri, R., Premoli Silva, I., Sprovieri, M., Tremolada, F., and Verga, D., 2002, Palaeoceanographic significance of the Tethyan 'Livello Selli' (Early Aptian) from the Hybla Formation, northwestern Sicily: biostratigraphy and high-resolution chemostratigraphic records. Palaeogeography, Palaeoclimatology, Palaeoecology, v. 185, pp. 175–196.

Bersezio, R., Erba, E., Gorza, M., and Riva, A., 2002, Berriasian–Aptian black shales of the Maiolica formation (Lombardian Basin, Southern Alps, Northern Italy): local to global events. Palaeogeography, Palaeoclimatology, Palaeoecology, v. 180, pp. 253–275.

Birkelund, T., Hancock, J.M., Hart, M.B., Rawson, P.F., Remane, J., Robaszynski, F., Schmid, F., and Surlyk, F., 1984, Cretaceous stage boundaries—Proposals. Bulletin of the Geological Society of Denmark, v. 33, pp. 3–20.

Bodin, S., Godet, A., Föllmi, K.B., Vermeulen, J., Arnaud, H., Strasser, A., Fiet, N., and Adatte, T., 2006a, The late Hauterivian Faraoni oceanic anoxic event in the western Tethys: Evidence from phosphorus burial rates. Palaeogeography, Palaeoclimatology, Palaeoecology, v. 235, pp. 245–264.

Bodin, S., Godet, A., Vermeulen, J., Linder, P., and Föllmi, K.B., 2006b, Biostratigraphy, sedimentology and sequence stratigraphy of the latest Hauterivian–early Barremian drowning episode of the Northern Tethyan margin (Altmann Member, Helvetic nappes, Switzerland). Eclogae Geologicae Helvetiae, v. 99, pp. 157–174.

Bodin S., Godet, A., Matera, V., Steinmann, P., Vermeulen, J., Gardin, S., Adatte, T., Coccioni, R., and Föllmi, K., 2007, Enrichment of redox-sensitive trace metals (U, V, Mo, As) associated with the late Hauterivian Faraoni ocanic anoxic event. International Journal of Earth Sciences, v. 96, pp. 327–341.

Bodin, S., Fiet, N., Godet, A., Matera, V., Westermann, S., Clément, A., Janssen, N.M.M., Stille, P., and Föllmi, K.B., 2009, Early Cretaceous (late Berriasian to early Aptian) palaeoceanographic change along the northwestern Tethyan margin (Vocontian Trough, southeastern France): $\delta^{13}C$, $\delta^{18}O$ and Sr-isotope belemnite and whole-rock records. Cretaceous Research, v. 30, pp. 1247–1262.

Braga, J.C., Company, M., Linares, A., Rivas, P., and Sandoval, J., 1982, Contribución al conocimiento bioestratigráfico del Hauteriviense-Barremense en la región de Jaén. Cuadernos de Geología Ibérica, v. 8, pp. 677–689.

Bralower, T.J., Leckie, R.M., Sliter, W.V., and Thierstein, H.R., 1995, An integrated Cretaceous microfossil biostratigraphy. In: Berggren, W.A., Kent, D.V., Aubry, M.P., and Hardenbol, J. (Eds.), Geochronology, Time Scales and Global Stratigraphic Correlation. SEPM, Special Publication 54, pp. 65–79.

Bürgl, H., 1956, Catálogo de las amonitas de Colombia, Parte I: Pulchelliidae. Boletín Geológico, v. 4, pp. 1–119.

Busnardo, R., 1965a, Le stratotype du Barrémien. 1.Lithologie et macrofaune. Colloque sur le Crétacé inférieur, 1963, Mémoires du Bureau de Recherches Géologiques et Minières, v. 34, pp. 101–116.

Busnardo, R., 1965b, Rapport sur l'étage Barrémien. Colloque sur le Crétacé inférieur, 1963, Mémoires du Bureau de Recherches Géologiques et Minières, v. 34, pp. 161–169.

Busnardo, R., 1984, Crétacé inférieur. Echelles biostratigraphiques. Ammonites. In: Debrand-Passard, S., Courbouleix, S., and Lienhardt, M.J. (Eds.), Synthèse géologique du Sud-Est de la France, Mémoires du Bureau de Recherches Géologiques et Minières, v. 125, pp. 292–294.

Busnardo, R., and Vermeulen, J., 1986, La limite Hauterivien–Barrémien dans la région stratotypique d'Angles (Sud-Est de la France). Comptes Rendus de l'Académie des Sciences, v. 302, série II, pp. 457–459.

Busnardo, R., Charollais, J., Weidmann, M., and Clavel, B., 2003, Le Crétacé inférieur de la Veveyse de Châtel (Ultrahélvetique des Préalpes externes; canton de Fribourg, Suisse). Révue de Paléobiologie, v. 22, pp. 1–174.

Busnardo, R., Granier, B., Clavel, B., and Charollais, J., 2013, Ammonitofaune du Barrémien de la coupe de L'Estellon (Baronnies, France): résultats biostratigraphiques préliminaires. Carnets de Géologie [Notebooks on Geology], Article 2013/03 (CG2013_A03), pp. 139–162.

Castro, J.M., Gea, G.A. de, Ruiz-Ortiz, P.A., and Nieto, L.M., 2008, Development of carbonate platforms on an extensional (rifted) margin: the Valanginian–Albian record of the Prebetic of Alicante (SE Spain). Cretaceous Research, v. 29, pp. 848–860.

Cecca, F., Marini, A., Pallini, G., Baudin, F., and Begouën, V., 1994a, A guide-level of the uppermost Hauterivian (Lower Cretaceous) in the pelagic succession of Umbria–Marche Apennines (Central Italy): the Faraoni Level. Rivista Italiana di Paleontologia e Stratigrafia, v. 99, pp. 551–568.

Cecca, F., Pallini, G., Erba, E., Premoli Silva, I., and Coccioni, R., 1994b, Hauterivian–Barremian chronostratigraphy based on ammonites, nannofossils, planktonic foraminifera and magnetic chrons from the Mediterranean domain. Cretaceous Research, v. 15, pp. 457–467.

Cecca, F., Faraoni, P., Marini, and Pallini, G., 1995, Field-trip across the representative sections for the upper Hauterivian–Barremian ammonite biostratigraphy in the Maiolica exposed at Monte Nerone, Monte Petrano and Monte Catria (Umbria–Marche Apennines). Memorie Descrittive della Carta Geologica d'Italia, v. 51, pp. 187–211.

Chang, S.C., Gao, K.Q., Zhou, C.F., and Jourdan, F., 2017, New chronostratigraphic constraints on the Yixian Formation with implications for the Jehol Biota. Palaeogeography, Palaeoclimatology, Palaeoecology, v. 487, pp. 399–406.

Channell, J.E.T., Cecca, F., and Erba, E., 1995, Correlations of Hauterivian and Barremian (Early Cretaceous) stage boundaries to polarity chrons. Earth and Planetary Science Letters, v. 134, pp. 125–140.

Channell, J.E.T., Erba, E., Muttoni, G., and Tremolada, F., 2000, Early Cretaceous magnetic stratigraphy in the APTICORE drill core and adjacent outcrop at Cismon (Southern Alps, Italy), and correlation to the proposed Barremian–Aptian boundary stratotype. Geological Society of America Bulletin, v. 112, pp. 1430–1443.

Clavel, B., Charollais, J., Schroeder, R., and Busnardo, R., 1995, Réflexions sur la biostratigraphie du Crétacé inférieur et sur sa complémentarité avec l'analyse séquentielle: exemple de l'Urgonien jurassien et subalpin. Bulletin de la Société Géologique de France, v. 166, pp. 663–680.

Clavel, B., Charollais, J., Conrad, M., Jan du Chêne, R., Busnardo, R., Gardin, S., Erba, E., Schroeder, R., Cherchi, A., Decrouez, D., Granier, B., Sauvagnat, J., and Weidmann, M., 2007, Dating and progradation

of the Urgonian limestone from the Swiss Jura to South-East France. Zeitschrift der Deutschen Gesellschaft für Geowissenschaften, v. 158, pp. 1025–1062.

Clavel, B., Busnardo, R., Charollais, J., Conrad, M., and Granier, B., 2009, Nouvelles données sur la répartition biostratigraphique des orbitolinidés à l'Hauterivien supérieur, au Barrémien et à l'Aptien inférieur dans le Sud-Est de la France et le Jura franco-suisse. Archives des Sciences, v. 62, pp. 125–146.

Clavel, B., Busnardo, R., Charollais, J., Conrad, M., and Granier, B., 2010, Répartition biostratigraphique des orbitolinidés dans la biozonation à ammonites (plate-forme urgonienne du Sud-Est de la France). Partie 1 : Hauterivien supérieur-Barrémien basal. Carnets de Géologie [Notebooks on Geology], Article 2010/06 (CG201_A06), pp. 1–53.

Clavel, B., Charollais, J., Busnardo, R., Granier, B., Conrad, R., Desjacques, P., and Metzger, J., 2014, La plate-forme carbonatée urgonienne (Hauterivien supérieur-Aptien inférieur) dans le Sud-Est de la France et en Suisse: synthèse. Archives des Sciences, v. 67, pp. 1–100.

Coccioni, R., 2020, Revised upper Barremian–upper Aptian planktonic foraminiferal biostratigraphy of the Gorgo a Cerbara section (central Italy). Newsletter on Stratigraphy, v. 53, pp. 275–295.

Coccioni, R., and Galeotti, S., 1993, Orbitally induced cycles in benthonic foraminiferal morphogroups and trophic structure distribution patterns from the Late Albian "Amadeus Segment" (Central Italy). Journal of Micropalaeontology, v. 12, 227–239.

Coccioni, R., and Premoli Silva, I., 1994, Planktonic foraminifera from the Lower Cretaceous of Rio Argos sections (southern Spain) and biostratigraphic implications. Cretaceous Research, v. 15, pp. 645–687.

Coccioni, R., Baudin, F., Cecca, F., Chiari, M., Galeotti, S., Gardin, S., and Salvini, G., 1998, Integrated stratigraphic, palaeontological, and geochemical analysis of the uppermost Hauterivian Faraoni Level in the Fiume Bosso section, Umbria–Marche Apennines, Italy. Cretaceous Research, v. 19, pp. 1–23.

Coccioni, R., Marsili, A., and Venturati, A., 2004, Chamber elongation in Early Cretaceous planktonic foraminifera: a case study from the Lower Hauterivian–Lower Aptian Rio Argos succession (southern Spain). Proceedings of the 1st Italian Meeting on Environmental Micropaleontology, 2002. Grzybowski Foundation, Special Publication 9, pp. 37–47.

Coccioni, R., Luciani, V., and Marsili, A., 2006, Cretaceous oceanic anoxic events and radially elongated chambered planktonic foraminifera: Paleoecological and paleoceanographic implications. Palaeogeography, Palaeoclimatology, Palaeoecology, v. 235, pp. 66–92.

Coccioni, R., Premoli Silva, I., Marsili, A., and Verga, D., 2007, First radiation of Cretaceous planktonic foraminifera with radially elongate chambers at Angles (Southeastern France) and biostratigraphic implications. Revue de Micropaléontologie, v. 50, pp. 215–224.

Company, M., Sandoval, J., and Tavera, J.M., 1992, Secuencias deposicionales en el Barremiense-Aptiense inferior de la Sierra del Corque (Cordillera Bética): consideraciones paleogeográficas. Revista de la Sociedad Geológica de España, v. 5, pp. 55–63.

Company, M., Sandoval, J., and Tavera, J.M., 1995. Lower Barremian ammonite biostratigraphy in the Subbetic Domain (Betic Cordillera, southern Spain). Cretaceous Research, v. 16, pp. 243–256.

Company, M., Sandoval, J., and Tavera, J.M., 2002, Ammonite bioevents and zonation of the uppermost Hauterivian in the Betic Cordillera (SE Spain). Documents des Laboratoires de Géologie de Lyon, v. 156, pp. 83–84.

Company, M., Sandoval, J., and Tavera, J.M., 2003, Ammonite biostratigraphy of the uppermost Hauterivian in the Betic Cordillera (SE Spain). Geobios, v. 36, pp. 685–694.

Company, M., Aguado, R., Sandoval, J., Tavera, J.M., Jiménez de Cisneros, C., and Vera, J.A. 2005, Biotic changes linked to a minor anoxic event (Faraoni Level, latest Hauterivian, Early Cretaceous). Palaeogeography, Palaeoclimatology, Palaeoecology, v. 224, pp. 186–199.

Company, M., Főzy, I., Sandoval, J., and Tavera, J.M., 2006, *Deitanites* n.g. and other related ammonites. Their significance within the family Holcodiscidae (Lower Cretaceous, Mediterranean region). Neues Jahrbuch für Geologie und Paläontologie, Monatshefte, v. 2006, pp. 1–14.

Company, M., Sandoval, J., Tavera, J.M., Aoutem, M, and Ettachfini, M., 2008. Barremian ammonite faunas from the western High Atlas, Morocco—biostratigraphy and palaeobiogeography. Cretaceous Research, v. 29, pp. 9–26.

Company, M., Sandoval, J., and Tavera J.M., 2010, Los géneros *Crioceratites* y *Pseudothurmannia* (Ancyloceratina, Ammonitida) del Hauteriviense superior (Cretácico inferior) de la Cordillera Bética. Resúmenes del III Congreso Ibérico de Paleontología y XXVI Jornadas de la Sociedad Española de Paleontología, 2010, pp. 96–99.

Company, M., Aguado, R., Baudin, F., Boulila, S., Coccioni, R., Deconinck, J.F., Frontalini, F., Giusberti, L., Martinez, M., Moiroud, M., Monna, F., O'Dogherty, L., Pellenard, P., Rawson, P.F., Riquier, L., Romero, G., Sandoval, J., Tavera, J.M., and Weissert, H., 2013, The Río Argos section (Caravaca Spain) candidate for GSSP of the lower boundary of the Barremian stage. Abstracts of 9th International Symposium on the Cretaceous System, 2013, p. 90.

Company, M., Aguado, R., Baudin, F., Boulila, S., Coccioni, R., Deconinck, J.F., Frontalini, F., Giusberti, L., Martinez, M., Moiroud, M., Monna, F., O'Dogherty, L., Pellenard, P., Rawson, P.F., Riquier, L., Romero, G., Sandoval, J., Tavera, J.M., and Weissert, H., 2017, The Barremian GSSP—state of the art. Abstracts of 10th International Symposium on the Cretaceous System, 2017. Berichte der Geologischen Bundesanstalt, v. 120, p. 54.

Concheyro, A., and Angelozzi, G.N., 2002, Nanofósiles calcáreos. In: Haller, M.J. (Eds.), Geología y recursos naturales de la provincia de Santa Cruz. Relatorio del XV Congreso Geológico Argentino, 2002, pp. 519–531.

Coquand, H., 1862, Sur la convenance d'établir dans le groupe inférieur de la formation crétacée un nouvel étage entre le néocomien proprement dit (couches à *Toxaster complanatus* et à *Ostrea Couloni*) et le néocomien supérieur (étage urgonien d'Alc. d'Orbigny). Bulletin de la Société Géologique de France, 2ème série, v. 19, pp. 531–541.

Déres, F., and Achéritéguy, J., 1980, Biostratigraphie des nannoconidés. Bulletin des Centres de Recherche Exploration-Production Elf Aquitaine, v. 4, pp. 1–53.

Erba, E., Channell, J.E.T., Claps, M., Jones, C., Larson, R., Opdyke, B., Premoli Silva, I., Riva, A., Salvini, G., and Torricelli, S., 1999, Integrated stratigraphy of the Cismon APTICORE (Southern Alps, Italy): a "reference section" for the Barremian–Aptian interval at low latitudes. Journal of Foraminiferal Research, v. 29, pp. 371–391.

Espitalié, J., Deroo, G., and Marquis, F., 1985, La pyrolyse Rock-Eval et ses applications. Revue de l'Institut Français du Pétrole, v. 40, pp. 563–579.

Etayo-Serna, F., 1968, Sinopsis estratigráfica de la región de Villa de Leiva y zonas próximas. Boletín de Geología, v. 21, pp. 19–32.

Feist, M., Lake, R. D., and Wood, C. J., 1995, Charophyte biostratigraphy of the Purbeck and Wealden of Southern England. Palaeontology, v. 38, pp. 407–442.

Fernández-López, S., 1997, Ammonites, clinos tafonómicos y ambientes sedimentarios. Revista Española de Paleontología, v. 12, pp. 102–128.

Fernández-López, S., Duarte, L.V., and Henriques, M.H.P., 2000, Ammonites from lumpy limestones in the lower Pliensbachian of Portugal: taphonomic analysis and palaeoenvironmental implications. Revista de la Sociedad Geológica de España, v. 13, pp. 3–15.

Fernando, A.G.S., Nishi, H., Tanabe, K., Moriya, K., Iba, Y., Kodama, K., Murphy, M.A., Okada, H., 2011, Calcareous nannofossil biostratigraphic study of forearc basin sediments: Lower to Upper Cretaceous Budden Canyon Formation (Great Valley Group), northern California, USA. Island Arc, v. 20, pp. 346–370.

Frau, C., Tendil, A.J.B., Masse, J.P., Richet, R., Borgomano, J.R., Lanteaume, C., and Robert, E., 2021, Revised biostratigraphy and regional correlations of the Urgonian southern Vercors carbonate platform, southeast France. Cretaceous Research, v. 124, 104773.

Frau, C., Tendil, A.J.B., and Lanteaume, C., 2023, New insights into the platform-to-basin anatomy of the Urgonian Bas-Vivarais Domain (Lower Cretaceous; SE France). Journal of Geography, Environment and Earth Science International, v. 27, pp. 19–47.

Friedrich, O., Reichelt, K., Herrle, J.O., Lehmann, J., Pross, J., and Hemleben, C., 2003, Formation of the Late Aptian Niveau Fallot black shales in the Vocontian Basin (SE France): evidence from foraminifera, palynomorphs, and stable isotopes. Marine Micropaleontology, v. 49, pp. 65–85.

Gale, A.S., Mutterlose, J., Batenburg, S., Gradstein, F.M., Agterberg, F.P., Ogg, J.G., and Petrizzo, M.R., 2020, The Cretaceous Period. In: Gradstein, F.M., Ogg, J.G., Schmitz, M.D., and Ogg, G.M. (Eds.), Geologic Time Scale 2020. Elsevier, Amsterdam, pp. 1023–1086.

Gea, G.A. de, 2004, Bioestratigrafía y eventos del Cretácico Inferior en las Zonas Externas de la Cordillera Bética. Universidad de Jaén, Jaén, 658 p.

Giraldo-Gómez, V.M., Petrizzo, M.R., Erba, E., and Bottini, C., 2022, Biostratigraphy, paleobathymetry and paleobiogeography of Lower Cretaceous benthic foraminifera from Shatsky Rise (ODP Leg 198) in the central Pacific Ocean. Cretaceous Research, v. 138, 105283.

Godet, A., Bodin, S., Föllmi, K.B., Vermeulen, J., Gardin, S., Fiet, N., Adatte, T., Berner, Z., Stüben, D., and van de Schootbrugge, B., 2006, Evolution of the marine stable carbon-isotope record during the Early Cretaceous: A focus on late Hauterivian and Barremian in the Tethyan realm. Earth and Planetary Science Letters, v. 242, pp. 254–271.

Goto, M., 2007, An Early Cretaceous ammonoid from the Itoshiro Subgroup of the Tetori Group in the Uchinami River area of Ohno City, Fukui Prefecture. Memoir of the Fukui Prefectural Dinosaur Museum, v. 6, pp. 27–34 (in Japanese).

Granier, B., Clavel, B., Moullade, M., Busnardo, R., Charollais, J., Tronchetti, G., and Desjacques, P., 2013, L'Estellon (Baronnies, France), a "Rosetta Stone" for the Urgonian biostratigraphy. Carnets de Géologie [Notebooks on Geology], Article 2013/04 (CG2013_A04), pp. 163–207.

Granier, B., Clavel, B., Busnardo, R., Charollais, J., Desjacques, P., and Bert, D., 2021. Biostratigraphic distribution of orbitolinids in the ammonite biozones (Urgonian platform of sotheastern France). Part 2: Barremian p.p. Carnets de Géologie, 21 (18), pp. 399–521.

Gressier, V., 2010, Contribution des producteurs carbonatés phytoplanctoniques à l'évolution isotopique ($\delta^{13}C$ et $\delta^{18}O$) des carbonates pélagiques des bassins Ouest téthysiens au cours de l'événement Valanginien (Weissert Event). PhD Thesis, Université Pierre et Marie Curie, Paris, 291 p. (unpublished).

Grosheny, D., Beaudoin, B., Morel, L., and Desmares, D., 2006, High-resolution biostratigraphy and chemostratigraphy of the Cenomanian/Turonian boundary event in the Vocontian Basin, southeast France. Cretaceous Research, v. 27, pp. 629–640.

Haq, B.U., 2014, Cretaceous eustasy revisited. Global and Planetary Change, v. 113, pp. 44–58

Hardenbol, J., Thierry, J., Farley, M.B., Jacquin, T., Graciansky, P.C. de, and Vail, P.R., 1998, Mesozoic and Cenozoic sequence chronostratigraphic framework of European basins. In: Graciansky, P.C. de, Hardenbol, J., Jacquin, T., and Vail, P.R. (Eds.), Mesozoic and Cenozoic sequence stratigraphy of European basins. SEPM, Special Publication 60, pp. 3–13 and Chart 5 (Cretaceous sequence chronostratigraphy).

Head, M.J., Aubry, M.P., Piller, W.E., and Walker, M., 2022, Standard Auxiliary Boundary Stratotype (SABS) approved to support the Global boundary Stratotype Section and Point (GSSP). Episodes, v. 46, pp. 99–100.

Hoedemaeker, P.J., 1992, Río Argos (Hauterivian–Barremian boundary). Excursion guide, 2nd Workshop of the Lower Cretaceous Cephalopod Team (IGCP Project 262: Tethyan Cretaceous Correlation), 1992, pp. 26–34.

Hoedemaeker, P.J., 1995, Ammonite distribution around the Hauterivian–Barremian boundary along the Río Argos (Caravaca, SE Spain). Géologie Alpine, Mémoire H.S., v. 20, pp. 219–277.

Hoedemaeker, P.J., 1998, Berriasian–Barremian sequences in the Río Argos succession near Caravaca (southeast Spain) and their correlation with some sections in southeast France. In: Graciansky, P.C. de, Hardenbol, J., Jacquin, T., and Vail, P.R. (Eds.), Mesozoic and Cenozoic sequence stratigraphy of European basins. SEPM, Special Publication, 60, pp. 423–441.

Hoedemaeker, P.J., 1999, A Tethyan–Boreal correlation of pre-Aptian Cretaceous strata: correlating the uncorrelatables. Geologica Carpathica, v. 50, pp. 101–124.

Hoedemaeker, P.J., 2013, Genus *Pseudothurmannia* Spath, 1923 and related subgenera *Crioceratites (Balearites)* Sarkar, 1954 and *C. (Binelliceras)* Sarkar, 1977 (Lower Cretaceous Ammonoidea). Revue de Paléobiologie, v. 32, pp. 1–209.

Hoedemaeker, P.J., and Bulot, L.G., 1990, Preliminary ammonite zonation for the Lower Cretaceous of the Mediterranean region. Géologie Alpine, v. 66, pp. 123–127

Hoedemaeker, P.J., and Herngreen, G.F.W., 2003, Correlation of Tethyan and Boreal Berriasian–Barremian strata with emphasis on strata in the subsurface of the Netherlands. Cretaceous Research, v. 24, pp. 253–275.

Hoedemaeker, P.J., and Leereveld, H., 1995, Biostratigraphy and sequence stratigraphy of the Berriasian–lowest Aptian (Lower Cretaceous) of the Río Argos succession, Caravaca, SE Spain. Cretaceous Research, v. 16, pp. 195–230.

Hoedemaeker, P.J., Company, M. Aguirre-Urreta, M.B., Avram, E., Bogdanova, T.N., Bujtor, L., Bulot, L.G., Cecca, F., Delanoy, G., Ettachfini, M., Memmi, L., Owen, H.G., Rawson, P.F., Sandoval, J., Tavera, J.M., Thieuloy, J.P., Tovbina, S.Z., and Vašíček, Z., 1993, Ammonite zonation for the Lower Cretaceous of the Mediterranean region; basis for the stratigraphic correlations within IGCP-Project 262. Revista Española de Paleontología, v. 8, pp. 117–120.

Hoedemaeker, P.J., Krs, M., Man, O., Parés, J.M., Pruner, P., and Venhodová, D., 1998, The Neogene remagnetization and petromagnetic study of the Early Cretaceous limestone beds from the Río Argos (Caravaca, Province of Murcia, SE Spain). Geologica Carpathica, v. 49, pp. 15–32.

Hoedemaeker, P.J., Reboulet, S., Aguirre-Urreta, M.B., Alsen, P., Aoutem, M., Atrops, F., Barragán, R., Company, M., González-Arreola, C., Klein, J., Lukeneder, A., Ploch, I., Raisossadat S.N., Rawson, P.F., Ropolo, P., Vašíček, Z., Vermeulen, J., and Wippich, M.G.E., 2003, Report on the 1st International Workshop of the IUGS Lower Cretaceous Ammonite Working Group, the 'Kilian Group' (Lyon, 11 July 2002). Cretaceous Research, v. 24, 89–94.

Holbourn, A., and Kuhnt, W., 2002, Cenomanian–Turonian palaeoceanographic change on the Kerguelen Plateau: a comparison with Northern Hemisphere records. Cretaceous Research, v. 23, pp. 333–349.

Imlay, R.W., 1960, Ammonites of Early Cretaceous age (Valanginian and Hauterivian) from the Pacific Coast States. Geological Survey Professional Papers, v. 3334-F, pp. 167–228.

Jacquin, T., Rusciadelli, G., Amedro, F., Graciansky, P.C. de, and Magniez-Janin, F., 1998, The North-Atlantic cycle: An overview of 2nd-order transgressive/regressive facies cycles in the Lower Cretaceous of Western Europe. In: Graciansky, P.C. de, Hardenbol, J., Jacquin, T., and Vail, P.R. (Eds.), Mesozoic and Cenozoic sequence stratigraphy of European basins. SEPM, Special Publication 60, pp. 399–409.

Janssen, N.M.M., 1997, Mediterranean Neocomian belemnites, part 1: Río Argos sequence (province of Murcia, Spain): The Berriasian–Valanginian and the Hauterivian–Barremian boundaries. Scripta Geologica, v. 114, pp. 1–55.

Janssen, N.M.M., and Főzy, I., 2004, Neocomian belemnites from the Bersek-hegy (Gerecse Mountains, Hungary), part I: Late Valanginian to earliest Barremian. Fragmenta Palaeontologica Hungarica, v. 22, pp. 27–49.

Janssen, N.M.M., and Főzy, I., 2005, Neocomian belemnites from the Bersek-hegy (Gerecse Mountains, Hungary), part II: Barremian. Fragmenta Palaeontologica Hungarica, v. 23, pp. 59–86.

Janssen, N.M.M., Clément, A., and Bont, W., 2012, Mediterranean Neo-

comian belemnites, part 4: belemnites of the Barremian stratotype section. Carnets de Géologie [Notebooks on Geology, Memoir 2012/02 (CG2012_M02), pp. 201–274.

Jeletzky, J.A., 1970, Marine Cretaceous biotic provinces and paleogeography of Western and Arctic Canada: illustrated by a detailed study of ammonites. Geological Survey of Canada, Paper 70-22, pp. 1–92.

Kakabadze, M.V., 1983, On the Hauterivian–Barremian correlation between the south of the USSR and certain southern and northern regions of Europe. Zitteliana, v. 10, pp. 501–508.

Kakabadze, M.V., and Hoedemaeker, P.J., 2010, New data on Early Cretaceous (Hauterivian–Barremian) heteromorphic ammonites from northern Germany. Scripta Geologica, v. 140, pp. 1–168.

Kemper, E., 1976, Geologischer Führer durch die Grafschaft Bentheim und die angrenzenden Gebiete mit einem Abriß der emsländischen Unterkreide. Das Bentheimer Land, v. 64, pp. 1–206.

Kemper, E., Rawson, P.F., and Thieuloy, J.P., 1981, Ammonites of Tethyan ancestry in the early Lower Cretaceous of north-west Europe. Palaeontology, v. 24, pp. 251–311.

Kilian, W., 1888, Description géologique de la Montagne de Lure (Basses-Alpes). Masson, Paris, 458 p.

Kilian, W., 1896, Notice stratigraphique sur les environs de Sisteron et contributions à la connaissance des terrains secondaires du Sud-Est de la France. Bulletin de la Société Géologique de France, 3ème série, v. 23 (1895), pp. 659–803.

Kilian, W., 1910, Erste Abteilung: Unterkreide (Palaeocretacicum). Zweite Lieferung: Das bathyale Palaeocretacicum im südostlichen Frankreich. C: Barrême-Stufe (Barrémien). In: Frech, F. (Ed.), Lethaea Geognostica; II Teil: Das Mesozoicum; and 3: Kreide. Schweizerbart, Stuttgart, pp. 234–279.

Klein, J., 2005, Lower Cretaceous Ammonites I. Perisphinctaceae 1: Himalayitidae, Olcostephanidae, Holcodiscidae, Neocomitidae, Oosterelliidae. In: Riegraf, W. (Ed.), Fossilium Catalogus I: Animalia, Backhuys, Leiden, 484 p.

Laskar, J., Fienga, A., Gastineau, M., and Manche, H., 2011. La2010: a new orbital solution for the long-term motion of the Earth. Astronomy & Astrophysics, v. 532, A89.

Leanza, H.A., and Hugo, C.A., 2011, Las Formaciones La Amarga y Lohan Cura (Cretácico Temprano) en el depocentro de Picún Leufú. In: Leanza, H.A., Arregui, C., Carbone, O., Danieli, J.C., and Vallés, J.M. (Eds.), Geología y recursos naturales de la provincia del Neuquén. Relatorio del XVIII Congreso Geológico Argentino, 2011, pp. 223–230.

Leereveld, H., 1995, Dinoflagellate cysts from the Lower Cretaceous Río Argos succession (SE Spain). LPP Contributions Series, v. 2, 175 p.

Leerereveld, H., 1997, Hauterivian–Barremian (Lower Cretaceous) dinoflagellate cyst stratigraphy of the western Mediterranean. Cretaceous Research, v. 18, pp. 421–456.

Lehmann, J., Ifrim, C., Bulot, L., and Frau, C., 2015. Paleobiogeography of Early Cretaceous ammonoids. In: Klug, C., Korn, D., De Baets, K., Kruta, I., and Mapes, R.H. (Eds.), Ammonoid Paleobiology: From macroevolution to paleogeography, Topics in Paleobiology, v. 44, pp. 229–257.

Li, M.S., Kump, L.R., Hinnov, L.A., and Mann, M.E., 2018. Tracking variable sedimentation rates and astronomical forcing in Phanerozoic paleoclimate proxy series with evolutionary correlation coefficients and hypothesis testing. Earth and Planetary Science Letters, v. 501, pp. 165–179.

Li, Y.J., Jicha, B.R., Yu, Z.Q., Wu, H.C., Wang, X.L., Singer, B.S., He, H.Y., and Zhou, Z.G., 2022, Rapid preservation of Jehol Biota in Northeast China from high precision $^{40}Ar/^{39}Ar$ geochronology. Earth and Planetary Science Letters, v. 594, 117718.

Lowrie, W., and Alvarez, W, 1984, Lower Cretaceous magnetic stratigraphy in Umbrian pelagic limestone sections. Earth and Planetary Science Letters, v. 71, pp. 315–328.

Lukeneder, A., 2012, New biostratigraphic data on an upper Hauterivian–upper Barremian ammonite assemblage from the Dolomites (Southern Alps, Italy). Cretaceous Research, v. 35, pp. 1–21.

Lukeneder, A., Soták, J., Jovane, L., Giorgioni, M., Savian, J.F., Halásová, E., Reháková, D., Jósza, Š., Kroh, A., Florindo, F., and Sprovieri, M., 2016, Multistratigraphic records of the Lower Cretaceous (Valanginian–Cenomanian) Puez key area in N Italy. Palaeogeography, Palaeoclimatology, Palaeoecolology, v. 447, pp. 65–87.

Maeda, H., and Seilacher, A., 1996, Ammonoid taphonomy. In: Landman, N.H., Tanabe, K., and Davis, R.A. (Eds.), Ammonoid paleobiology. Topics in Paleobiology, v. 13, pp. 543–578.

Malumián, N., Náñez, C., 2002, Los foraminíferos, su significado geológico y ambiental. In: Haller, M.J. (Ed.), Geología y recursos naturales de la provincia de Santa Cruz. Relatorio del XV Congreso Geológico Argentino, 2002, pp. 481–493.

Martín-Closas, C., 2015, Cosmopolitanism in Northern Hemisphere Cretaceous Charophyta (Clavatoroidae). Palaeogeography, Palaeoclimatology, Palaeoecology, v. 438, pp. 9–23.

Martín-Closas, C., and Wang, Q.F., 2008, Historical biogeography of the lineage *Atopochara trivolvis* Peck 1941 (Cretaceous Charophyta). Palaeogeography, Palaeoclimatology, Palaeoecology, v. 260, pp. 435–451.

Martín-Closas, C., Clavel, B., Schroeder, R., Charollais, J., and Conrad, M.A., 2009, Charophytes from the Barremian–lower Aptian of the Northern Subalpine Chains and Jura Mountains, France: correlation with associated marine assemblages. Cretaceous Research, v. 30, pp. 49–62.

Martinez, M., 2018, Mechanisms of preservation of the eccentricity and longer-term Milankovitch cycles in detrital supply and carbonate production in hemipelagic marl-limestone alternations. In: Montenari, M. (Ed.), Cyclostratigraphy and Astrochronology. Stratigraphy & Timescales, v. 3, pp. 189–218.

Martinez, M., Pellenard, P., Deconinck, J.F., Monna, F., Riquier, L., Boulila, S, Moiroud, M., and Company, M., 2012. An orbital floating time scale of the Hauterivian–Barremian GSSP from a magnetic susceptibility signal (Río Argos, Spain). Cretaceous Research, v. 36, pp. 106–115.

Martinez, M., Deconinck, J.F., Pellenard, P., Riquier, L., Company, M., Reboulet, S., and Moiroud, M., 2015. Astrochronology of the Valanginian–Hauterivian stages (Early Cretaceous): Chronological relationships between the Paraná–Etendeka large igneous province and the Weissert and the Faraoni events. Global and Planetary Change, v. 131, pp. 158–173.

Martinez, M., Aguado, R., Company, M., Sandoval, J., and O'Dogherty, L., 2020. Integrated astrochronology of the Barremian Stage (Early Cretaceous) and its biostratigraphic subdivisions. Global and Planetary Change, v. 195, 103368.

Matsukawa, M., 2017, Barremian to Aptian (Lower Cretaceous) ammonite faunas of the Kochi Basin, southwest Japan. Bulletin of Tokyo Gakugei University, Division of Natural Sciences, v. 69, pp. 197–222.

Matsukawa, M., 2018, Barremian (Lower Cretaceous) ammonite fauna of the Arida Formation, Wakayama, Japan. Bulletin of Tokyo Gakugei University, Division of Natural Sciences, v. 70, pp. 99–119.

Matsukawa, M., 2022, Barremian–Aptian ammonite biostratigraphy of the Sanchu Cretaceous, Japan. Cretaceous Research, v. 137, 105245.

Matsukawa, M., and Asahara, T, 2010, Stratigraphy of the Tetori Group in the Uchinamigawa District, border area of Ishikawa and Fukui prefectures, central Japan, and correlation between its Hakusan Area and Kuzuryugawa Region. Bulletin of Tokyo Gakugei University, Division of Natural Sciences, v. 62, pp. 119–130 (in Japanese).

Matsukawa, M., and Fukui, M., 2009, Hauterivian–Barremian marine molluscan fauna from the Tetori Group in Japan and late Mesozoic marine transgressions in East Asia. Cretaceous Research, v. 30, pp. 615–631.

Matsukawa, M., and Obata, I., 2015, Barremian–Albian (Early Cretaceous) ammonite faunas of the Katsuuragawa Basin, southwest Japan.

Cretaceous Research, v. 56, pp. 25–52.
Matsukawa, M., Ito, M., Nishida, N., Koarai, K., Lockley, M.G., and Nichols, D.G., 2006, The Cretaceous Tetori biota in Japan and its evolutionary significance for terrestrial ecosystems in Asia. Cretaceous Research, 27, pp. 199–225.
Matsukawa, M., Fukui, M., Koarai, K., Asakura, T., and Aono, H, 2007, Discovery of a third marine transgression in the Tetori Group base on the restudy of stratigraphy of the group in Hida–Furukawa region, Gifu Prefecture, Japan. Jourrnal of the Geological Society of Japan, v. 113, pp. 417–437 (in Japanese).
McArthur, J.M., Janssen, N.M.M., Reboulet, S., Leng, M.J., Thirlwall, M.F., and van de Schootbrugge, B., 2007, Palaeotemperatures, polar ice-volume, and isotope stratigraphy (Mg/Ca, $\delta^{18}O$, $\delta^{13}C$, $^{87}Sr/^{86}Sr$): The Early Cretaceous (Berriasian, Valanginian, Hauterivian). Palaeogeography, Palaeoclimatology, Palaeoecology, v. 248, pp. 391–430.
Moiroud, M., Martinez, M., Deconinck, J.F., Monna, F., Pellenard, P., Riquier, L., and Company, M., 2012. High-resolution clay mineralogy as a proxy for orbital tuning: Example of the Hauterivian–Barremian transition in the Betic Cordillera (SE Spain). Sedimentary Geology, v. 282, pp. 336–346.
Moreno-Sánchez, M., and Hincapié-Jaramillo, G., 2010, Estudio de isótopos de carbono (delta ^{13}C) y estroncio ($^{87}Sr/^{86}Sr$) en los depósitos cretáceos-terciarios de la Cordillera Oriental. Universidad de Caldas, Manizales, 93 p.
Moullade, M., 1984, Intérét des petits foraminifères benthiques "profonds" pour la stratigraphie et l'analyse des paléoenvironnements océaniques mésozoiques. Proceedings of the 2nd International Symposium on Benthic Foraminifera, 1983, pp. 429–464.
Moullade, M., Tronchetti, G., Kuhnt, W., and Masse, J.P., 2000, Les Foraminifères benthiques et planctoniques du stratotype historique de l´Aptien inférieur dans la région de Cassis-La Bédoule (SE France). In: Moullade, M., Tronchetti, G., and Masse, J.P. (Eds.), Le stratotype historique de l´Aptien inférieur (Bédoulien) dans la région de Cassis-La Bédoule (SE France). Géologie Méditerranéenne, v. 25 (3–4) (1998), pp. 187–225.
Mourgues, F.A., 2007, *Sabaudiella* Vašíček & Hoedemaeker (Ancyloceratidae, Ammonoidea) in the Andean Lower Cretaceous Chañarcillo back-arc basin, northern Chile. Proceedings of the 4th European Meeting on the Palaeontology and Stratigraphy of Latin America, 2007. Cuadernos del Museo Geominero, v. 8, pp. 267–271.
Murphy, M.A., 1975, Paleontology and stratigraphy of the lower Chickaball Mudstone (Barremian–Aptian) in the Ono Quadrangle, northern California. University of California Publications in Geological Sciences, v. 113, pp. 1–52.
Musacchio, E. A., 1989, Biostratigraphy of non-marine Cretaceous of Argentina based on Calcareous microfossils. Proceedings of the 3rd International Cretaceous Symposium, 1987, pp. 811–850.
Mutterlose, J., 1989, Faunal and floral distribution in late Hauterivian rhythmic bedded sequences and their implications. Proceedings of the 3rd International Cretaceous Symposium, 1987, pp. 691–713.
Mutterlose, J., 1992, Migration and evolution patterns of floras and faunas in marine Early Cretaceous sediments of NW Europe. Palaeogeography, Palaeoclimatology, Palaeoecology, v. 94, pp. 261–282.
Mutterlose, J., and Ruffell, A., 1999, Milankovitch-scale palaeoclimate changes in pale–dark bedding rhythms from the Early Cretaceous (Hauterivian and Barremian) of eastern England and northern Germany. Palaeogeography, Palaeoclimatology, Palaeoecology, v. 154, pp. 133–160.
Mutterlose, J., and Wiedenroth, K., 2009, Neue Tagesaufschlüsse der Unter-Kreide (Hauterive–Unter-Apt) im Großraum Hannover–Braunschweig: Stratigraphie und Faunenführung. Berliner paläobiologische Abhandlungen, v. 10, pp. 257–288.
Mutterlose, J., Bodin, S., and Fähnrich, L., 2014, Strontium-isotope stratigraphy of the Early Cretaceous (Valanginian–Barremian): Implications for Boreal–Tethys correlation and paleoclimate. Cretaceous Research, v. 50, pp. 252–263.
Noè, L.F., and Gómez-Pérez, M., 2020, Plesiosaurs, palaeoenvironments, and the Paja Formation Lagerstätte of central Colombia: An overview. In: Gómez, J., and Pinilla-Pachon, A.O. (Eds.), The Geology of Colombia, volume 2: Mesozoic, Servicio Geológico Colombiano, Bogotá, pp. 441–483.
Nyong E.E., and Ramanathan, R., 1985, A record of oxygen deficient paleoenvironments in the Cretaceous of the Calabar Flank, SE Nigeria. Journal of African Earth Sciences, v. 3, pp. 455–460.
Obata, I., and Matsukawa, M., 2007, Barremian–Aptian (Early Cretaceous) ammonoids from the Choshi Group, Honshu (Japan). Cretaceous Research, v. 28, pp. 363–391.
Obata, I., and Matsukawa, M., 2009, Some ammonoids from the Barremian and probable Albian of the Choshi Peninsula, Japan. Bulletin of Tokyo Gakugei University, Division of Natural Sciences, v. 61, pp. 97–103.
Ogg, J.G., 2020, Geomagnetic Polarity Time Scale. In: Gradstein, F.M., Ogg, J.G., Schmitz, M.D., and Ogg, G.M. (Eds.), Geologic Tine Scale 2020. Elsevier, Amsterdam, pp. 159–192.
Pan, Y.X., Zhu, R.X., John, S., and Zhou, Y.X., 2001, Magnetic polarity ages of the fossil-bearing strata at the Sihetun section, West Liaoning: A preliminary result. Chinese Science Bulletin, v. 46, pp. 1473–1476.
Patarroyo, P., 2000, Distribución de amonitas del Barremiano de la Formación Paja en el sector de Villa de Leyva (Boyacá, Colombia), Biostratigrafía. Geología Colombiana, v. 25, pp. 149–162
Patarroyo, P., 2004, Die Entwicklung der Ammoniten der Familie Pulchelliidae aus dem Barrême von Zentral-Kolumbien (Südamerika). Revue de Paléobiologie, v. 23, pp. 1–65.
Patarroyo, P., 2020, Barremian deposits of Colombia: A special emphasis on marine successions. In: Gómez, J., and Pinilla-Pachon, A.O. (Eds.), The Geology of Colombia, volume 2: Mesozoic, Servicio Geológico Colombiano, Bogotá, pp. 403–439.
Perch-Nielsen, K., 1985, Mesozoic calcareous nannofossils. In: Bolli, H.M., Saunders, J.B., Perch-Nielsen, K. (Eds.), Plankton stratigraphy. Cambridge University Press, Cambridge, pp. 329–426.
Pérez-Cano, J., Bover-Arnal, T., and Martín-Closas, C., 2020, Barremian charophytes from the Maestrat Basin. Cretaceous Research, v. 115, 104544.
Pérez-Cano, J., Bover-Arnal, T., and Martín-Closas, C., 2021, Barremian–early Aptian charophyte biostratigraphy revisited. Newsletters on Stratigraphy, v. 55, pp. 199–230.
Pictet, A., 2021, New insights on the Early Cretaceous (Hauterivian–Barremian) Urgonian lithostratigraphic units in the Jura Mountains (France and Switzerland): the Gorges de l'Orbe and the Rocher des Hirondelles formations. Swiss Journal of Geosciences, v. 114, 18.
Popenoe, W.P., Imlay, R.W., and Murphy, M.A., 1960, Correlation of the Cretaceous formations of the Pacific Coast (United States and northwestern Mexico). Bulletin of the Geological Society of America, v. 71, pp. 1491–1540.
Premoli Silva, I., Soldan, D.M., and Petrizzo, M.R., 2018, Upper Hauterivian–upper Barremian planktonic foraminiferal assemblages from the Arroyo Gilico section (southern Spain). Journal of Foraminiferal Research, v. 48, pp. 314–355.
Rawson, P.F., 1971, Lower Cretaceous ammonites from north-east England: the Hauterivian genus *Simbirskites*. Bulletin of the British Museum (Natural History), Geology, v. 20, pp. 25–86.
Rawson, P.F., 1983, The Valanginian to Aptian stages—current definitions and outstanding problems. Zitteliana, v. 10, pp. 493–500.
Rawson, P.F., 1995, The "Boreal" Early Cretaceous (Pre-Aptian) ammonite sequences of NW Europe and their correlation with the western Mediterranean faunas. Memorie Descrittive della Carta Geologica d'Italia, v. 51, pp. 121–130.
Rawson, P.F., Avram, E., Baraboshkin, E.J., Cecca, F., Company, M., Delanoy, G., Hoedemaeker, P.J., Kakabadze, M., Kotetishvili, E., Leereveld, H., Mutterlose, J., Salis, K. von, Sandoval, J., Tavera, J.M., and

Vašíček, Z., 1996, The Barremian stage. Bulletin de l'Institut Royal des Sciences Naturelles de Bélgique, v. 66-supp., pp. 25–30.

Reboulet, S., Klein, J., Barragán, R., Company, M., González-Arreola, C., Lukeneder, A., Raisossadat S.N., Sandoval, J., Szives, O., Tavera, J.M., Vašíček, Z., and Vermeulen, J., 2009, Report on the 3rd International Meeting of the IUGS Lower Cretaceous Ammonite Working Group, the "Kilian Group" (Vienna, Austria, 15th April 2008). Cretaceous Research, v. 30, 496–502.

Reboulet, S., Szives, O., Aguirre-Urreta, M.B., Barragán, R., Company, M., Frau, C., Kakabadze, M.V., Klein, J., Moreno-Bedmar, J.A., Lukeneder, A., Pictet, A., Ploch, I., Raisossadat S.N., Vašíček, Z., Baraboshkin, E.J., and Mitta V.V., 2018, Report on the 6th International Meeting of the IUGS Lower Cretaceous Ammonite Working Group, the Kilian Group (Vienna, Austria, 20th August 2017). Cretaceous Research, v. 91, 100–110.

Rey, J., 1993, Análisis de la cuenca subbética durante el Jurásico y el Cretácico en la transversal Caravaca-Vélez Rubio. Universidad de Granada, Granada, 460 p.

Rey, J., 1995, Sedimentation answers to local tectonic events in a pelagic swell (Subbetic Zone, province of Murcia, Spain). Bulletin de la Société Géologique de France, v. 166, pp. 479–491.

Riccardi, A.C., 1984, Las zonas de amonitas del Cretácico de la Patagonia (Argentina y Chile). Memoria del III Congreso Latinoamericano de Paleontología, 1984, pp. 396–405.

Riccardi, A.C., Aguirre-Urreta, M.B., and Medina, F.A., 1987, Aconeceratidae (Ammonitina) from the Hauterivian–Albian of southern Patagonia. Palaeontographica A, v. 196, pp. 105–185.

Rodríguez-Tovar, F.J., and Uchmann, A., 2017, The Faraoni event (latest Hauterivian) in ichnological record: The Río Argos section of southern Spain. Cretaceous Research, v. 79, pp. 109–121.

Roth, P.H., and Thierstein, H.R., 1972, Calcareous nannoplankton: Leg 14 of the Deep Sea Drilling Project. Initial Reports of the Deep Sea Drilling Project, v. 14, pp. 421–485.

Ruiz-Ortiz, P.A., Gea, G.A. de, and Castro, J.M., 2006, Timing of canyon-fed turbidite deposition in a rifted basin: The Early Cretaceous turbidite complex of the Cerrajón Formation (Subbetic, Southern Spain). Sedimentary Geology, v. 192, pp. 141–166.

Sano, S., 2015, New view of the stratigraphy of the Tetori group in central Japan. Memoir of the Fukui Prefectural Dinosaur Museum, v. 14, pp. 25–61.

Sauvage, L., Riquier, L., Thomazo, C., Baudin, F., and Martinez, M, 2013, The late Hauterivian Faraoni "Oceanic Anoxic Event" at Río Argos (southern Spain): An assessment on the level of oxygen depletion. Chemical Geology, v. 340, pp. 77–90.

Schlagintweit, F., and Bucur, I.I., 2021, The late Berriasian early evolutionary burst of the Orbitolinidae: New insights into taxonomy, origin, diversification and phylogeny of the family based on data from eastern Serbia. Carnets de Géologie, 21 (15), pp. 343–382.

Seilacher, A., 2007, Trace fossil analysis. Springer, Berlin, 225 p.

Sissingh, W., 1977, Biostratigraphy of Cretaceous calcareous nannoplankton. Geologie en Mijnbouw, v. 56, pp. 37–65.

Szives, O., Moreno-Bedmar, J.A., Aguirre-Urreta, M.B., Company, M., Frau, C., López-Horgue, M., Pictet, A., Ploch, I., Salazar, C., Barragán, R., Latil, J.L., Lehmann, J., Robert, E., and Reboulet, S., 2023, Report on the 7th International Meeting of the IUGS Lower Cretaceous Ammonite Working Group, the Kilian Group (Warsaw, Poland 21st August 2022): State of the art on the current Standard Ammonite Zonation of the Western Tethyan Mediterranean Province. Cretaceous Research, v. 153, 105716.

Tremolada, F., Erba, E., De Bernardi, B., and Cecca, F., 2009, Calcareous nannofossil fluctuations during the late Hauterivian in the Cismon core (Venetian Alps, northeastern Italy) and in selected sections of the Umbria–Marche Basin (central Italy): paleoceanographic implications of the Faraoni Level. Cretaceous Research, v. 30, pp. 505–514.

Tronchetti, G., and Grosheny, D., 1991, Les assemblages de foraminifères benthiques au passage Cénomanien-Turonien à Vergons, S-E France. Geobios, v. 24, pp. 13–31.

Vašíček, Z., and Hoedemaeker, P.J., 2003, Small Berriasian, lower Valanginian and Barremian heteromorphic ammonites from the Río Argos succession (Caravaca, southeast Spain). Scripta Geologica, v. 125, pp. 11–33.

Vašíček, Z., Michalík, J., and Borza, K., 1983, To the "Neocomian" biostratigraphy in the Krížna-Nappe of the Strážovské Vrchy Mountains (Northwestern Central Carpathians). Zitteliana, v. 10, pp. 467–483.

Veen, G.W. van, 1966, Note on a Jurassic–Cretaceous section in the Subbetic SW of Caravaca (prov. Murcia, Spain). Geologie en Mijnbouw, v. 45, pp. 391–397.

Veen, G.W. van, 1969. Geological investigations in the region west of Caravaca, south-eastern Spain. PhD thesis, University of Amsterdam, 143 pp. (unpublished).

Vera, J.A., 2001, Evolution of the South Iberian continental margin. In: Ziegler, P.A., Cavazza, W., Robertson, A.H.F., and Crasquin-Soleau, S. (Eds.), Peri-Tethyan rift/wrench basins and passive margins. Mémoires du Muséum National d'Histoire Naturelle, v. 186, pp. 109–143.

Vera, J.A., Arias, C., García-Hernández, M., López-Garrido, A.C., Martín-Algarra, A., Martín-Chivelet, J., Molina, J.M., Rivas, P., Ruiz-Ortiz, P.A., Sanz de Galdeano, C., and Vilas, L., 2004. Las Zonas Externas Béticas y el Paleomargen Sudibérico. In: Vera, J.A. (Ed.), Geología de España. Sociedad Geológica de España e Instituto Geológico y Minero de España, Madrid, pp. 354–361.

Vermeulen, J., 2003, Étude stratigraphique et paléontologique de la famille des Pulchelliidae (Ammonoidea, Ammonitina, Endemoceratacea). Géologie Alpine, Mémoire H.S., v. 42 (2002), pp. 1–333.

Vermeulen, J., 2005, Boundaries, ammonite fauna and main subdivisions of the stratotype of the Barremian. Géologie Alpine, série "Colloques et excursions", v. 7, pp. 147–173.

Vermeulen, J., Mascarelli, E., Borro, A., Lazarin, P., Lépinay, P., and Leroy, L., 2018, La limite Hauterivien-Barrémien à Barrême, sud-est de la France. Annales du Muséum d'Histoire Naturelle de Nice, v. 33, pp. 23–31.

Wang, Q.F., Lu, H.N., and Yang, J.L., 2008, Charophytes. In: Chang, M.M., Chen, P.J., Wang, Y.Q., Wang, Y., and Miao, D.S. (Eds.), The Jehol fossils the emergence of feathered dinosaurs, beaked birds and flowering plants. The Shanghai Scientific and Technical Publishers, Shangai, pp. 162–165.

Wang, Z., and Lu, H.N., 1982, Classification and evolution of Clavatoraceae with notes on its distribution in China. Bulletin of Nanjing Institute of Geology and Paleontology, Academia Sinica, v. 4, pp. 77–104 (in Chinese).

Westermann, G.E.G., 2000, Marine faunal realms of the Mesozoic: review and revision under the new guidelines for biogeographic classification and nomenclature. Palaeogeography, Palaeoclimatology, Palaeoecology, v. 163, pp. 49–68.

Yu. Z.Q., Wang, M., Li, Y.J., Deng, C.L., and He, H.Y., 2021, New geochronological constraints for the Lower Cretaceous Jiufotang Formation in Jianchang Basin, NE China, and their implications for the late Jehol Biota. Palaeogeography, Palaeoclimatology, Palaeoecology, v. 583, 110657.

Zhang, Y., Ogg, J.G., Minguez, D., Hounslow, M.W., Olaussen, S., Gradstein, F.M., and Esmeray-Senlet, S., 2021, Magnetostratigraphy of U–Pb-dated boreholes in Svalbard, Norway, implies that magnetochron M0r (a proposed Barremian–Aptian boundary marker begins at 121.2 ± 0.4 Ma. Geology, v. 49, pp. 733–737.

Zhong, Y.T., Huyskens, M.H., Yin, Q.Z., Wang, Y.Q., Ma, Q., and Xu, Y.G., 2021, High-precision geochronological constraints on the duration of 'Dinosaur Pompeii' and the Yixian Formation. National Science Review, v. 8, nwab063.

Zhu, R.X., Pan, Y.X., Shi, R.P., Liu, Q.S., and Li, D.M., 2007, Palaeomagnetic and $^{40}Ar/^{39}Ar$ dating constraints on the age of the Jehol Biota and the duration of deposition of the Sihetun fossil-bearing lake sediments, northeast China. Cretaceous Research, v. 28, pp. 171–176.

Miguel Company is 'Profesor Titular' (senior lecturer) at the Univesity of Granada (Spain) and chair of the Barremian Working Group of the International Subcommission on Cretaceous Stratigraphy. He teaches general and applied palaeontology. His research interests focus on taxonomy, evolution, palaeoecology, palaeobiogeography and biostratigraphy of Early Cretaceous ammonites from the Tethyan Realm.

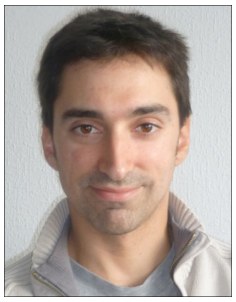

Mathieu Martinez is 'Maître de Conférences' (senior lecturer) at the University of Rennes, in Laboratory Géosciences Rennes. He teaches sedimentology and paleoclimatology. His research interests focus on the impact of the Milankovitch cycles on deep-time biogeochemical cycles and sedimentary records.

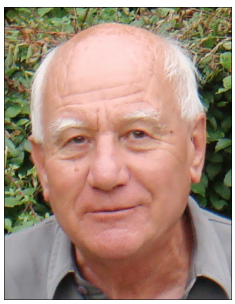

Peter F. Rawson is Emeritus Professor at University College London and former chair of the Barremian Working Group of the International Subcommission on Cretaceous Stratigraphy. His research is focused on Late Jurassic to Early Cretaceous global biogeography, palaeogeography, sea levels and climate, and on Early Cretaceous ammonite faunas from the Boreal Realm and South America (Argentina).

Appendix. Taxonomic index

Alphabetic list of the taxa mentioned in the text and figures

Calcareous nannofossils

Assipetra infracretacea (Thierstein, 1973) Roth, 1973
Assipetra terebrodentarius (Applegate et al. in Covington & Wise, 1987) Rutledge & Bergen in Bergen, 1994
Axopodorhabdus dietzmannii (Reinhardt, 1965) Wind & Wise, 1983
Biscutum constans (Górka, 1957) Black in Black & Barnes, 1959
Braarudosphaera bigelowii (Gran & Braarud, 1935) Deflandre, 1947
Calcicalathina oblongata (Worsley, 1971) Thierstein, 1971
Chiastozygus Gartner, 1968
Conusphaera rothii (Thierstein, 1971) Jakubowski, 1986
Cretarhabdus conicus Bramlette & Martini, 1964
Cretarhabdus loriei Gartner, 1968
Crucibiscutum Jakubowski, 1986
Cruciellipsis cuvillieri (Manivit, 1966) Thierstein, 1971
Cyclagelosphaera margerelii Noël, 1965
Cyclagelosphaera rotaclypeata Bukry, 1969
Diazomatolithus lehmanii Noël, 1965
Discorhabdus ignotus (Górka, 1957) Perch-Nielsen, 1968
Haqius circumradiatus (Stover, 1966) Roth, 1978
Haqius ellipticus (Grün *in* Grün & Allemann, 1975) Bown, 1992 emend. Bown, 2005
Hayesites irregularis (Thierstein in Roth & Thierstein, 1972) Applegate et al. in Covington & Wise, 1987
Helenea chiastia Worsley, 1971
Hemipodorhabdus gorkae (Reinhardt, 1969) Grün in Grün & Allemann, 1975
Lithraphidites bollii (Thierstein, 1971) Thierstein, 1973
Lithraphidites carniolensis Deflandre, 1963
Manivitella pemmatoidea (Deflandre in Manivit, 1965) Thierstein, 1971
Micrantholithus Deflandre *in* Deflandre & Fert, 1954
Micrantholithus hoschulzii (Reinhardt, 1966) Thierstein, 1971
Micrantholithus obtusus Stradner, 1963
Micrantholithus spinulentus Aguado, 2012
Micrantholithus stellatus Aguado in Aguado et al., 1997
Mitosia infinita Worsley, 1971
Nannoconus Kamptner, 1931
Nannoconus bermudezii Brönnimann, 1955
Nannoconus bucheri Brönnimann, 1955
Nannoconus circularis Déres & Achériteguy, 1980
Nannoconus globulus Brönnimann, 1955
Nannoconus grandis Déres & Achériteguy, 1980
Nannoconus kamptneri Brönnimann, 1955
Nannoconus steinmannii Kamptner, 1931
Nannoconus wassallii Brönnimann, 1955
Owenia partita (Varol *in* Al-Rifaiy et al., 1990) Bown in Kennedy et al., 2000
Palaeomicula maltica (Worsley, 1971) Varol & Jakubowski, 1989
Percivalia fenestrata (Worsley, 1971) Wise, 1983
Retecapsa angustiforata Black, 1971
Retecapsa crenulata (Bramlette & Martini, 1964) Grün in Grün & Allemann, 1975
Rhagodiscus asper (Stradner, 1963) Reinhardt, 1967
Rotelapillus crenulatus (Stover, 1966) Perch-Nielsen, 1984
Sollasites Black, 1967
Speetonia colligata Black, 1971
Staurolithites mitcheneri (Applegate & Bergen, 1988) Rutledge & Bown, 1998 in Bown et al., 1998
Staurolithites siesseri Bown in Kennedy et al., 2000
Staurolithites stradneri (Rood et al., 1971) Bown in Bown & Cooper, 1998
Tegumentum stradneri Thierstein *in* Roth & Thierstein, 1972
Tranolithus gabalus Stover, 1966
Tubodiscus frankiae Bown, 2005
Watznaueria Reinhardt, 1964
Watznaueria barnesiae (Black in Black & Barnes, 1959) Perch-Nielsen, 1968
Watznaueria biporta Bukry, 1969
Watznaueria cynthae Worsley, 1971
Watznaueria fossacincta (Black, 1971) Bown in Bown & Cooper, 1989
Watznaueria ovata Bukry, 1969
Zeugrhabdotus Reinhardt, 1965
Zeugrhabdotus diplogrammus (Deflandre in Deflandre & Fert, 1954) Burnett in Gale et al., 1996
Zeugrhabdotus embergeri (Noël, 1958) Perch-Nielsen, 1984
Zeugrhabdotus noeliae Rood et al., 1971
Zeugrhabdotus trivectis Bergen, 1994
Zeugrhabdotus xenotus (Stover, 1966) Burnett in Gale et al., 1996

Dinoflagellate cysts

Aprobolocysta eilema Duxbury, 1977
Exiguisphaera phragma Duxbury, 1979
Subtilisphaera perlucida (Alberti, 1959) Jain & Millepied, 1973
Subtilisphaera scabrata Jain & Millepied, 1973
Subtilisphaera senegalensis Jain & Millepied, 1973
Palaecysta complicata (Neale & Sarjeant, 1962) Williams & Fensone, 2016

Dasycladalean algae

Angioporella neocomiensis Conrad & Masse, 1989
Deloffrella hauteriviana (Masse, 1999 in Masse et al., 1999) Granier, 2013
Suppiluliumaella corbarica (Jaffrezo, 1973) Carras, 1995

Charophytes

Ascidiella iberica var. *iberica* Grambast, 1966
Ascidiella stellata var. *lata* Martín-Closas, 1996
Ascidiella stellata var. *stellata* (Martín-Closas & Grambast-Fessard, 1986) Martín-Closas ex Schudack, 1993
Ascidiella triquetra (Grambast, 1969) Martín-Closas, 1996
Atopochara trivolvis var. *triquetra* (Grambast, 1968) Martín-Closas, 1996
Clavator calcitrapus var. *jiangluoensis* (Wang & Li in Wang & Lu, 1982) Pérez-Cano, Bover-Arnal & Martín-Closas, 2020
Clavator grovesii var. *gautieri* (Grambast, 1979) Martín-Closas, 1996
Clavator harrisii var. *dongjingensis* (Hu & Zeng, 1981) Martín-Closas 2000
Clavator harrisii var. *harrisii* Peck, 1941
Clavator harrisii var. *reyi* (Grambast-Fessard, 1980) Martín-Closas, 1996
Globator maillardii var. *trochiliscoides* (Grambast, 1966) Martín-Closas, 1996
Globator maillardii var. *biutricularis* Vicente & Martín-Closas, 2013
Hemiclavator adnatus (Martín-Closas & Grambast-Fessard, 1986)

Schudack, 1989
Hemiclavator neimongolensis var. *posticecaptus* (Martín-Closas & Grambast-Fessard, 1986) Martín-Closas, 1996.
Pseudoglobator fourcadei Grambast, 1969

Planktonic foraminifera
Favusella hoterivica (Subbotina, 1953)
Globigerinelloides paragottisi Verga & Premoli Silva, 2003
Hedbergella Bronnimann & Brown, 1958
Hedbergella aptiana Bartenstein, 1965
Hedbergella delrioensis (Carsey, 1926)
Hedbergella excelsa Longoria, 1974
Hedbergella infracretacea (Glaessner, 1937)
Hedbergella laculata (Banner, Copestake & White, 1993)
Hedbergella praetrocoidea Kretchmar & Gorbachik in Gorbachik, 1986
Hedbergella sigali Moullade, 1966
Lilliputianella eocretacea (Neagu 1975)
Lilliputianella pauliani (Neagu, 1975)
Lilliputianella roblesae (Obregón de la Parra, 1959)
Lilliputianella semielongata (Longoria, 1974)
Lilliputianella similis (Longoria, 1974)

Small benthic foraminifera
Ammodiscus Reuss, 1862
Astacolus Montfort, 1808
Conorotalites bartensteini (Bettenstaedt, 1952)
Conorotalites intercedens (Bettenstaedt, 1952)
Dorothia Plummer, 1931
Dorothia kummi (Zedler, 1961)
Dorothia ouachensis (Sigal, 1952)
Dorothia praeoxycona Moullade, 1966
Dorothiinae Balakhmatova, 1972
Gavelinella Brotzen, 1942
Gavelinella barremiana Bettenstaedt, 1952
Glomospirella Plummer, 1945
Laevidentalina Loeblich & Tappan, 1986
Lenticulina Lamarck, 1804
Polimorphinidae Orbigny, 1839
Reussoolina Colom, 1956
Spirillina Ehrenberg, 1843
Textularia bettenstaedti Bartenstein & Oertli, 1977

Large benthic foraminifera
Cribellopsis schroederi Arnaud-Vanneau, 1980
Eopalorbitolina pertenuis (Foury, 1968)
Orbitolinopsis buccifer Arnaud-Vanneau & Thieuloy, 1972
Orbitolinopsis cuvillieri Moullade, 1960
Orbitolinopsis kiliani (Henson, 1948)
Paleodictyoconus beckerae Clavel et al., 2009
Palorbitolina lenticularis (Blumenbach, 1805)
Valserina primitiva Schroeder et al., 1969
Valserina turbinata (Foury, 1968)
Vanneauina vercorii (Arnaud-Vanneau, 1980)

Ammonites
Abrytusites neumayri (Haug, 1889)
Acrioceras meriani (Ooster, 1860)
Acrioceras ramkrishnai Sarkar, 1955
Ammonites ligatus Orbigny, 1841
Amorina fumisugium (Uhlig, 1883)
Amorina paxillosa (Uhlig, 1883)
Anahamulina gaspardae Vermeulen & Vašíček, 2011
Anahamulina pictetiformis (Busnardo in Busnardo et al, 2003)
Anahamulina subcylindrica (Orbigny, 1850)
Arnaudiella wiedmanni Vermeulen, 1998
Balearites angulicostatus (Orbigny, 1841)
Balearites balearis (Nolan, 1894)
Balearites binelli (Astier, 1851)
Balearites krenkeli (Sarkar, 1955)
Barremites Kilian, 1913
Barremites psilotatus (Uhlig, 1883)
Barremites tenuicinctus (Sarasin & Schöndelmayer, 1901)
Buergliceras jimenezi Vermeulen, Company, Sandoval & Tavera, 2010
Craspedodiscus Spath, 1924
Craspedodiscus discofalcatus (Lahusen, 1874)
Craspedodiscus gottschei (Koenen, 1904)
Craspedodiscus variabilis (Rawson, 1971)
Crioceratites duvalii Leveillé, 1837
Criocratites villiersianus (Orbigny, 1842)
Cryptocrioceras yrigoyeni (Leanza, 1970)
Discoidellia apenninica (Cecca, Faraoni & Marini, 1998)
Discoidellia favrei (Ooster, 1860)
Discoidellia masylaea (Coquand, 1852)
Discoidellia vermeuleni (Cecca, Faraoni & Marini, 1998)
Emericiceras emericii (Léveillé, 1837)
Emericiceras honnoratianum (Orbigny, 1842)
Emericiceras thiollierei (Astier, 1851)
Favrella wilckensi (Favre, 1908)
Fissicostaticeras rarocinctum (Koenen, 1902)
Garroniceras morloti (Ooster, 1860)
Hamulina Orbigny, 1850
Hamulinites munieri (Nicklès, 1894)
Hamulinites nicklesi Avram, 1999
Hatchericeras Stanton, 1901
Hatchericeras patagonense Stanton, 1901
Hemihoplitidae Spath, 1924
Hertleinites aguila (Anderson, 1938)
"*Holcodiscus*" *evolutus* Fallot & Termier, 1923
Homeomorphites varicostatus (Riccardi & Aguirre-Urreta, 1989)
Hypophylloceras semistriatum (Orbigny, 1841)
Kotetishvilia compressissima (Orbigny, 1841)
Kotetishvilia nicklesi (Hyatt, 1903)
Lyticoceras nodosoplicatum (Kilian & Reboul, 1915)
Lytoceras anisoptychum Uhlig, 1883
Lytoceras densifimbriatum Uhlig, 1883
Lytoceras subfimbriatum (Orbigny, 1841)
Malgasaynella besairiei (Collignon, 1949)
Megacrioceras doublieri (Jaubert, 1856)
Neolissoceras subgrasianum (Drushchits, 1960)
Nicklesia pulchella (Orbigny, 1841)
Olcostephanus Neumayr, 1875
Paracrioceras spathi Kemper, Rawson & Thieuloy, 1981

Paracrioceras strombecki (Koenen, 1902)
Paraspinoceras Sarkar, 1955
"*Paraspinoceras*" *evolutum* (Fallot & Termier, 1923)
Paraspiticeras Kilian, 1910
Phyllopachyceras infundibulum (Orbigny, 1841)
Phyllopachyceras winkleri (Uhlig, 1882)
Plesiospitidiscus Breistroffer, 1947
Plesiospitidiscus subdifficilis (Karakasch, 1907)
Protaconeceras Casey, 1954
Protaconeceras patagoniense (Favre, 1908)
Pseudothurmannia Spath, 1923
Pseudothurmannia catulloi (Parona, 1898)
Pseudothurmannia mortilleti (Pictet & de Loriol, 1858)
Pseudothurmannia ohmi (Winkler, 1868)
Pseudothurmannia picteti Sarkar, 1955
Pseudothurmannia pseudomalbosi (Sarasin & Schöndelmayer, 1901)
Pseudovaldedorsella compsensis (Kilian, 1910)
Psilotissotia chalmasi (Nicklès, 1890)
Psilotissotia colombiana (Orbigny, 1842)
Raspailiceras Wright, 1956
Sabaudiella Vašíček & Hoedemaeker, 2003
Sabaudiella argosensis Vašíček & Hoedemaeker, 2003
Sabaudiella riverorum Aguirre-Urreta & Rawson, 2012
Sabaudiella simplex Busnardo in Busnardo et al, 2003
Sanmartinoceras africanum insignicostatum Riccardi, Aguirre-Urreta & Medina, 1987
Scaphites yvani Puzos, 1832
Shasticrioceras Anderson, 1938
Shasticrioceras patricki Murphy, 1975
Silesitidae Hyatt, 1900
Subsaynella sayni (Paquier, 1900)
Subpulchellia fouquei (Nicklès, 1894)
Taveraidiscus alcoyensis (Nicklès, 1890)
Taveraidiscus heeri (Ooster, 1860)
Taveraidiscus hugii (Ooster, 1860)
Taveraidiscus intermedius (Orbigny, 1841)
Taveraidiscus kiliani (Paquier, 1900)
Taveraidiscus oosteri (Sarasin & Schöndelmayer, 1901)
Taveraidiscus querolensis (Busnardo in Busnardo & David, 1957)
Taveraidiscus vandeckii (Orbigny, 1850)
Vasicekina autinae Vermeulen, 2010
Veveysiceras arbeitae Vermeulen, Lazarin, Lépinay, Leroy & Mascarelli, 2013

Belemnites
Belemnites minaret Raspail, 1829
Duvalia dilatata (Blainville, 1827)
Duvalia pontica Shvetsov, 1913
Duvalia silesiaca Uhlig, 1902
Hibolites subfusiformis (Raspail, 1829)
Hibolites jaculiformis Shvetsov, 1913

Ichnofossils
Chondrites Sternberg, 1833
Planolites Nicholson, 1873
Rhizocorallium Zenker, 1836
Thalassinoides Ehrenberg, 1944
Trichichnus Frey, 1970
Zoophycos Massalongo, 1855